Deciphering the transcriptional states of Müller glia and their progeny in the regenerating zebrafish retina

D I S S E R T A T I O N

zur Erlangung des akademischen Grades

Doctor of Philosophy (Ph.D.)

vorgelegt

dem Bereich Mathematik und Naturwissenschaften der Technischen Universität Dresden

von

Laura Celotto

Eingereicht am

Die Dissertation wurde in der Zeit von Dezember 2018 bis Dezember 2022 an der Professur für Molekulare Entwicklungsgenetik der TU Dresden angefertigt.

To my beloved auntie Nunù

Per la mia amata zia Nunù

TABLE OF CONTENT

SUMMARY

The retina is the neural tissue situated at the back of the eyes that samples the visual scene and sends the processed information to the brain. Millions of people worldwide suffer from retinal diseases that affect mainly the light sensing photoreceptors or retinal ganglion cells, the output neurons projecting to the brain. Despite promising attempts in the fields of gene therapy and cell transplantation, a definitive cure for retinal diseases is still missing.

Research on highly regenerative organisms like zebrafish (*Danio rerio*) offers an attractive perspective to inform gene as well as cell transplantation-based therapies to treat retinal pathologies. Indeed, the zebrafish retina has the same structure and function as the human retina, including the presence of all retinal neurons as well as Müller glia, glial cells that provide structural and metabolic support.

Remarkably, and differently from mammalian species, zebrafish Müller glia behave additionally as stem cells upon tissue damage. In this context, Müller glia re-enter the cell cycle and generate retinal progenitors that eventually differentiate to all retinal neurons.

In the last twenty years, there has been a considerable effort to understand the molecular mechanisms underlying zebrafish Müller glia reprogramming to pro-regenerative stem cells and retinal progenitor production. However, a comprehensive study of the molecular identity of Müller glia, Müller glia-derived retinal progenitors as well as regenerated progeny in uninjured and lesioned conditions is still missing. Furthermore, although retinal progenitors regenerate all retinal neurons, independently of the specific retinal cell type that has been mostly affected by the tissue damage, it is not known whether *all* regenerated progeny integrate and rewire into the existing circuitry.

The present study had two aims:

- **First**, it aimed to provide a comprehensive description of Müller glia, Müller glia-derived progenitors as well as regenerated progeny in uninjured and light-lesioned retina at 44 hours as well as at 4 and 6 days post-lesion.
- **Second**, it aimed to establish a CreER^{T2} recombinase-based strategy to allow genetic access to follow and manipulate Müller glia-derived progenitors and their progeny during regeneration.

To achieve the first aim, a short-term lineage tracing strategy was devised using the two fluorescent reporters *Tg(gfap:mCherry)* and *Tg(pcna:EGFP)* labelling Müller glia and proliferating cells, respectively. Double transgenic animals were employed to sort for Müller glia, Müller glia-derived progenitors as well as regenerated progeny from the uninjured and light-lesioned retina. Subsequently, 10x Genomics, single cell RNA sequencing was performed to characterize their transcriptome and to deduct their differentiation trajectories during retina regeneration.

The sequencing experiment showed the presence of a glial and a neurogenic trajectory in the regenerating retina up to 6 days post-lesion. The glial trajectory starts with non-reactive Müller glia, characterized by canonical glial markers, and continues with injury-reactive Müller glia at 44 hours post-lesion, which upregulate genes associated with glia reprogramming and inflammation as well as proliferation. These early reactive Müller glia divide and generate cells belonging to a population with a hybrid identity that becomes eminent at 4 days post-lesion and is characterized by marker genes of both Müller glia and progenitors. A glial self-renewal and a neurogenic trajectory depart from the hybrid cell population. While the glial self-renewal trajectory feeds back to the non-reactive Müller glia cell population, the neurogenic trajectory continues with neurogenic progenitors, which progressively express markers of restricted fate competence and eventually regenerate several retinal neurons. The birthdate order of the regenerated progeny recapitulates the order observed during retinal development to a great extent. Indeed, retinal ganglion cells and red cone photoreceptors are born at 4 days post-lesion, followed by blue cones, amacrine and bipolar cells at 6 day post-lesion. Regenerated rod photoreceptors as well as horizontal cells were not detected among the sorted progeny, despite detection of their committed precursors.

To achieve the second aim, genetic access to Müller glia-derived cells was established using the *TgBAC(mmp9:CreET^{t2},cryaa:EGFP);Tg(Olactb:loxP-DsRed2-loxP-EGFP)* double transgenic line. The injury-induced promoter *mmp9* is expressed in reactive Müller glia and drives the expression of CreER^{T2}. Upon administration of the metabolite 4-hydroxytamoxifen, CreER^{T2} catalyses recombination in the Cre-dependent reporter *Tg(Olactb:loxP-DsRed2-loxP-EGFP)*, resulting in the expression of EGFP under the control of the broadly expressed *Olactb* promoter. Subsequently, recombined cells, which include progenitors and progeny, express EGFP permanently. Two time points of 4-hydroxytamoxifen intraperitoneal injection were tested to achieve efficient recombination: 6 hours post-lesion, corresponding to 2 hours prior to onset of *mmp9*

in reactive Müller glia, and 24 hours post-lesion. In both cases, a substantial number of EGFP-positive, Müller glia-derived cells was observed in the regenerating retina at 4 days post-lesion. The majority of the EGFP-positive cells co-localized with PCNA-positive nuclei and corresponded most likely to progenitors. Importantly, EGFP-positive cells were neither observed in the light-lesioned, ethanol injected controls nor in the uninjured, 4-hydroxytamoxifen-injected controls, indicating tight control of CreER^{T2}.

In conclusion, the current PhD thesis provides a comprehensive description of the transcriptome of Müller glia, Müller glia-derived retinal progenitors and regenerated progeny. Moreover, it establishes a CreER^{T2}-based approach to study the composition as well as long-term integration of Müller glia-derived cells in the regenerated retina and allow their genetic manipulations in future studies.

1. INTRODUCTION

Zebrafish (*Danio rerio*) are teleost fish that live in the freshwaters of east India. During the seventies of the last century, zebrafish have been introduced as research model organisms to study development and regeneration in vertebrates[1]. Zebrafish release hundreds of fertilized eggs from a single pairing event, which is advantageous for the genetic study of embryonic development. Importantly, zebrafish embryos are transparent, hence suitable for live imaging microscopy experiments to follow developmental processes *in vivo*. Finally, zebrafish have the remarkable ability to regenerate a variety of organs upon damage, including the fin, heart, pancreas, liver, as well as neural tissues like spinal cord, brain and retina[2–6]. Warm-blooded vertebrates, including mammals, do not possess such extensive regeneration capacity.

1.1 THE RETINA: A WINDOW TO THE WORLD

The retina is the neuronal tissue laying at the back of our eye that samples the visual scene in a first step, before reaching the brain (Figure 1)[7]. The retinal structure is highly conserved across vertebrates, and consists of three nuclear layers that alternate with two plexiform layers[8–10]. The cell bodies of the different retinal neurons arrange in layers with an impressively regular pattern, thus one can infer the identity of a neuron just by looking at the position of its nucleus[11]. The outer nuclear layer hosts the cell bodies of rod and cone photoreceptors, the cells that first sense and process incoming light. Photoreceptors connect to bipolar cells, the second order neurons that further rely the processed visual information to retinal ganglion cells in the ganglion cell layer. Finally, retinal ganglion cells convey the visual information through their axons that collect in the optic nerve and project to the brain. Connections between photoreceptors, bipolar cells and retinal ganglion cells form the vertical pathway of the retina, which main neurotransmitter is glutamate[11]. The vertical retinal pathway conveys light-ON and light-OFF responses to the brain. Cells in the horizontal pathway of the retina, that is the inhibitory horizontal and amacrine cells, fine tune the vertical pathway[11]. Horizontal cells locate to the outer half of the inner nuclear layer and synapse with photoreceptors and bipolar cells in the outer plexiform layer, where they regulate colour contrast detection[12,13]. Finally, amacrine cells locate to the inner half of the inner nuclear layer, with a subset of them, called displaced amacrine cells, locating to the ganglion cell layer. Amacrine cells synapse with bipolar and retinal ganglion cells in the inner plexiform layer, regulating detection of luminance, light motion and

direction[12]. In addition to neurons, the inner nuclear layer contains the cell bodies of Müller glia, which are the main glial cell type of the retina providing structural, metabolic and trophic support to the tissue[14].

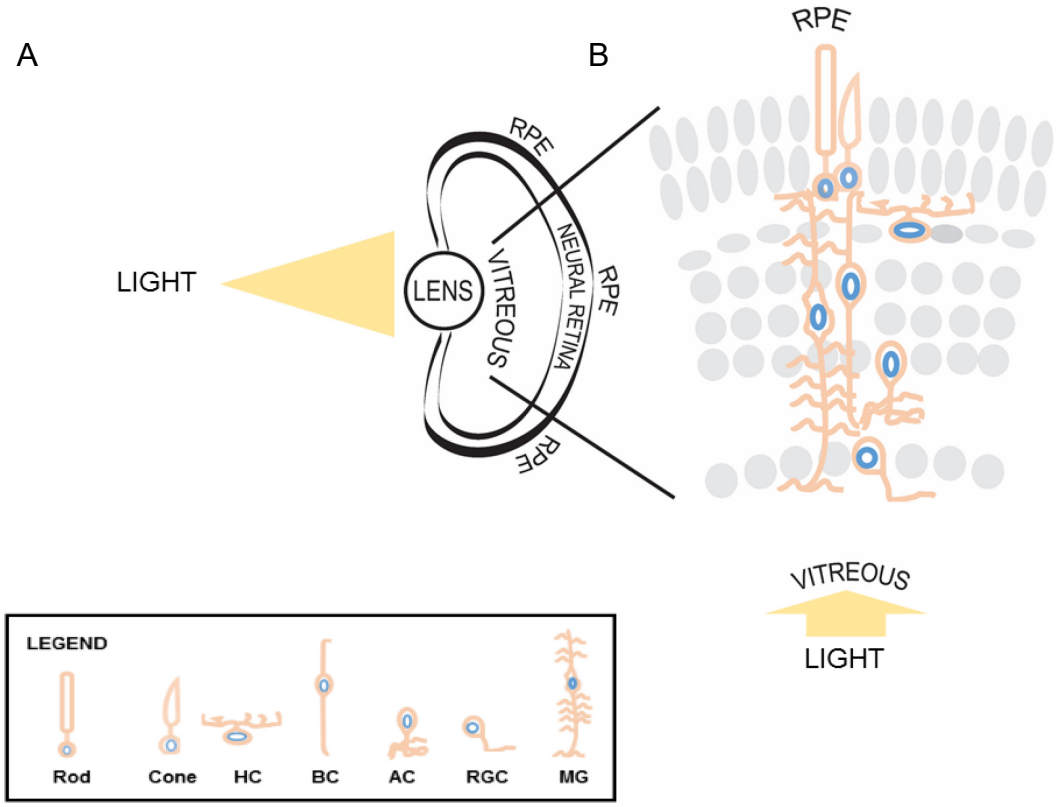

Figure 1. The vertebrate retina. A. Scheme of the vertebrate retina. **B.** Schematic histology of the retinal layers. ONL, outer nuclear layer; OPL, outer plexiform layer; INL, inner nuclear layer; IPL, inner plexiform layer; GCL, ganglion cell layer. In the legend: HC, horizontal cell; BC, bipolar cell; AC, amacrine cell; RGC, retinal ganglion cell; MG, Müller glia; RPE, retinal pigmented epithelium.

1.1.1 Photoreceptors

The vertebrate retina has rod and cone photoreceptors, the “antennae” detecting light at the very back of the eye, where they occupy the outer nuclear layer. Rods are highly light sensitive cells, and can detect as low as one photon, hence mainly working under scotopic or dim light conditions. Conversely, cones are less light sensitive than rods, but display a faster light response and are involved in high acuity and colour vision[15,16]. Photoreceptors sense light due to opsins, which are G protein-coupled receptors that bind the chromophore *11-cis-retinal*, a derivative of vitamin A. Rhodopsin is the photopigment of rods and preferentially detects light at 501 nm[17], whereas cone photoreceptors are classified in several spectral categories, according to the type of expressed opsins[12,13]. Each cone opsin has a preferred peak of absorption at specific light wavelengths, allowing for selective colour detection. The zebrafish retina has four

spectral classes of cones[18]: short, single UV cones (peak of absorption at 360 nm)[19], long, single blue cones (peak of absorption at 415 nm), and double red/green cones[17,20–22]. The latter are two morphologically distinct, but electrically coupled, cones that express two different opsins: the principal cone expresses red opsins (peak of absorption at 565 nm), while the accessory cone expresses green opsins (peak of absorption at 477 nm) [8,12-14]. Cone photoreceptors organize in a highly ordered mosaic in the zebrafish retina, with rows of red/green cones alternating with rows of blue and UV cones, so that blue cones always flank red cones and UV cones always flank green cones[23,24]. Rod photoreceptors arrange in four corners surrounding a central UV cone[25]. Photoreceptors are highly polarized neurons, organized in five compartments: the outer segment, the connecting cilium, the inner segment, the cell body with the nucleus, and the synapse[16]. The outer segment is a long, specialized primary cilium that assumes a rod-like shape in rod photoreceptors and a conical shape in cone photoreceptors[16,26]. Rod outer segments contain stacks of membranous disks that are separated from the surrounding plasma membrane, whereas cone outer segments are actual invagination of the plasma membrane[27,28]. The outer segment connects to the inner segment via the connecting cilium, enriched with mitochondria, lysosomes and other organelles. The inner segment is contiguous to the cell body hosting the nucleus and, from the cell body, a short axon ends up in the synapse with bipolar and horizontal cells, the so-called ribbon synapse[16].

1.1.2 Bipolar cells

Bipolar cells are the second order neurons in the glutamatergic vertical pathway of the retina that collect luminance, colour and spatial information from photoreceptors to relay them to retinal ganglion cells, the output of the retina[12,29]. Bipolar cells have their nuclei in the inner nuclear layer, and extend a distal dendritic tree that connects with photoreceptors in the outer plexiform layer, and a proximal axon with variable varicosities that terminates in the inner plexiform layer[30]. The zebrafish retina has 17 different classes of bipolar cells, based on their physiology as well as morphology of axonal ramification in the inner plexiform layer: six ON, seven OFF and four ON/OFF bipolar cells[30]. ON bipolar cells depolarize in response to light stimulation and express metabotropic glutamate receptors as well as a glutamate transporter forming a chloride channel [9,29,31]. OFF bipolar cells express ionotropic AMPA and kainite glutamate receptors and hyperpolarize in response to light stimulation[31]. ON/OFF bipolar cells exhibit both ON and OFF responses[32]. ON and OFF responses are segregated in

different *strata* or laminae of the inner plexiform layer, where bipolar cell axons synapse with amacrine and retinal ganglion cells [12,31,32]. ON bipolar cells, which specifically express protein kinase C alpha and beta (PKCα and PKCβ)[32], terminate with their axons in the proximal strata 4 to 6 of the inner plexiform layer[30]. OFF bipolar cells axons terminate in the distal strata 1 to 3 of the inner plexiform layer, whereas ON/OFF cells terminate both in ON and OFF strata[30]. The diversity of bipolar cell types raises to 33 distinct classes, based on their differential dendritic trees that sample information from different combination of photoreceptors in the outer plexiform layer[33]. Differently from mammals, zebrafish lack an exclusive rod bipolar cell, having only bipolar cells that receive signals from both cone and rod photoreceptors[33].

1.1.3 Horizontal cells

Horizontal cells are interneurons that modulate the synapse between photoreceptor and bipolar cells in the outer nuclear layer. Their nuclei locate in the outer half of the inner nuclear layer, where they form a layer with the major nuclear axis arranged in parallel to the retinal surface[8,9]. Horizontal cells are the first stop in the horizontal pathway of the retina and are involved in contrast detection and modulation via mechanisms of colour opponency[13]. Colour opponency is a type of neural computation used to detect colour changes by comparing the activity of at least two photoreceptor types, each sensing different light wavelengths[13]. Horizontal cells selectively express the neurotransmitter GABA as well as GAD67, which is an enzyme that synthesizes GABA[34,35]. Zebrafish have four different classes of horizontal cells: H1, H2 and H3, which sample information from cone photoreceptors, and H4 that samples exclusively from rod photoreceptors[12,36,37].

1.1.4 Amacrine cells

Amacrine cells are the second stop in the horizontal pathway and regulate the synapse between bipolar and retinal ganglion cells in the inner plexiform layer of the retina via feedback as well as feedforward mechanisms[12]. A gross categorization distinguishes narrow, medium and large field amacrine cells, depending on the size of their dendritic tree[38]. Like bipolar cells, amacrine cell axons terminate in different *strata* of the inner plexiform layer, depending on the sampling of light ON, light OFF and light ON/OFF signals[30]. Overall, there are 28 different classes of amacrine cells in the zebrafish retina, based on their morphology as well as dendritic and axonal ramification[38]. Like horizontal cells, amacrine cells are interneurons that express calcium binding proteins,

GABA as well as other modulatory neurotransmitters, including glycine, noradrenaline, acetylcholine and parvalbumin[34,35,39–42]. In particular, a specific class of amacrine cells called starburst amacrine cells release both GABA and acetylcholine and modulate the detection of light motion by a subtype of retinal ganglion cells[43,44].

1.1.5 Retinal ganglion cells

Retinal ganglion cells are the last neurons in the retinal vertical pathway and the sole output of the vertebrate retina[9,12]. They extract features from the visual scene, like chromaticity, luminance transition and edges, light motion and direction. Retinal ganglion cells sample the inputs coming from bipolar as well as amacrine cell, with which they synapse in the inner plexiform layer[45]. Retinal ganglion cells are glutamatergic neurons, which axons collect in the optic nerve projecting to the optic tectum and to additional nine extra-tectal regions in the zebrafish brain[34,46–48]. The zebrafish retina has more than 30 different retinal ganglion cell types, depending on their morphology and physiology. A recent study used single cell RNA sequencing of *Tg (isl2b:RFP)* retinal ganglion cells from larval and adult zebrafish and classified 32, transcriptionally unique retinal ganglion cells in the zebrafish retina, which identity and function are largely established already during the larval stages[49].

1.2 THE DEVELOPMENT OF THE VERTEBRATE RETINA

The development of the vertebrate retina is a highly conserved process that follows two principles. First, despite the great heterogeneity of cells populating the tissue, both retinal neurons and Müller glia derive from a common pool of multipotent retinal progenitor cells (RPCs)[8,50–53]. Second, retinal cell populations arise in waves according to a conserved order, in which retinal ganglion cells are born first, followed by cones, horizontal cells, amacrine cells, rods and bipolar cells (Figure 2). Müller glia is the latest cell type to be born[8,54–58].

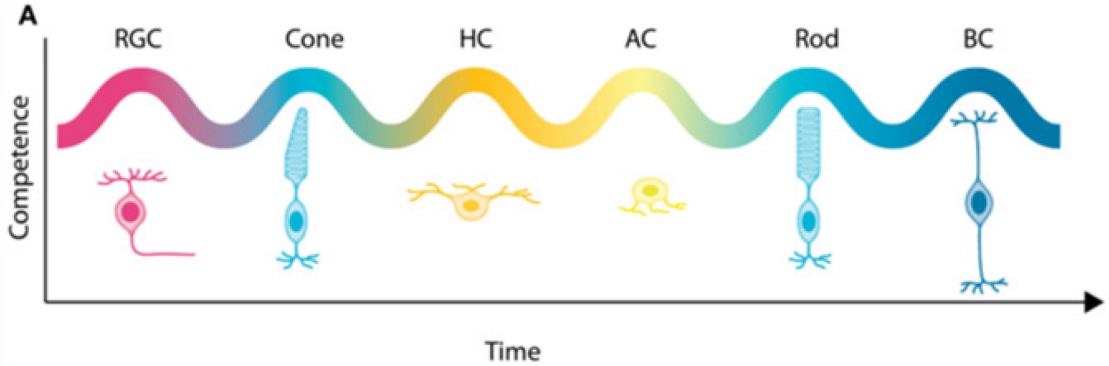

Figure 2. The developmental birthdate order of retinal cells. Neurons (and, later, Müller glia, not shown here) arise in subsequent, but overlapping, waves of production by RPCs that change their competence during retinogenesis.

Figure modified from *Neuronal Migration and Lamination in the Vertebrate Retina – Amini R., Rocha Martins M., and Norden C., Frontiers in Neuroscience, 2018.*

1.2.1 Atoh7 and the beginning of retinal neurogenesis

In the early phases of retinogenesis, the retina is a pseudostratified epithelium populated by proliferating RPCs expressing markers like *pax6*, *vsx2*, *six3*, and *nr2e1*[53,59–63]. An early study found that retinal neurogenesis in zebrafish starts at around 28 hours post-fertilization (hpf) in the ventro-nasal position, with the birth of the first retinal ganglion cells, followed by the rest of the ganglion cell layer, the inner nuclear and, eventually, the outer nuclear layer[64]. At a single-cell level, the birthdate order of retinal neurons is the one described above[58]. Live imaging led to the discovery that *atoh7* is one of the earliest neurogenic markers, expressed by RPCs right before their mitotic division on the apical side of the retina[65–67]. Progenitors expressing *atoh7* divide asymmetrically and generate one retinal ganglion cell and a sister cell that can be either an amacrine cell or a precursor of photoreceptors or of horizontal cells[65,66,68]. Importantly, amacrine and horizontal cells arise when subsets of RPCs downregulate Atoh7 and upregulate Ptf1a, which directly inhibits Atoh7 and starts the inhibitory cell lineage[38,69]. Conversely, bipolar cells and Müller glia derive from distinct Vsx2-positive RPCs that do not arise within the Atoh7 lineage, although a very recent study claims that Atoh7-positive RPCs eventually might have the **potency** to generate bipolar cells too[60,68].

1.2.2 Committed precursors in the zebrafish retina

Committed precursors have unique molecular and morphological features, and, usually, terminally divide to generate two cells of the same type (Figure 3)[8,56].

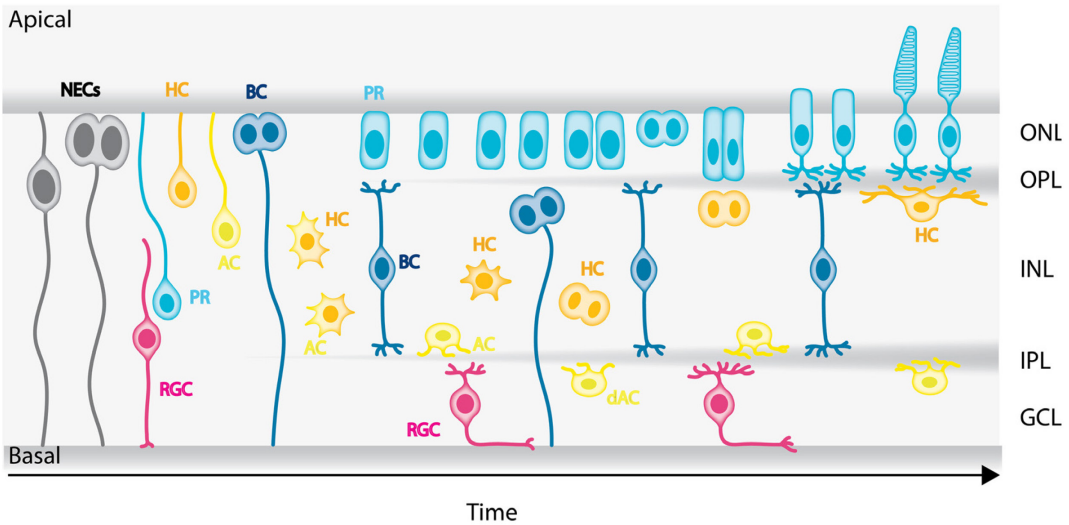

Figure 3. Committed precursors in the developing zebrafish retina. Neuroepithelial cells (NECs) divide asymmetrically and generate retinal ganglion cells (RGC), and photoreceptor precursors (PR), horizontal cell precursors (HC) or amacrine cells as well as displaced amacrine cells (AC, dAC). Bipolar cells arise from distinct, dedicated precursors (BC). ONL, outer nuclear layer; OPL, outer plexiform layer; INL, inner nuclear layer; IPL, inner plexiform layer; GCL, ganglion cell layer. Figure modified from *Neuronal Migration and Lamination in the Vertebrate Retina – Amini R., Rocha Martins M., and Norden C., Frontiers in Neuroscience, 2018.*

For instance, precursors of red cones in the developing zebrafish retina express *thrb* and assume a rectangular morphology in the outer nuclear layer, where they terminally divide to produce two cone photoreceptors that express long-wave length opsins (*opn1lw1* or *opn1lw2*)[70]. In addition, horizontal cells derive from committed precursors that terminally divide in the future horizontal cell layer, have multipolar morphology and express Ptf1a and Prox1[71]. Finally, a subset of bipolar cells derive from apical and non-apical divisions of Vsx1-positive precursors[56]. Vsx1-positive precursors, in turn, arise from Vsx2-positive RPCs, which generate also the rest of bipolar cells as well as Müller glia. Retinal lamination in the zebrafish is complete at around 72 hpf.

1.3 HER MAJESTY THE MÜLLER GLIA

Müller glia are the main glial cells of the vertebrate retina. The word “glia” comes from the ancient Greek and means “glue”. Indeed, glial cells of the nervous system glue together neurons, that is, they form a net of cells providing neurons with metabolic and mechanical support[14,72–74]. This is particularly evident for Müller glia, which function and cellular structure are suitable to support the health of retinal neurons. Müller glia are large cells that span the entire thickness of the retina and have a polygonal-shaped nucleus locating to the middle/basal row of the inner nuclear layer. They extend a long, apical process that eventually connects to the outer limiting membrane of the retina, and a basal process that terminates with an end-foot in the inner limiting membrane, which separates the retina from the vitreous. Additional, highly ramified processes extend laterally from the main glial cell body, ensheating virtually every neuron and synapse in the retina[14,74]. This highly complex morphology makes the Müller glia exquisite sentinels of the retinal extracellular milieu and the neuronal wellbeing. For instance, Müller glia control the ionic as well as neurotransmitter balance by expressing ionic, GABA and glutamate transporters. Once transported in the Müller glia, GABA and glutamate are metabolized to glutamine by the enzyme glutamine synthetase (GS), a specific marker in all vertebrate glia. Next, glutamine is re-transported back to neurons to feed glutamate synthesis[72,75–77]. Additionally, Müller glia regulate the re-cycling of the retinal pigments of cone photoreceptors, behave as “optic fibres” to

facilitate light conduction to photoreceptors, and, in overall, ensure the lamination as well as mechanical robustness of the retina[78,79]. Müller glia development and maturation are stepwise processes starting with the late retinal progenitor cell, which in mammals shares many genes with mature Müller glia[80,81]. Interestingly, transcription factors that regulate Müller glia development, like Vsx2, Nr2e1, Sox2 and Sox9, are expressed also by proliferating, multipotent RPCs in the developing retina[61,62,82–90]. Some of these factors, like Sox2, are even markers of mature Müller glia in the adult retina[86]. Eventually, upregulation of GS expression as well as the appearance of a high K^+ conductance mark Müller glia maturation[91–94]. Because of their apical-basal, polarized morphology and their molecular signature, Müller glia are considered to be similar to late-stage retinal progenitors or as cells that *retain* a progenitor footprint[6,80,95]. This is particularly evident in the retina of vertebrates with high regenerative capacities, like teleosts, and, in particular, zebrafish.

1.3.1 Müller glia: the stem cells of the central zebrafish retina

Early studies of the teleost retina showed that the adult tissue retains two stem cell niches that ensure continuous retinal growth throughout the fish lifespan: the ciliary marginal zone (CMZ) and the rod precursors[96–100]. The CMZ corresponds to the peripheral area of the retina, where the tissue meets the iris epithelium, and includes stem and progenitor cells. It generates all retinal neurons in the adult retina, except for rods, and expresses many of the stem cell markers found in the embryo, such as multipotency and neurogenic genes, like *vsx2*, *pax6*, and *atoh7,* as well as proliferation genes like *pcna*[100,101]. Rod photoreceptors derive from rod precursors at the base of the outer nuclear layer[102]. A study from the Raymond lab showed that Müller glia are responsible for rod genesis in the retina[95]. They found that rod progenitors come from slowly cycling Müller glia in the inner nuclear layer, and form a cluster of fusiform cells migrating along the glia towards the outer nuclear layer, where they eventually become rod precursors. Rod precursors lay in the adult outer nuclear layer as a reserve for mature rods[95]. The sequence of marker genes expressed in the rod lineage is the same as the one regulating their development in the embryonic retina, and includes transcription factors like Neurod1, Crx and Nr2e3[95,103,104]. Importantly, and differently than in the mammalian retina[105], Crx and Nr2e3 in the developing fish retina label progenitors of both cone and rod photoreceptors, which share a similar appearance when still at the immature state[58,103]. In addition to be the stem cells of the rod lineage,

zebrafish Müller glia have the astonishing capacity to boost their stem cell potential and eventually regenerate all retinal neurons upon tissue damage.

1.3.2 Müller glia lead retina regeneration in zebrafish

During the early 2000s, Vihtelic and Hyde showed that exposure of zebrafish to a constant, intense light for 7 days caused photoreceptor apoptosis within 1 day from the lesion and triggered a proliferative response in the inner nuclear layer of the retina[106]. Specifically, they documented the appearance of PCNA-positive, fusiform nuclei that peaked in number at 4 days post lesion (dpl) and closely associated with GFAP-positive, Müller glia fibers. At 28 dpl, regenerated rods and cones were observed in the outer nuclear layer, but the cone mosaic appeared disorganized as compared to the uninjured controls. Later, Yurco and Cameron observed similar elongated, proliferating nuclei of cells associating with Müller glia in a laser-lesioned retina[107]. Finally, between 2006 and 2007, three papers from the Goldman, Hyde and Raymond lab showed that Müller glia were the source of proliferating cells in the lesioned retina. First, Fausett and Goldman used a transgenic fish line in which GFP reports for a fragment of the *alpha tubulin 1 (tuba1a)* promoter[108]. Alpha tubulin1 is a microtubule protein highly expressed by progenitors and immature neurons during development of the central nervous system[109,110]. They showed that *tuba1a*:GFP was induced in fish retinae exposed to a stab injury that had ablated several retinal neurons. GFP was specifically induced in Müller glia that expressed BrdU as early as 2 dpl. GFP was further retained by BrdU-positive cells forming a cluster around a central Müller glia that the authors interpreted as neurogenic[106,107,111,112], Müller glia-derived progenitors[108]. These progenitors peaked in proliferation at 4 dpl, and shared with Müller glia the expression of *pax6*, a marker of multipotency, as well as very similar cytoplasm and nucleus appearance, as shown by electron microscopy. Eventually, lineage tracing of GFP-positive cells derived from injury reactive Müller glia showed that they expressed markers of Müller glia as well as retinal ganglion, amacrine, and bipolar cells at 7 and 11 dpl. The authors concluded that Müller glia are the stem cells that trigger a pro-regenerative response in the stab lesioned retina of zebrafish. They divide at 2 dpl, and generate multipotent progenitors that amplify and eventually migrate to several retinal layers to produce all retinal neurons and Müller glia[108]. One year later, Fimbel and colleagues described a similar sequence of events in the ouabain lesioned retina[113]. Ouabain is a toxin that inhibits the sodium/potassium pump and ablates preferentially retinal ganglion and amacrine cells when injected in the vitreous at low

concentrations (2 μM)[114,115]. The authors used the transgenic fish line *Tg(gfap:EGFP),* to label Müller glia, and immunohistochemistry for PCNA to label proliferating cells in uninjured and ouabain-lesioned conditions. They found that EGFP-positive Müller glia started to express PCNA at 2 dpl; at 3 dpl, the number of EGFP/PCNA-double positive glia reached a peak, and then decreased again at 5 and 7 dpl. In the meantime, ***gfap:*EGFP-negative**, but PCNA-positive, elongated cells associating with *gfap:*EGFP-positive Müller glia appeared at 5 dpl, scattered in the inner as well as outer nuclear layers. The authors used the transgenic fish line *Tg(olig2:EGFP)* and showed that the majority of PCNA-positive cells at 5 dpl were also *olig2*:EGFP-positive, where *olig2* is a developmental marker of retinal progenitors[116]. Finally, they showed that new retinal ganglion and amacrine cells were regenerated within 60 dpl. In particular, using the *Tg(atoh7:EGFP)* line they found that regenerated ganglion cells derived from *atoh7* expressing progenitors, similarly to what happens during retinogenesis[65,117]. The authors concluded that Müller glia proliferate at 2 dpl and generate proliferating progenitors that eventually replace missing retinal ganglion and amacrine cells upon ouabain-mediated lesion. Progenitors express known developmental markers, like *olig2* and *atoh7*[113]. Later in the same year, Bernardos and colleagues described Müller glia proliferation and subsequent production of progenitors using the *Tg(gfap:GFP)* line in the diffuse light-lesioned retina[95]. In this paradigm, an intense (≥ 100.000 lux) bright light is applied for 30 minutes to freely swimming fish, which have been previously dark-adapted, to ablate rod and cone photoreceptors in the central/dorsal area of the retina. Again, Müller glia proliferated as early as 2 dpl and produced PCNA-, Pax6-double positive retinal progenitors that peaked in proliferation at 4 dpl. Of note, the authors reported that Pax6 was not an exclusive marker of progenitors, but it was expressed, albeit weakly, already by Müller glia in uninjured conditions. Progenitors eventually migrated along Müller glia fibers to the outer nuclear layer, where they expressed the photoreceptor precursor marker Crx, and regenerated first mature cones at 6 dpl[95].

Subsequent studies on retina regeneration further investigated the molecular dynamics that trigger retina regeneration upon different lesion paradigm[6,118–120]. In all cases, Müller glia start a response organized in four phases (Figure 4):[120]

- **Müller glia activation and partial de-differentiation**;

- **Müller glia asymmetric division and Müller glia-derived progenitor production**;
- **Progenitor proliferation;**
- **Progenitor differentiation and retinal architecture restoration**.

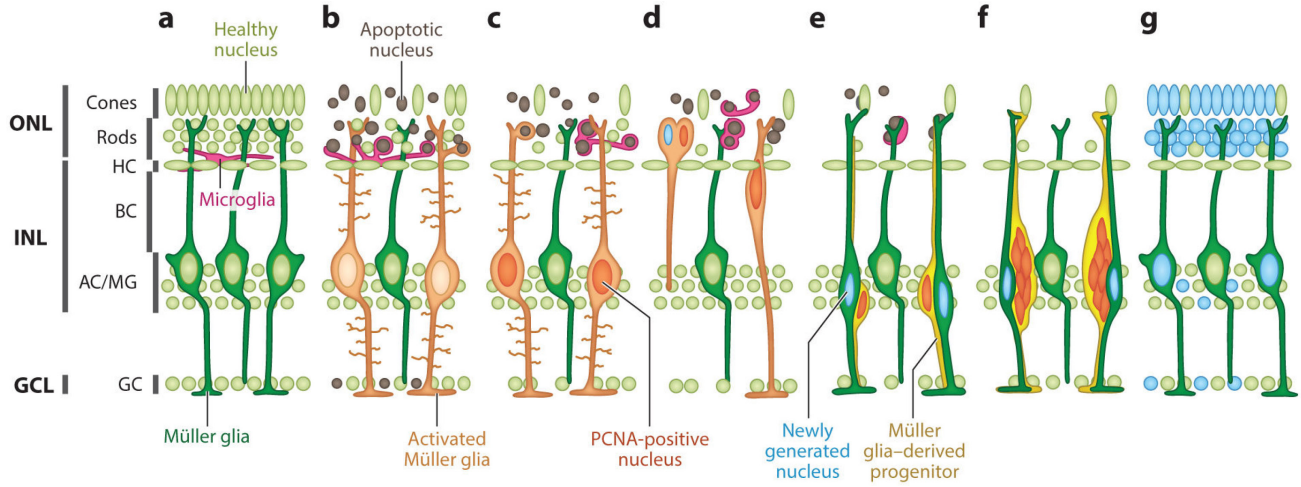

Figure 4. Schematic illustration of retina regeneration upon light lesion. **a.** Uninjured retina. **b.** Exposure to light triggers apoptosis mainly in the outer nuclear layer (ONL), where photoreceptors reside, but some rare, apoptotic nuclei locate to other retinal layers, like the ganglion cell layer (GCL). Microglia phagocyte dying rods and cones, while a subset of Müller glia (MG) become activated in the inner nuclear layer (INL) engulfing photoreceptors too. **c.** Activated MG, still engulfing dying photoreceptors, start expressing PCNA, a marker of proliferation. **d.** MG nuclei migrate to the ONL and undergo asymmetric cell division that generate a self-renewed, MG nucleus (light blue) and a Müller glia-derived progenitor nucleus (orange). **e.** The newly generated, post-mitotic MG nucleus (blue nucleus in the green cell) and the Müller glia-derived progenitor nucleus (orange nucleus in the yellow cell) return back to the INL. **f.** Only the Müller-glia derived progenitor keeps proliferating, generating clusters of proliferating nuclei that associate with self-renewed MG. **g.** Regenerated photoreceptors, as well as INL and GCL cells, (blue nuclei) appear in the ONL at 30 dpl. MG is back to quiescence. HC: horizontal cells; BC: bipolar cells; GC: ganglion cells. Modified from *Reprogramming of Müller glia to regenerate neurons – Lahne M., Nagashima M., Hyde D.R., and Hitchcock P.F., Annual Review of Vision Science, 2020.*

- <u>Müller glia *activation* and *partial* de-differentiation: 0-2 dpl</u>

When fish are exposed to a bright light, photoreceptors undergo apoptosis, with a peak of cell death between 16-24 hpl[106,121,122]. Dying photoreceptors release extracellular signals like tumor necrosis alpha (TNFα) that, together with additional unknown cues, signals the Müller glia ongoing tissue damage[123]. Müller glia, from now on referred to as MG, become **reactive** (Figure 4b). Activated MG exert an inflammatory-like response by phagocytosis of dying photoreceptors and by expression of matrix metalloproteases like *mmp9*, growth factors like *hbegfa*, and cytokines of the interleukin family like *crlf1a*[121,124–128]. In the meantime, microglia, the resident immune

cells of the retina become amoeboid and phagocyte dying rods and cones[124]. TNFα is necessary and sufficient to trigger MG **reactivity** and **partial de-differentiation**[123,129]. Activation of MG comprises the MG upregulation of the transcription factor Stat3, the proneural basic Helix Loop Helix (bHLH) factor Ascl1a and the pluripotency, RNA-binding protein Lin-28, in this order, between 6 and 16 hpl[122,130–133]. In particular, Ascl1a is essential to directly induce the multipotency transcript *lin-28* in MG. Lin-28 protein, in turn, binds to and decreases the availability of *let-7* miRNAs, a family of micro RNAs that promote the differentiated state of MG[132]. Additionally, Yap1 and Hmga1a are necessary for MG reactivity in the early phase of retina regeneration, since knock down of Yap1 or Hmga1a decreases significantly the number of MG that re-enter the cell cycle[134]. Finally, activation of MG also involves upregulation of developmental markers of progenitors like *pax6* and *vsx2*, which are already weakly expressed by MG in uninjured conditions[101,108,135]. **Partial de-differentiation** of MG is a term introduced by Lenkowski and Raymond to describe the fact that MG lose some characteristics of differentiated cells upon injury, for instance downregulation of certain glial-specific markers like *rlbp1a* and *glula*[6,113,136,137]. Importantly, it is debated whether *gfap* and the corresponding GFAP protein, the main marker of zebrafish MG, is downregulated by de-differentiated MG. Some reports claim that GFAP protein and *gfap* transcript are transiently upregulated during retinal regeneration[95,138,139], others show *gfap* downregulation, either *before* MG express PCNA or *after* cell cycle re-entry[113,136]. Lenkowski and Raymond state that, independently of the level of expression, *gfap* (and GFAP) is a specific marker of MG in injured and uninjured conditions. Additionally, MG keep their apical/basal morphology and their lateral processes throughout the regeneration response, hence the nomenclature *partial* de-differentiation of MG[5,6,108,119,137].

In all cases, Ascl1a is sufficient to induce the expression of proliferating cell antigen A (**PCNA**), a marker of proliferation (DNA replication and mitosis) in reprogrammed MG in the zebrafish retina (Figure 4c)[130,132,140]. MG proliferation is necessary to trigger successful regeneration of photoreceptors, since knock down of PCNA causes MG apoptosis, which impairs retinal repair[141].

- <u>Müller glia asymmetric division (30 hpl-2 dpl)</u>

Reactive MG re-enter the cell cycle at around 30 hpl, when they upregulate PCNA in the inner nuclear layer (Figure 4c). Immunohistochemistry of retinal sections as well

as live imaging studies of retinal explants have shown that proliferating MG undergo interkinetic nuclear migration, a phenomenon described for neuropeithelial RPCs in the developing retina[137,142]. After DNA replication (S phase of the cell cycle) that occurs in the inner nuclear layer, MG nucleus migrate to the outer nuclear layer, where it undergoes a single, **asymmetric cell division**. The results of this cell division is the production of a renewed MG and a MG-derived progenitor (Figure 4d)[135,137,142]. Afterwards, both MG and progenitor nuclei migrate back to the inner nuclear layer (Figure 4e).

- Progenitor amplification (2-4 dpl)

While the renewed MG re-differentiate back to a non-reactive (quiescent) state, MG-derived progenitors undergo interkinetic nuclear migration and keep proliferating, forming a cluster of cells at around the central MG (Figure 4f)[6,108,120,137]. Peak of progenitor proliferation varies between 4 and 5 dpl, depending on the lesion paradigm. In the light-lesioned retina, the peak is observed at 4 dpl, a time point when some progenitors have already initiated migration to the outer nuclear layer, where they are going to differentiate into photoreceptors[95,106,108,113,137]. However, some migration to the basal inner nuclear layer, as well as to the ganglion cell layer, occurs as well[143].

- Progenitor differentiation and retinal architecture restoration (4-30 dpl)

Progenitors start differentiating to retinal neurons at around 4 dpl. At 30 dpl, retina regeneration is complete and the layered retinal architecture is restored[95,106,126,143]. Interestingly, despite the type of applied lesion paradigm, MG-derived RPCs eventually regenerate several retinal neurons, in addition to those preferentially ablated by the injury[143]. For instance, in a light-lesioned retina, where mainly rods and cones die, RPCs eventually produce also retinal ganglion as well as amacrine cells, in addition to photoreceptors. However, RPCs that have migrated to the outer nuclear layer are more proliferative than RPCs that have migrated to the rest of the retinal layers in a light-lesioned retina. Conversely, in neurotoxin-induced retinal lesions (for instance via the application of NMDA or ouabain) retinal ganglion and amacrine cells are selectively ablated, and RPCs generating the latter cell types proliferate more than those generating photoreceptors. Hence, there is a **proliferative bias** of RPCs that differentiate to the lost neuronal cell type in the regenerating zebrafish retina, but MG regenerate *extra*-neurons in addition to those affected by the lesion[143].

1.4 THE REVOLUTION OF SINGLE CELL RNA SEQUENCING

Genomic studies involving bulk RNA sequencing, microarray analysis as well as RT-PCR have been performed on dissociated retinae as well as Fluorescent Activated Cell Sorted (FACS) MG and MG-derived cells in several lesion paradigms[122,126,133,134,138,144,145]. These studies either characterized the early events of MG reactivity and RPC production[134] or investigated broadly the molecular identity of RPCs at a population level, most of the times discussing the gene ontology of the different phases of retina regeneration. This cell population-based approach allows the identification of genes that are upregulated or downregulated in **discrete events** of retina regeneration. For instance, these studies identified the early (16 hpl) upregulation of genes associated with cell clearance, cell growth, and inflammatory-like response, like complement precursor genes, matrix metalloproteases genes (*mmp9*), genes coding for growth factors (*hbegfa*), cell migration (*cxc4rb*) and immune function (*lcp1*, coding for the immune protein L-plastin)[126]. Moreover, these studies showed downregulation of glutamine synthetase genes *glula* and *glulb* as well as upregulation of *stat3*, involved in MG activation[122]. They identified also genes associated with MG and RPC proliferation as well as Notch signalling and, starting from 4 dpl, neurogenesis (*pcna*, *her 4.1*, *olig2*, *atoh7*, *nr2e3*)[122]. However, the major drawback of bulk sequencing and microarray-based studies is the **averaging** of gene expression across multiple cell populations and lack of single cell resolution of the transcriptome[146,147]. In other words, while these approaches allow the profiling of the transcriptional landscape of cell populations and the associated events, they do not enable to know whether *all* the cells in a population share the upregulation of the same genes or whether there is transcriptional heterogeneity within the cell population itself. Moreover, microarrays and bulk RNA sequencing are not able to profile the transcriptome of rare events, like *intermediate* cell states that locate in a trajectory of differentiation from stem cells to progeny. In this context, the advent of single cell RNA sequencing (scRNAseq) platforms has revolutionized the fields of genomics, developmental and regenerative biology. scRNAseq allows profiling the transcriptome of thousands of single cells and capturing molecular heterogeneity in cell populations[146–149]. Moreover, by identifying transcriptional similarities between cell states or populations, scRNAseq aligns them in a trajectory of differentiation, enabling to study cell lineages and fate choices[134,147,150,151]. scRNAseq is a constantly evolving technology, with the droplet-based, 10x Genomics being the most currently used

platform[152]. Droplet-based scRNAseq uses microfluidics chips organized in eight, parallel channels, where each channel hosts oil, the single cell solution, barcoded gel beads and the outcome of the emulsion reaction at the core of the technology (Figure 5).

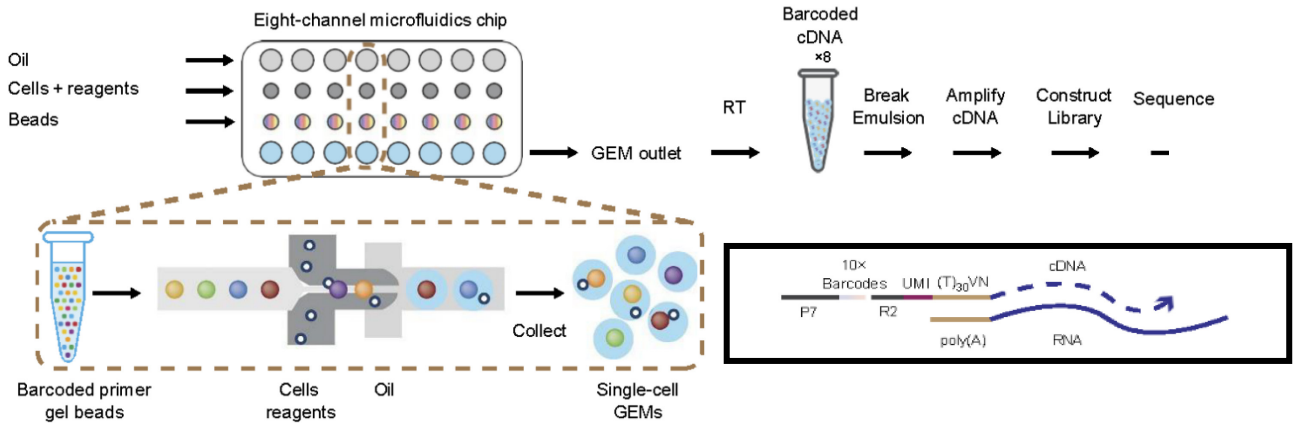

Figure 5. 10x Genomics, droplet-based scRNAseq platform. Upper part. A microfluidic chip has eight parallel channels, each hosting oil, cells and gel beads that eventually are combined in a Gel Emulsion (GEM) droplet. Cell lysis, mRNA capture and reverse transcription (RT) occur within the GEM. Barcoded cDNA is amplified and subsequent cDNA libraries sequenced. **Dotted, brown frame.** A detail of the microfluidic reaction that leads to the formation of single GEMs. **Black frame.** Detail of the barcoded oligonucleotides that harbour primers for sequencing (P7), 10x Barcodes that index beads, a unique molecular identifier (UMI) that indexes the transcript, a poly-dT sequence $(T)_{30}VN$ that hybridizes specifically to the 3'poly-A of a mRNA. Modified from *Massively parallel digital transcriptional profiling of single cells – Zheng et al., Nature Communications, 2017*.

In the droplet-based technology, a stream of **barcoded gel beads** captures single cells so that a single cell interacts with a single bead, and both are eventually encapsulated in an oil-droplet. Each bead is coated with a collection of oligonucleotides consisting of a **10x barcode** and a **unique molecular identifier** sequence (Figure 5, black-framed insert). The 10x barcode is shared by all the oligonucleotides belonging to a bead and identifies a single bead, hence the single cell associated with it. By contrast, the UMI sequence varies among oligonucleotides in a bead and identifies individual mRNA transcripts resulting from the lysis of the single cell associated with the single bead. In addition to the barcodes and the unique molecular identifier, oligonucleotides coating the gel beads harbour sequencer adapters (for later Illumina-based sequencing), primers for reverse transcription, and a 30 base pairs-long oligod-T sequence that hybridizes with the 3'-polyA tail of a complementary mRNA. Cell lysis and reverse transcription of hybridized mRNAs to complementary cDNAs occur in the droplet. Subsequently, the droplet emulsion is broken and the transcribed cDNAs amplified and sequenced by next generation, short-read Illumina sequencers. Downstream

bioinformatic analysis include extraction of information regarding the cell-barcode, UMI and RNA reads, alignment of the reads to a reference genome and gene identification, counting of UMIs and reads, identification of beads uniquely associated with cells. Eventually, a cell by gene matrix is generated, where each cell is associated with a set of genes[152]. Further bioinformatic analysis is applied to this raw matrix, including quality control, normalization and feature extraction. Quality control enables discarding of low quality cells that have a low number of sequenced counts (≈ less than 2000), detected genes (≈ less than 500) and high counts of mitochondrial reads (more than 15%). Normalization aims to scale the count data to obtain the *actual* relative gene abundance between cells, and correct for the variability inherent to each step (droplet formation, reverse transcription, library preparation and sequencing) that might affect the final number of counts per cell in the matrix. Feature extraction identifies highly variable genes, that is, those genes showing the highest variance across the single cell dataset, which is assumed to be informative about the cell identity/status[150,153]. However, the number of highly variable genes is still in the order of thousands genes, which complicates to visualize cell populations in a two or three dimensional transcriptome space. Hence, dimensionality reduction methods like principal component analysis[154], t-distributed stochastic neighbour embedding (t-SNE)[155] and Uniform Approximation and Projection (UMAP)[156] have been developed to visualize individual cells in space by selecting only a few, descriptive dimensions (e.g. marker genes) per cell. In a transcriptome map, cells sharing a similar transcriptome locate closer in space and belong to the same cluster, which has a specific colour. Cluster annotation occurs usually by inspection of the top 100, upregulated genes per cluster, which are obtained by applying statistic tests (e.g. t-test) between a single cluster and the rest of the clusters in a dataset.

1.5 THE USE OF THE CRE-LOXP TECHNOLOGY FOR CELL LINEAGE TRACING

Cre recombinase is a site-specific recombinase that binds the DNA at specific target sites to catalyse recombination between two DNA sequences. Specifically, Cre binds the DNA at loxP (locus of crossover (x) in P1) sites, which consist of a couple of 13 base pair-long, palindromic DNA sequences that flank an 8 base pair-long central spacer. The direction and orientation of the loxP sites determine the outcome of the recombination event, which can be **deletion** or **reversion** of a DNA sequence (Figure 6A). If the two loxP sites flanking the DNA sequence are oriented in the head-to-head direction, the sequence is reverted upon Cre-binding[157,158]. If the two loxP sites are

head-to-tail oriented, the binding of Cre results in the excision of the intervening DNA sequence, which is irreversibly eliminated as a circular molecule harbouring one of the who loxP sites (Figure 6A). The use of Cre recombinases has revolutionized reverse genetics, allowing for conditional knock-in as well as knock-out of selected DNA sequences as well as genetic fate mapping studies. Importantly, Cre recombinases enable to introduce a genetic modification in a controlled and cell-specific manner in the adult animals, bypassing embryonic lethality that is associated with genetic mutations introduced in the germline[158]. One application of the Cre-loxP system occurs in lineage tracing studies of developmental and regenerative biology. Lineage tracing experiments allow the study of cell fate choices of stem cell-derived progeny in developing and regenerated tissue. The establishment of the ligand-inducible CreER^{T2} system represents an important advancement for lineage tracing experiments[159–161]. In this system, the Cre protein is fused with the human estrogen receptor, which has been modified to bind the tamoxifen metabolite 4-hydroxytamoxifen, but not cell-endogenous hormones, with high affinity. In the absence of tamoxifen, the CreER^{T2} complex is retained in the cytoplasm of the cell. Once in the cell, tamoxifen is metabolized to 4-hydroxytamoxifen (4-OHT), which binds CreER^{T2} and induces a conformational change of the complex. Subsequently, CreER^{T2} enters the nucleus, binds the loxP sites and catalyses DNA recombination[160].

By controlling the time of tamoxifen, or its direct metabolite 4-OHT, administration, temporal control of Cre-mediated recombination is possible. In lineage tracing experiments, a cell-specific promoter drives CreER^{T2} expression. A second promoter drives the expression of a Cre-dependent reporter (Figure 6B)[3,162–164]. For instance, a loxP-flanked DsRed2 gene, followed by a second, different fluorescent reporter, like EGFP. In the absence of tamoxifen or 4-OHT, CreER^{T2} is retained in the cytoplasm, resulting in the expression of DsRed2, hence cells are red-labelled. Upon tamoxifen or 4-OHT administration and binding to CreER^{T2}, CreER^{T2} moves to the cell nucleus and catalyses the excision of the loxP-flanked DsRed2 cassette. As a result, the recombined cell will be permanently expressing the EGFP cassette and green-labelled. If the recombined cell is a proliferating cell, like a stem or a progenitor cell, all the resulting progeny will be permanently labelled in green, hence identifiable as deriving

from the first recombined cell (Figure 6B). This is very advantageous to study fate choices in developing as well as regenerating systems.

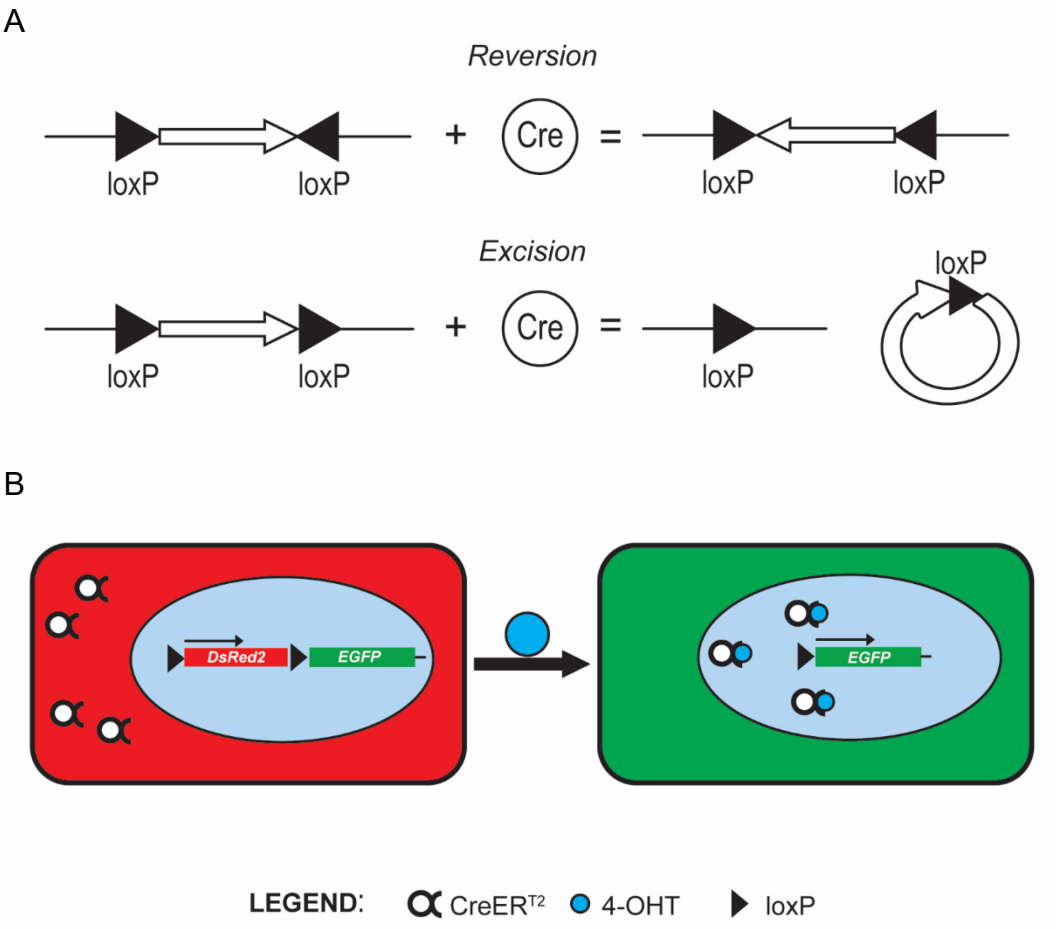

Figure 6. Cre-loxP recombination and lineage tracing. A. Cre recombinase catalyses DNA reversion when bound to head-to-head oriented loxP sites and DNA excision when bound to head-to-tail oriented loxP sites. **B.** Application of CreER^{T2}-mediated DNA excision for lineage tracing. In the left cell, CreR^{T2} remains in the cytoplasm and a cell specific promoter drives the expression of the DsRed2 reporter; hence, the cell is visualized as red fluorescent. Upon 4-OHT administration, the metabolite binds the CreER^{T2} complex, which moves to the nucleus and catalyses the excision of the DsRed2 reporter cassette, with subsequent expression of EGFP. The cell fluorescence switches from red to green.

1.6 WHY STUDYING RETINA REGENERATION IN ZEBRAFISH

Currently, there are 2.2 billion people suffering from near or distance vision impairment[165]. Retinal diseases are variable in nature and severity and the most common ones fall in three categories: age-related macular degeneration, glaucoma and retinitis pigmentosa[166]. Age-related macular degeneration and retinitis pigmentosa are photoreceptors diseases: in the former, defects of the retinal pigmented epithelium, which covers the apical side of the retina and provides metabolic support to photoreceptors, result in the progressive degeneration of cones and, at late stages,

rods. Retinitis pigmentosa comprises a highly heterogeneous group of genetically inheritable diseases characterized by the progressive degeneration of rods, followed by cone loss and, eventually, blindness[167]. Finally, glaucoma is a disease of retinal ganglion cells that degenerate most commonly because of increased intraocular pressure[166]. Currently, definitive cures for these diseases are lacking, especially in cases when cell loss has become irreversible. The most promising treatments of retinal diseases rely on gene therapy and the use of retinal implants[168,169]. Gene therapy uses adeno-associated viruses as vectors to deliver the correct form of a mutated gene in the retinae of visually impaired patients. Retinal implants, instead, rely on electronics and optogenetics to stimulate the activity of residual neurons in the degenerating retina.

In the meantime, pre-clinical research is improving the use of human stem cell-derived retinal organoids to model and study retinal diseases and related therapies *in vitro*[168]. In particular, retinal organoids developed from human-induced pluripotent stem cells could be a useful source for cell transplantation-based therapies[170,171]. For example, successful transplantation and integration of human retinal organoid-derived cone photoreceptors has been recently documented in a mouse model of degenerating retina. However, the yield of transplantable cones is currently insufficient to treat late-stage degenerative diseases of the retina, when cell loss is almost complete[172].

Research on highly regenerative animals like zebrafish can provide significant information to trigger endogenous regeneration in the mammalian retina. Knowledge of the transcriptional network that promotes reprogramming of zebrafish MG to a neurogenic cell could inform gene therapy strategies to provide the mammalian MG with the reprogramming factors necessary for the endogenous production of new retinal neurons. Mouse MG have shown of cell cycle re-entry and neuron regeneration when treated with growth factors like EGF[173–176]. However, the response is not as robust as in fish, and, more importantly, regenerated neurons do not include photoreceptors, which are the most affected cells in the diseases of the mammalian retina[173,175,177]. Knowledge of the molecular mechanisms that ensure MG-derived RPCs production as well as RPC differentiation to *all* retinal neurons in the zebrafish retina can inform cell transplantation-based therapies, for instance regarding the improvement of the photoreceptor yield *in vitro*[170].

AIMS OF THE STUDY

The zebrafish retina can regenerate all retinal neurons upon several lesion paradigms, thanks to the stem cell properties of the Müller glia. Upon tissue damage, Müller glia become reactive by engaging in two responses. First, they express inflammation-associated genes, like cytokines, growth factors and tissue metalloproteases, and via phagocytosis of dying neurons. Second, they *partial* de-differentiate and third they re-enter the cell cycle, to undergo asymmetric cell division and generate a self-renewed Müller glia and a Müller glia-derived progenitor. While self-renewed Müller glia re-differentiate back to quiescence, progenitors continue proliferating and eventually regenerate all retinal neurons and repair the lesion within 30-60 dpl. What is still missing in the retina regeneration field is a **comprehensive** characterization of the **transcriptome** of Müller glia and Müller glia-derived retinal progenitors **at a single cell level**. This knowledge is needed to fully understand the transition from cell phases and cell fate commitment. Moreover, a single cell characterization of the emergence of progenitors from Müller glia and of the regenerated progeny from progenitors is lacking. Finally, it is unknown whether all the regenerated neurons correctly **integrate** into the extant retinal circuit. This PhD thesis aimed at applying a short-term lineage tracing strategy using the *Tg(pcna:EGFP);Tg(gfap:mCherry)* double transgenic line, enabling sorting and enrichment of Müller glia, Müller glia-derived progenitors and regenerated progeny after a light lesion up to 6 days post-lesion, followed by single cell RNA sequencing. Moreover, it aimed at establishing a long term, **Cre recombinase**-based lineage tracing strategy to investigate the **long-term integration** of Müller glia-derived cells in the existent retinal circuit of the diffuse light-lesioned zebrafish retina.

The following scientific questions were addressed experimentally:

1. Is there any transcriptional heterogeneity of Müller glia, Müller glia-derived progeny and regenerated progeny in the light-lesioned retina?
2. Do regenerated progeny arise according to the developmental birthdate order in the light-lesioned retina?
3. Can we use single cell RNA sequencing to find new marker genes of Müller glia, Müller glia-derived progenitors and regenerated progeny in the light-lesioned retina?
4. Can we use CreER^{T2} mediated recombination to investigate long-term integration of Müller glia-derived cells in the existent retinal circuitry?

2. MATERIALS

2.1 Technical device

APPLICATION	DEVICE
Confocal microscope	Laser scanning 780, Zeiss Axio Imager.Z1
Fluorescent microscope	Widefield ApoTome, Zeiss Axio Imager.Z1
Cryostat	CryoStar Nx70, Thermo Scientific
Light source (For light lesion)	EXFO X-Cite 120W, EXFO Photonic Solutions
Stereomicroscope	Olympus MVX10
Tube rotor	Myltenyi Biotec MACSmix rotator
PCR Machine	Eppendorf Mastercycler ep Gradient 5
Thermomixer	Eppendorf Thermomixer® Comfort
FACS	BD FACS Aria III
cDNA library quality control	Agilent Fragment Analyzer 5200
Deep Sequencing	Illumina NextSeq500

2.2 Transgenic lines

LINE	CITATION
Tg(pcna:EGFP)	Described here
Tg(gfap:nls-mCherry)	Described here and in [4]
TgBAC(mmp9:CreERt2,cryaa:EGFP);Tg(Olactb:loxP-DsRed2-loxP-EGFP)	Described in [163]

2.3 Kits

APPLICATION	COMPANY	IDENTIFIER
Papain dissociation System	Worthington Biochemical	LK003150
10x Chromium single - cell	10x Genomics	v3 chemistry
Total RNA purification kit	Norgen Biotek Coporation	17200
cDNA synthesis	Roche	4379012001
Cloning	Thermo Fisher	TOPO TA® cloning dual promoter
Gel and DNA recovery kit	Zymo Research	D4002
Plasmid recovery	Thermo Fisher	Gene Jet Plasmid Miniprep k0503

Plasmid recovery	Macherey - Nagel	Nucleo Bond® Xtra Midi
FISH amplification kit	AKOYA Biosciences®	TSA™ Plus Cyanine 3

2.4 Primers

NAME	SEQUENCE
crlf1a	**Fw**_CTCACAAAACTCGCAACCAGG
crlf1a	**Rev**_GGATCCATTAACCCTCACTAAAGGGAACGTGGCCACTTTTGAGTCCA
id1	**Fw**_GGATATTTAGGTGACACTATAGAAGAGCATGTGGTGAACTGTCA
id1	**Rev**_GGATTAATACGACTCACTATAGGG CACAAACACACACGCGTATC
hmgb2b	**Fw**_GCAGACATGTCGCGATGAAC
hmgb2b	**Rev**_TTAACTGAACCCGTCGGTCG
onecut2	**Fw**_GGCTTGGGCTCCATACACAG
onecut2	**Rev**_ACGCTTTGGTGCAAGTGCTG

2.5 Reagents

APPLICATION	COMPANY	IDENTIFIER
NBT/BCIP stock solution	Roche	11681451001
DIG-Blocking reagent	Roche	11096176001
Calcein blue, AM	Invitrogen	C1429
Neutral protease (Dispase®)	Worthington Biochemical	LS02100
DAPI	Thermo Scientific	62248
4-Hydroxytamoxifen	Sigma Aldrich	H7904

2.6 Buffers

BUFFER	PREPARATION
20x SSC	175.3 g NaCl, 88.2 g HOC(COONa)(CH2COONa)2 · 2H2O, adjust pH to 6 with acetic acid in DEPC water
ISH wash	50% deionized formamide, 1x SSC in DEPC water
MABT	100 mM maleic acid, 150 mM NaCl, adjust pH to 7.5 with NaOH, 0.1% Tween 20, in DEPC water, filter
Staining buffer	100 mM NaCl, 50 mM MgCl2, 100 mM Tris base, pH = 9.5, 0.1% Tween 20 in DEPC water
TNT	100 Tris HCl, pH = 7.5, 150 mM NaCl, 0.1% Tween 20 in DEPC water

2.7 Antibodies

Primary

NAME, DILUTION	SPECIES	COMPANY	REFERENCE
Zrf1, 1:250	Mouse, monoclonal, IgG1	ZIRC	AB_10013806, [108]
mCherry, 1:500	Rabbit, polyclonal	Takara	632475, [178]
GFP, 1:2000	Chicken, polyclonal	Abcam	ab13970, [179]
PCNA; 1:500	Mouse, monoclonal IgG2a	Dako	M0879, [3]
anti-Digoxigenin-AP Fab fragments, 1:2000		Roche	11093274910, [4]
anti- Digoxigenin-POD Fab fragments, 1:2000		Roche	11207733910, [4]

Secondary

NAME	FLUOROPHORE	DILUTION	COMPANY
Alexa® anti-mouse IgG1	633	1:500	Invitrogen
Alexa® anti-mouse IgG2a	633	1:500	Invitrogen
Alexa® anti-chicken	488	1:500	Invitrogen
Alexa® anti-rabbit	555	1:500	Invitrogen

3. METHODS

3.1 Animals

Zebrafish (*Danio rerio*) were raised as previously described[180]. Adult fish that were 6-12 months old and of either sex were used for all experiments. WT animals were in the AB background. Fish were kept according to FELASA guidelines[181]. All animal experiments were conducted according to the guidelines and under supervision of the Regierungspräsidium Dresden (permit: TVV 44/2017). All efforts were made to minimize animal suffering and the number of animals used.

3.2 Transgenic lines

For the generation of the *Tg(pcna:EGFP)*, the BAC CH73-140L11, containing more than 100 kb of the genomic *pcna* locus, was obtained from the BACPAC resource centre. A cassette containing EGFP and a polyadenylation signal was recombined at the starting ATG of exon 1. First, FRTgb- neo-FRT and EGFP cassettes where amplified by PCR. Then, they were amplified and merged by fusion PCR with primers carrying 50 nucleotides of homology of the targeting sequence. Recombineering of the BAC was performed as previously described[182]. BAC DNA was purified and about 50 pg of BAC DNA were injected into fertilized eggs at the one cell stage. F0 were raised and incrossed. F1 were identified by visual screening for GFP expression and raised. The *Tg(gfap:nls-mCherry)* line was generated as previously described[4]. In addition to the line described in Lange et al. (tud117tg), a second independent insertion was isolated, which displays a stronger expression in MG and was hence used for this PhD thesis. The *TgBAC(mmp9:CreERt2,cryaa:EGFP);Tg(Olactb:loxP-DsRed2-loxP-EGFP)* was generated as previously described[163].

3.3 Light injury

WT AB, *Tg(pcna:EGFP);Tg(gfap:nls-mCherry)* and *TgBAC(mmp9:CreERt2,cryaa:EGFP);Tg(Olactb:loxP-DsRed2-loxP-EGFP)* fish were dark adapted for 3 days. Diffuse light lesion was performed as previously described in my lab[121]. Up to 4 fish were exposed for 30 min to a bright light (light intensity ≥ 100.000 lux) in a beaker containing system water (300 ml), positioned 3 cm away from the light bulb of a metal halide lamp (EXFO X-Cite 120W, EXFO Photonic Solutions, Mississauga, Ontario, Canada). Afterwards, lesioned animals were put back to system tanks in normal light conditions. Uninjured fish controls were dark adapted and processed in parallel.

3.4 Dissociation of retinae to a single cell suspension

Uninjured and light-lesioned *Tg(pcna:EGFP);Tg(gfap:nls-mCherry)* fish were exposed to a lethal overdose (0.2%) of MS-222 (Sigma)[183]. Subsequently, each cornea was poked with a needle, and tweezers were used to remove the lens. Then, the retinae were isolated and put in a dissociation solution of papain (16 U/ml), dispase (0.2 U/ml) and DNAse (168 U/ml) in Earle's Balanced Salt Solution (EBSS, Worthington Biochemical Corporation). Up to 6 retinae were put in 1.7 ml of dissociation solution.

Tissue was digested for 30 minutes at 28°C, and then calcein blue (final concentration: 1µM, Invitrogen) was added for 10 minutes at 28°C to stain for living cells. At the end of the enzymatic digestion, mechanical trituration was applied using fire-polished glass pipettes of decreasing diameter to improve retinae dissociation. Cells were centrifuged (300 g) at 4°C, for 6 minutes. The cell pellet was re-suspended in EBSS supplemented with DNAse (100 U/ml) to eliminate residual DNA, and albumin ovomucoid inhibitor (1:10 of stock solution, Worthington Biochemical Corporation) to stop papain action. The single cell solution was finally filtered using 20 µm filters and put on ice, ready for Fluorescent Activated Cell Sorting (FACS). Each single cell suspension was obtained by pooling 8 retinae (from 4 fish, 2 males and 2 females) of uninjured and light-lesioned *Tg(pcna:EGFP);Tg(gfap:nls-mCherry)* animals. Uninjured WT AB, *Tg(gfap:nls-mCherry)* and *Tg(pcna:EGFP)* fish were used to prepare single cell suspensions of dissected retinae for setting the single fluorophore gates in flow cytometry. Additionally, a calcein only stained single cell suspension was prepared from uninjured WT AB fish retinae for the setting of the calcein gate in the flow cytometry.

3.5 Flow cytometry and FACS

Cell sorting was performed with the help of Katja Bernhardt and Erwin Weiss from the CMCB Flow Cytometry facility. A BD FACSAria™ III cell sorter was used for flow cytometry and FACS. mCherry was detected with a 561 nm excitation laser and a 610/20 nm band pass filter, EGFP using with a 488 nm laser and a 530/30 nm band pass filter and calcein blue with a 405 nm laser and a 450/40 nm band pass filter. Forward and side scatters were used to gate cells among all the events in the single cell suspension and to gate singlets among those cells. mCherry-positive only as well as EGFP-positive only gates were set in comparison to the unstained, WT control. Calcein blue positive, single cells were eventually gated as living cells (60.000 living cells from uninjured, 44 hpl and 4 dpl samples, 41.389 living cells from 6 dpl sample). Each sorted sample, containing 15.000 cells, was put on ice and sent to the CMCB Deep Sequencing Facility for single cell RNA sequencing (scRNAseq).

3.6 (Droplet based) single cell RNA sequencing

The whole 10x Genomics single cell RNA sequencing on sorted cells has been performed by Juliane Bläsche from the DRESDEN-concept Genome Center- Technische Universität Dresden- Center for Molecular and Cellular Bioengineering

(CMCB). Andreas Petzold, from the same Center, has been performed pre-processing of the raw sequencing data with CellRanger.

Single cell transcriptome sequencing was performed following the 10x Genomics Single cell transcriptome workflow[152]. 15.000 FACS-sorted cells were recovered in BSA-coated tubes containing 5 ul PBS with 0.04% BSA. Cell samples were carefully mixed with Reverse Transcription Reagent (Chromium Single Cell 3' Library Kit v3) and loaded onto a Chromium Single Cell B Chip to reach a recovery of 10.000 cells per sample. The samples were processed according to the guidelines of the 10x Genomics user manual for single cell 3' RNA-seq v3. Briefly, the droplets were directly subjected to reverse transcription, the emulsion was broken and cDNA was purified using silane beads (Chromium Single Cell 3' Gel Bead Kit v2). After cDNA amplification with 11 cycles, samples were purified with 0.6x volume of SPRI select beads to remove fragments of DNA that were smaller than 400 base pairs. cDNA quality was checked using the Agilent Fragment Analyzer 5200 (NGS Fragment Kit). 10 ul of the resulting cDNA were used to prepare single cell RNA seq libraries - involving fragmentation, dA-Tailing, adapter ligation and 11 cycles of indexing PCR following manufacturer's guidelines. After quantification, both libraries were sequenced on an Illumina NextSeq500 in 75 base pair paired-end mode, generating 45-109 million fragments per transcriptome library. The raw sequencing data was processed with the 'count' command of the Cell Ranger software (v2.1.0) provided by 10X Genomics. To build the reference, the zebrafish genome (GRCz11) as well as gene annotation (Ensembl 90) were downloaded from Ensembl and the annotation was filtered with the 'mkgtf' command of Cell Ranger (options: '—e attribute=gene_biotype:protein_coding --attribute=gene_biotype:lincRNA –attribute=gene_biotype:antisense'). Genome sequence and filtered annotation were then used as input to the 'mkref' command of Cell Ranger to build the appropriate Cell Ranger.

3.7 Bioinformatic analysis

The whole bioinformatic analysis has been done by Dr. Fabian Rost from the DRESDEN-concept Genome Center- Technische Universität Dresden- Center for Molecular and Cellular Bioengineering (CMCB)

The complete software stack for the analysis is available as a Singularity container (https://gitlab.hrz.tu-chemnitz.de/dcgc-bfx/singularity/singularity-single-cell, tag 1f5da0b). The count matrices generated with Cell Ranger were further analysed using

scanpy 1.8.2 (https://genomebiology.biomedcentral.com/articles/10.1186/s13059-017-1382-0). For quality control, cells with less than 2.000 counts, less than 500 detected genes, more than 15% mitochondrial reads or more than 60% of the counts in the top 50 highest expressed genes were removed. Counts were normalised with the size factors computed with calculateSumFactors from scran 1.18.5 (min.mean=0.1)[184]. Normalised counts were log-transformed using the numpy function log1p. The top 4000 highly variable genes were detected using the scanpy function scanpy.pp.highly_variable_genes (n_top_genes=4000). Cell cycle scores were computed using scanpy.tl.score_genes_cell_cycle on each sample separately. As genes associated to S-phase, the *mcm5*, *pcna*, *tyms*, *fen1*, *mcm2*, *mcm4*, *rrm1*, *unga*, *gins2*, *mcm6*, *cdca7a*, *dtl*, *prim1*, *uhrf1*, *si:dkey-185e18.7*, *hells*, *rfc2*, *rpa2*, *nasp*, *rad51ap1*, *gmnn*, *wdr76*, *slbp*, *ccne2*, *ubr7*, *pold3*, *msh2*, *atad2*, *rad51*, *rrm2*, *cdc45*, *cdc6*, *exo1*, *tipin*, *dscc1*, *blm*, *casp8ap2*, *usp1*, *pola1*, *chaf1b*, *brip1* and *e2f8* were used. As genes associated to G2/M phase, the genes *hmgb2a*, *cdk1*, *nusap1*, *ube2c*, *birc5a*, *tpx2*, *top2a*, *ndc80*, *cks2*, *nuf2*, *cks1b*, *mki67*, *tmpoa*, *cenpf*, *tacc3*, *smc4*, *ccnb2*, *ckap2l*, *aurkb*, *bub1*, *kif11*, *anp32e*, *tubb4b*, *gtse1*, *kif20ba*, *si:ch211-69g19.2*, *jpt1a*, *cdc20*, *ttk*, *kif2c*, *rangap1a*, *ncapd2*, *dlgap5*, *si:ch211-244o22.2*, *cdca8*, *ect2*, *kif23*, *hmmr*, *aurka*, *anln*, *lbr*, *ckap5*, *cenpe*, *ctcf*, *nek2*, *g2e3*, *gas2l3*, *cbx5* and *selenoh* were used. Principal component analysis (PCA) was performed on highly variable genes (function scanpy.pp.pca using svd_solver='arpack'). A k-nearest-neighbour (knn) graph was computed using scanpy.pp.neighbors and a UMAP was computed using scanpy.tl.umap. Clustering was performed with scnapy.tl.leiden (resolution= 0.01). For the three resulting clusters, marker genes were computed using scanpy.tl.rank_genes_groups. Two small clusters identified as microglia and low-quality cells were removed from the downstream analysis. Detection of highly variable genes PCA was performed as described above on the remaining cells. A new knn graph (this time with n_neighbors= 50) and a new UMAP were computed. Embedding densities were computed using scanpy.tl.embedding_density. Clustering was performed in multiple steps, always using scanpy.tl.leiden: First, the data were clustered with the resolution parameter set to 0.45. Next, cluster 10 was subclustered with resolution 0.1 and cluster 0 was subclustered with resolution 0.2. Marker genes of the resulting 15 clusters were computed with scanpy.tl.rank_genes_groups. Differential expression analysis of pairs of clusters was performed by subsetting the

data to cells from those two clusters and computing differentially expressed genes with scanpy.tl.rank_genes_groups.

3.8 Cluster annotation

Cluster annotation and biological interpretation of the dataset were done by me

Cluster annotation was performed following several steps. Initially, clusters were annotated by inspection of the top 100 upregulated genes per cluster, the time point at which each cluster appeared and cluster cell cycle profile. Genes were annotated by consulting the ZFIN database (http://zfin.org/) and Pubmed (https://pubmed.ncbi.nlm.nih.gov/) indexed literature about retina development and regeneration. More specifically, lists of marker genes from Hoang et al., 2020 were examined [134] as a reference for cell cluster annotation. After the initial identification of cell clusters, a finer characterization was performed by conduction of differential gene expression analysis for clusters that shared a similar identity. Occasionally (e.g., in the case of horizontal cell precursor marker *ptf1a*), the UMAP profile of known candidates from retina development or regeneration was plotted. Eventually, the expression of selected genes was checked via *in situ* hybridization, fluorescent *in situ* hybridization and immunohistochemistry on retina cryosections.

3.9 4-hydroxytamoxifen injections for Cre-recombination

Uninjured and light-lesioned *TgBAC(mmp9:CreERt2,cryaa:EGFP);Tg(Olactb:loxP-DsRed2-loxP-EGFP)* fish were used for $CreER^{T2}$ recombinase-based lineage tracing. $CreER^{T2}$-mediated recombination was induced by intraperitoneal injections of 10 µl 4-hydroxytamoxifen (4-OHT, Sigma Aldrich) dissolved to a final concentration of 2.5 mM in 10% ethanol/phosphate buffer (Kuscha and Brand, unpublished). 4-OHT was injected either at 6 hpl, 2 hours before *mmp9* is upregulated in the light lesioned retina[125], or at 24 hpl. In parallel, light-lesioned fish were injected with 10 µl 10% ethanol/phosphate buffer either at 6 hpl or at 24 hpl as vehicle controls. Finally, uninjured fish were injected with 2.5 mM 4-OHT in parallel to injected, light-lesioned animals and additional uninjured, untreated fish were used as controls. All the uninjured and light-lesioned animals were eventually processed at 4 dpl for cryosectioning and immunohistochemistry.

3.10 Tissue preparation and cutting

Fish heads were fixed with 4% paraformaldehyde in 0.1 M phosphate buffer (PB, pH: 7.4) overnight, at 4°C. Subsequently, fixed heads where decalcified and cryoprotected in 20% EDTA and 20% sucrose in 0.1M PB (pH: 7.5) overnight, at 4°C. Heads were eventually embedded in 7.5% gelatin, 20% sucrose in 0.1M PB and sectioned (12 or 14 μm) at the cryostat.

3.11 Synthesis of probes for *in situ* hybridization

Retinae harvested at 4 dpl (when selected transcripts were highly enriched) were dissected and sonicated at 4°C to extract total RNA. RNA extraction was performed with the total RNA purification kit and following manufacturer's instructions (Norgen Biotek Corporation). cDNA transcription was done using the first strand cDNA synthesis kit (Roche), followed by PCR to amplify fragments of interest by using the primer pairs listed in the "Materials" section. The resulting amplicon was purified using the gel and DNA recovery kit (Zymo Research) and cloned in a TOPO TA® vector (Thermo Fisher). E coli bacteria were transformed with the vector and cultured overnight at 37°C. On the next day, colonies were further cultured in LB medium supplemented with 1:2000 ampicillin overnight at 37°C, shaking. Mini-prep (Gene Jet Plasmid Miniprep kit k0503, Thermo Fisher) was subsequently applied to the cultures for DNA extraction. Purified plasmids were sent for sequencing (Eurofins) to check the insert sequence. Insert-positive colonies were further enriched in LB/ampicillin cultures for midi-prep (Nucleo Bond® Xtra Midi, Macherey – Nagel) and purified plasmids were linearized to transcribe anti-sense, digoxigenin labelled (DIG) RNA probes. Probes were stored at -20°C. Probes for *crlf1a*, *hmgb2b*, *onecut1*, *onecut2* were transcribed from a TOPO TA® cloned insert. Instead, the *id1* probe was transcribed directly from the PCR – amplified cDNA using SP6-conjugated forward and T7-conjugated reverse primers.

3.12 *in situ* hybridization

in situ hybridization and fluorescent *in situ* hybridization were performed on 3 fish per lesioned time point and on 3 uninjured controls in parallel. Cryosections were dried for 30 minutes at room temperature, then permeabilized by washing two times for 10 minutes in phosphate buffer saline supplemented with 0.3% Triton X-100 (PBSTx). Probes for *in situ* hybridization were denatured by heating up at 70°C for 10 minutes and vortexing. Sections were incubated overnight in denatured probes in a water bath at 62°C. The day after, sections were rinsed three times (once for 15 minutes, followed

by two washes of 30 minutes each) in washing buffer (“Materials”) at 62°C. Then, in the chromogenic *in situ* hybridization, sections were washed twice in MABT (“Materials”) for 30 minutes each and incubated with 2% digoxigenin blocking reagent (“Materials”) in MABT for 1 hour at room temperature. In the case of fluorescent *in situ* hybridization, sections were washed in TNT buffer (“Materials”), and afterwards incubated with 2% digoxigenin blocking reagent in TNT buffer. Then, sections were incubated with the AP-conjugated, anti-digoxigenin antibody (chromogenic *in situ* hybridization, 1:2000) or with the POD-conjugated, anti-digoxigenin antibody (fluorescent *in situ* hybridization, 1:2000) overnight, at 4°C. The next day, sections were washed four times for 20 minutes each in MABT (chromogenic *in situ* hybridization) or three times for 10 minutes each in TNT buffer (fluorescent *in situ* hybridization) at room temperature. Afterwards, sections for chromogenic *in situ* hybridization were washed for 5 minutes in staining buffer (“Materials”) and finally incubated with 20 µl/ml NBT/BCIP stock solution diluted in the staining buffer, at room temperature, to develop the chromogenic reaction. Time of incubation varied between three hours and overnight, depending on the target mRNA and probe concentration. In the case of fluorescent *in situ* hybridization, after TNT washes, sections were incubated for 30 minutes with 1:200 Cy3-Tyramide in TSA amplification buffer (Akoya Biosciences®), at room temperature. Finally, sections from chromogenic *in situ* hybridization were washed three times with PBS, for 10 minutes each. Sections were mounted in 70% glycerol in PBS, ready for bright field microscopy. Fluorescent *in situ* hybridization sections were rinsed three times in PBS, for 10 minutes each, and afterwards, incubation with primary antibody for immunohistochemistry was performed as described below.

3.13 Immunohistochemistry

Immunohistochemistry was perfomed as previously described in my lab[2,3]. Sections were dried at room temperature for 30 minutes and washed 3 times in PBSTx for 10 minutes. Primary antibodies, diluted in PBSTx, were applied overnight at 4°C (refer to “Materials” for detailed use of primary antibodies). For the retrieval of proliferating cell nuclear antigen (PCNA), sections were immersed in 10 mM sodium citrate (pH: 6) for 6 minutes at a temperature higher than 80°C. Subsequently, they were washed, and the anti-PCNA antibody was applied. After primary antibody incubation, sections were rinsed three times in PBSTx for 10 minutes, then Alexa® fluorophore conjugated, secondary antibodies in PBSTx were applied for 2 hours at room temperature (refer to

“Materials” for detailed use of secondary antibodies). Sections were washed three times in PBS, and then DAPI (4′,6-Diamidino-2-phenyl-indol-dihydrochlorid) was applied to counterstain nuclei. Sections were finally mounted in 70% glycerol in PBS, and stored at 4°C. Each staining used to validate scRNAseq results was performed on 3 animals per time point upon injury and on 3 uninjured fish controls in parallel. The number of animals used for immunohistochemistry on retinal sections cut from the *TgBAC(mmp9:CreERt2,cryaa:EGFP);Tg(Olactb:loxP-DsRed2-loxP-EGFP)* line is indicated in the correspondent figure captions.

3.14 Microscopy

Bright field images of *in situ* hybridizations and pictures in Figure 8 were acquired with the Widefield ApoTome microscope (Zeiss Axio Imager.Z1) using the 20x/0.8 Plan-Apochromat, Air, DIC objective. Images in Figure 7, Figure 15 and 17 were acquired with the laser scanning confocal microscope 780 (Zeiss Axio Imager.Z1) using the 40x/1.2 C-Apochromat, Water, DIC, Zeiss (Figures 7 and 15) and the 20x/0.8 Plan-Apochromat, Air, DIC, Zeiss (Figure 17), respectively. The same confocal microscope, with the correspondent 40x objective, was used to acquire images of the $CreER^{T2}$ recombinase-based immunohistochemistry (Figure 24). In order to minimize crosstalk in multicolour specimens, acquisition of the diverse fluorescent channels was sequential.

3.15 Image acquisition and processing

The Zeiss ZEN blue V 2012 software was used to process images acquired in bright field. The extended depth of focus function (contrast method) was applied to raw, bright field images to project the chromogenic signal of the optical stack to a single plane. Fiji[185] software was used for the processing of fluorescent images, including contrast adjustments, image crop and rotation. Figure panels were assembled using the software Adobe Illustrator CC 2015.3. The plot in Figure 22 was obtained using Microsoft Excel 2016.

3.16 Statistics

Marker genes were ranked by their test statistic computed with a t-test for each gene, comparing cells within the cluster to the cells outside the cluster, as implemented by the scanpy function tl.rank_genes_groups. The same was done for the identification of differentially expressed genes between pairs of clusters.

3.17 Data availability

All the sequencing data supporting the results of this study have been deposited at https://singlecell.broadinstitute.org/single_cell/reviewer_access/5a29ec20-d572-4461-bfd3-cb8973c05f33 and are accessible through BioProject ID SCP1973.

4. RESULTS

PART I

4.1 Isolation of individual MG, RPCs and regenerated progeny using fluorescent reporters

Previous studies of retina regeneration in zebrafish have largely addressed MG reprogramming and RPCs production[106,108,123,126,130,135–137,141]. Instead, the molecular identity and cell fate choices of RPCs have been less investigated, and mostly at a population level[126,133,134,138,143,144,186–188]. Here, the transcriptome of MG and MG-derived RPCs was sequenced and their differentiation trajectories towards regenerated retinal neurons were analyzed at a single cell level. To this aim, a strategy to isolate and enrich for individual MG, RPCs and regenerated progeny was devised using retinae of uninjured and light-lesioned zebrafish transgenic line carrying the two fluorescent reporters *pcna*:EGFP and *gfap*:mCherry. EGFP expression occurs under the regulatory elements of proliferating cell nuclear antigen (*pcna*), a known marker of proliferation, and was used to label actively dividing cells and their short-term progeny thanks to the persistence of EGFP. Conversely, mCherry is under the regulatory elements of glial fibrillary acidic protein (*gfap*), a known marker of zebrafish MG. Both transgenes recapitulate the endogenous gene expression in the adult retina (Figure 7). Immunohistochemistry against PCNA co-labeled *pcna*:EGFP-positive cells mainly in the ciliary marginal zone, one of the stem cells niches in the adult zebrafish retina[95,101]. Occasional *pcna*:EGFP/PCNA-double positive cells were also detected in the central retina (Figure 7A). The Zrf1 antibody, which stains selectively for zebrafish MG, labeled virtually all *gfap*:mCherry-positive cells in the central retina as well as the ciliary marginal zone[95] (Figure 7B). The expression of the two fluorescent reporters EGFP and mCherry was addressed at three different time points in the light-lesioned retina. First, 44 hours post light lesion (hpl) that is 2 hours after MG are about to complete or have completed their asymmetric cell division that generates the first Müller glia-derived RPCs[137]. Second, 4 days post light lesion (dpl), which is the peak of RPC proliferation[95,108] and third, 6 dpl, when the first regenerated cone photoreceptors arise[95].

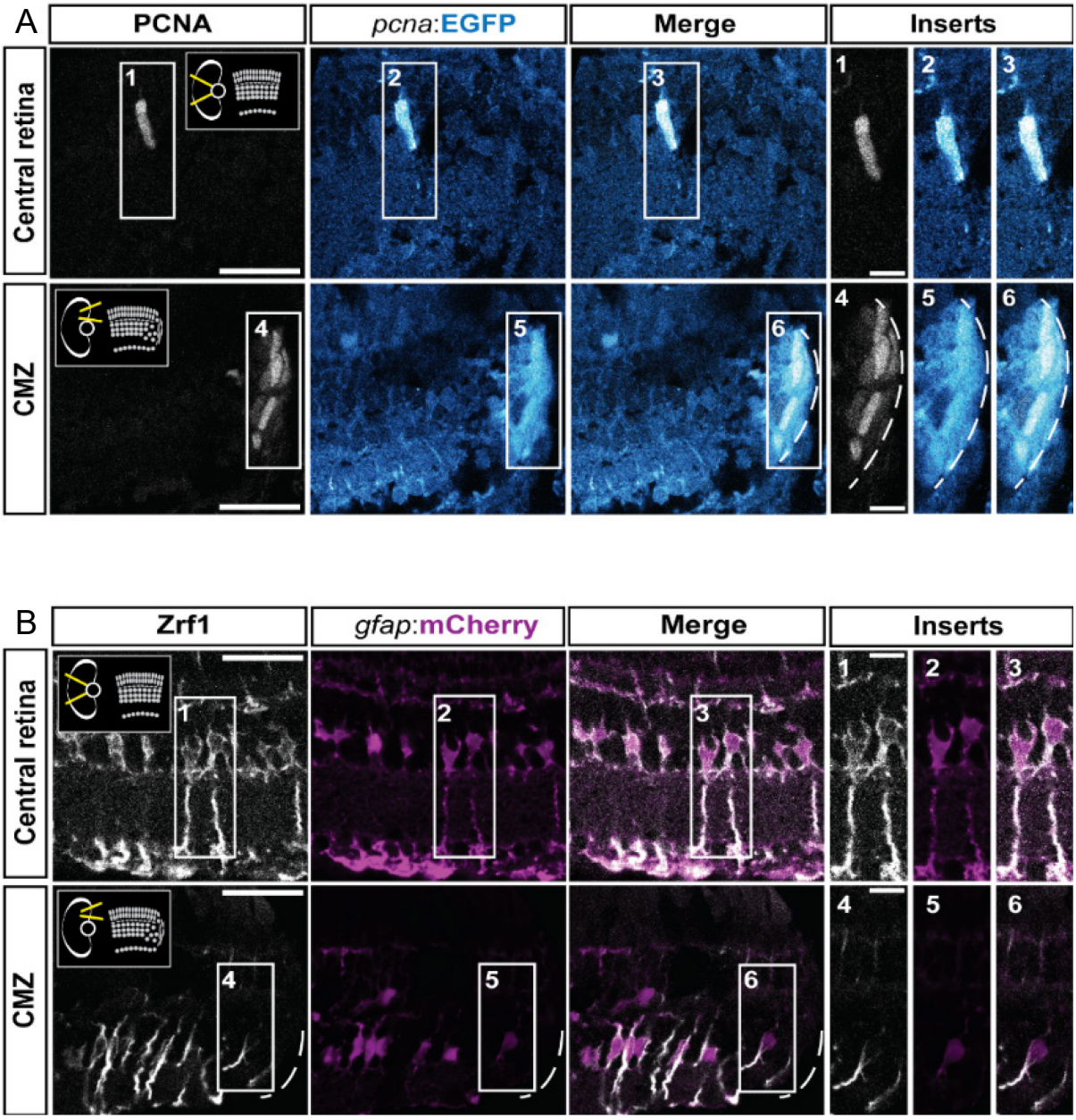

Figure 7. Characterization of the fluorescent reporter lines *Tg(pcna:EGFP)* and *Tg(gfap:mCherry)* in double transgenic animals. A. Confocal images of immunohistochemistry for the proliferation marker PCNA (grey) and EGFP (blue) on retinal sections of *Tg(pcna:EGFP);Tg(gfap:mCherry)* fish (N= 3 animals). Schemes in the thumbnails on the top-right and top-left of the PCNA panels indicate the region of interest, either the central retina or the ciliary marginal zone (CMZ). **B.** Confocal images of immunohistochemistry detecting Zrf1-positive MG (magenta) and mCherry on retinal sections of *Tg(pcna:EGFP);Tg(gfap:mCherry)* fish (N= 3 animals). Scale bar: 30 µm for main panels, 10 µm for inserts.

Immunohistochemistry against EGFP and mCherry in double transgenic *Tg(pcna:EGFP);Tg(gfap:mCherry)* animals corroborated the expression of the transgenes in the central retina at the indicated time points (Figure 8).

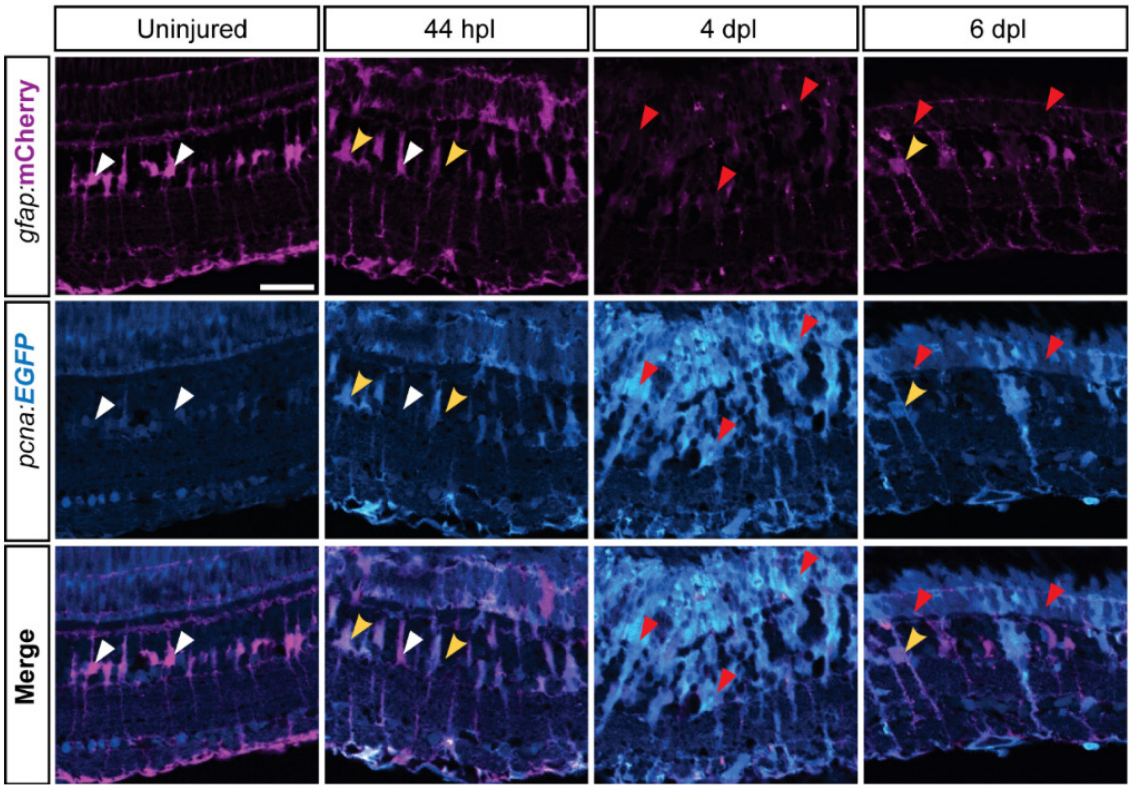

Figure 8. Expression of *Tg(pcna:EGFP);Tg(gfap:mCherry)* in the regenerating retina. Apotome images show endogenous immunofluorescence of EGFP and mCherry driven by *Tg(pcna:EGFP)* and *Tg(gfap:mCherry)*, respectively, on retinal sections collected in uninjured as well as lesioned conditions. White arrowheads indicate mCherry-positive, EGFP-negative MG. Yellow arrowheads indicate mCherry-/EGFP-double positive MG. Red arrowheads indicate low-mCherry-/EGFP-double positive, putative RPCs. N= 3 animals. Scale bar: 30 µm.

In the uninjured, central retinae EGFP signal was undetectable, while strong mCherry expression was observed, consistent with expression in homeostatic, non-proliferating MG (white arrowheads). Instead, numerous EGFP/mCherry double-positive cells arose at 44 hpl, which presumably stained reactive, proliferating MG (yellow arrowheads). At 4 dpl, overall mCherry expression was significantly reduced, in agreement with the described downregulation of the *gfap* promoter, whereas EGFP was strongly found throughout the retinal layers, matching the reported peak in proliferation of MG-derived RPCs (red arrowheads)[95,108,113,136]. Finally, at 6 dpl, mCherry expression increased again, while EGFP signal became less prominent.

The persistence of the intrinsic fluorescence of EGFP and mCherry reporters during retina regeneration was exploited to isolate MG, MG-derived RPCs and regenerated progeny at a single cell level. Accordingly, only MG express mCherry in uninjured, central retinae, but activate EGFP expression during the asymmetric cell division that occurs upon light lesion at 44 hpl (Figure 9A). Early MG-derived RPCs inherit the mCherry protein from dividing MG and slowly degrade/dilute the reporter in subsequent proliferations. Hence, MG-derived RPCs are identified as EGFP-positive, but *low* mCherry-positive at 4 dpl. At 6 dpl, RPCs start migrating to the other retinal layers and have further diluted the mCherry reporter, thus show a weaker mCherry fluorescence, but retain EGFP expression, since their last cell divisions are still ongoing. Similarly, RPC-derived, regenerated neurons show even lower levels of mCherry fluorescence, and low EGFP signal during subsequent cell differentiation at 6 dpl. Retinae of uninjured and light-lesioned samples were dissected in agreement with this rationale, and dissociated to single cell suspensions followed by FACS and droplet-based, 10x Genomics scRNAseq (Figure 9B). Flow cytometry confirmed the logic underlying the described sorting strategy (Figure 9C). All samples contained non-fluorescent and EGFP-positive only cells, in agreeement with the fact that non-proliferating and proliferating cells populate the adult zebrafish retina.

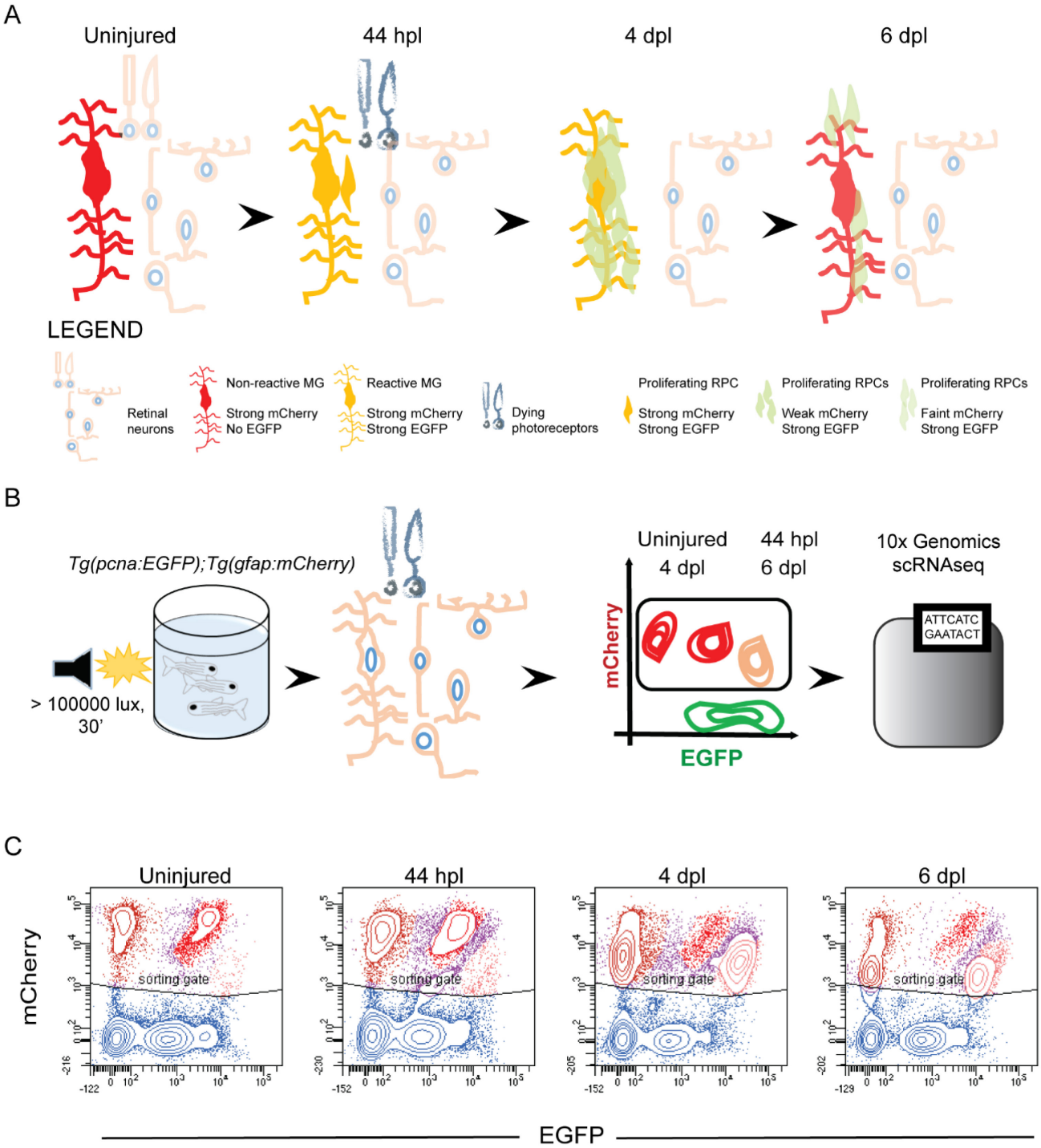

Figure 9. Use of fluorescent reporters for single cell isolation of MG, RPCs and regenerated progeny. A. Schematic illustration of the logic used to isolate individual cells from regenerating retinae of double transgenic *Tg(pcna:EGFP);Tg(gfap:mCherry)* fish. In the uninjured retina, MG show high levels of mCherry, but absence of EGFP. Upon light lesion, which results in dying rod and cone photoreceptors, mCherry-positive MG turn on also EGFP at 44 hours post lesion (hpl). At 4 days post lesion (dpl), MG still express strong mCherry and EGFP levels. Instead, proliferating RPCs show weak mCherry, but strong EGFP fluorescence. Finally, MG have lost the EGFP signal at 6 dpl, and express mCherry only. RPCs, which start migrating and differentiating, have further diluted mCherry and EGFP. **B.** Illustration of the workflow for the scRNAseq experiment. Uninjured and light-lesioned retinae (44 hpl, 4 dpl, 6 dpl) of *Tg(pcna:EGFP);Tg(gfap:mCherry)* fish were dissociated to a single cell suspension. Following fluorescent activated cell sorting **of mCherry-positive only and EGFP/mCherry-double positive** cells, droplet-based, 10x Genomics scRNAseq was applied to single cells. **C.** Flow cytometry plots depicting EGFP and

mCherry fluorescence recorded from retinal cells dissociated at the indicated time points. **Cells in the sorting gate include mCherry-positive only as well as mCherry/EGFP-double positive cells**. Number of sorted cells: 15.000 resulting from the pooling of 8 retinae from 4 (2 males and 2 females) fish.

Moreover, mCherry only-positive cell populations were present at all sampled time points, likely corresponding to non-reactive MG found in *homeostatic* (that is, uninjured) conditions. In addition to cells expressing only either EGFP or mCherry, EGFP/mCherry-double positive cells were detected in all samples, including the uninjured one, consistently with proliferating MG that is evident in the homeostatic central retina (see Figure 7A). The EGFP/mCherry-double positive population increased at 44 hpl, presumably including reactive, that is reprogrammed and de-differentiated (see above) MG cells. At 4 dpl, the expanded EGFP/mCherry-double positive cell population was still present, but displayed a lower mCherry fluorescence, and increased EGFP fluorescence, in agreement with the appearance of MG-derived RPCs that peak in prolifeartion at this time point[95,108]. At 6 dpl, the EGFP/mCherry-double positive cell population displayed a further decreased mCherry intensity. In order to profile the transcriptome of individual MG, RPCs and progeny of the uninjured and light-lesioned retinae, retinal samples were prepared at the before-mentioned time points (uninjured, 44 hpl, 4 dpl, 6 dpl) and eventually 15.000 cells per time point were sorted. A sorting gate that included both mCherry-positive only and EGFP/mCherry-double positive cells was applied at the sampled time points (Figure 9C). Non-fluorescent as well as EGFP-positive only cells were not sorted. To summarize, the devised short-term lineage tracing strategy allows the isolation of individual MG and MG-derived cells of the regenerating zebrafish retina. Subsequently, sorted cells can be subjected to droplet-based,10x Genomics scRNAseq.

4.2 15 different cell clusters were annotated by scRNAseq in the light-lesioned retina

10x Genomics scRNAseq was employed to sequence the transcriptome of the sorted cells. 13.139 cells passed the sequencing quality control, and a median of 1.407 genes and 4.061 mean read counts per cell was detected. Initially, three clusters for the entire dataset were annotated (Figure 10). Indeed, a core dataset, containing MG, RPCs and retinal neurons, and two additional clusters that represented microglia and low-quality cells were annotated (Figure 10A, B). Both microglia and low-quality cell populations were excluded from the subsequent analysis.

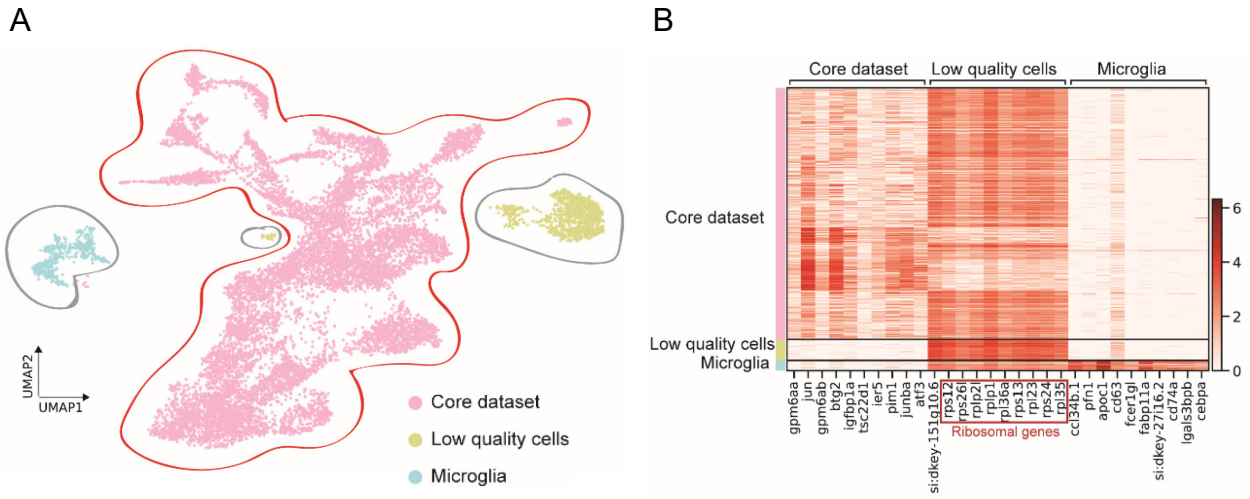

Figure 10. **Original scRNAseq dataset. A.** UMAP of the original scRNAseq dataset, which contained a core retinal cluster (circled in red) and two clusters annotated as microglia and low-quality cells (circled in grey). **B.** Heat map showing the expression of the top 10 marker genes per cluster of the original dataset. Number of cells in the original dataset: 13.139.

The core dataset was re-clustered and eventually included 11.690 cells belonging to fifteen annotated, different cell populations (Figure 11A). From left to right on the UMAP the **progressive emergence** of clusters of MG, MG-derived RPCs and regenerated progeny was observed. Cell population identity was assigned by inspection of the top 100, upregulated marker genes per cluster (Appendix 1). In particular, four clusters of MG (clusters 1 to 4), which located to the left and middle portion of the map, and five RPC clusters (clusters 5 to 9), positioned on the right side of the map, were identified. Regenerated progeny branched from the RPCs and included retinal ganglion (cluster 10), amacrine (cluster 13) and bipolar cells (cluster 15) at the bottom-right, as well as red and blue cones (clusters 11 and 12) at the top-right of the map. Additionally, a second cluster of amacrine cells (cluster 14) separated from the first amacrine cell cluster. To investigate how the composition of cells changed during the sampled time course of regeneration, computation of embedding densities plots was conducted for each time point (Figure 11B).

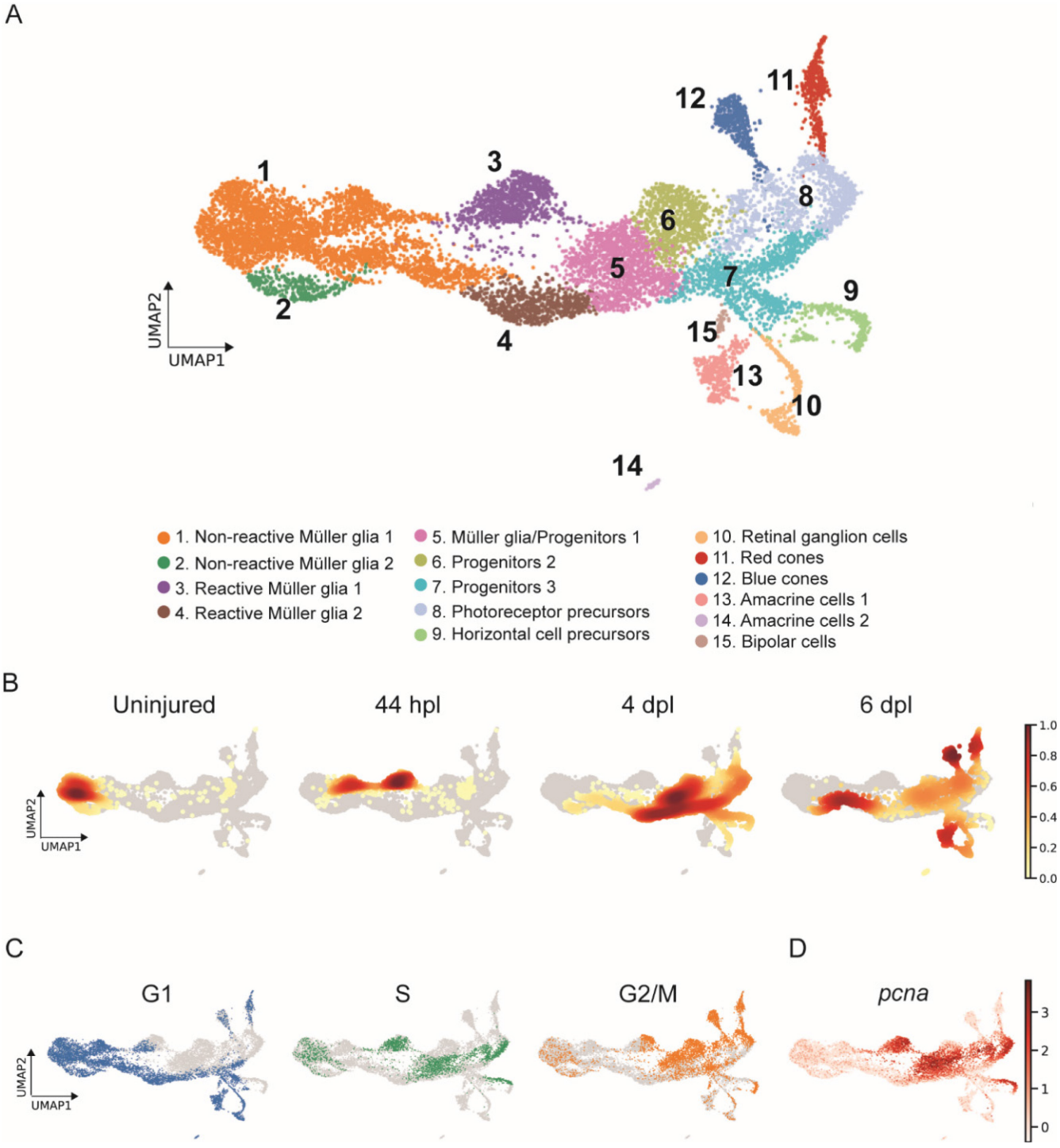

Figure 11. scRNAseq identifies 15 different cell populations in the light-lesioned retina. A. Core dataset depicted on the uniform manifold approximation and projection (UMAP) map. Notice the *progressive* emergence of MG, RPCs and progeny clusters from left to right. Cluster identity is indicated in the figure legend. **B.** Normalized cell densities on the UMAP for the 4 different samples (uninjured, 44 hpl, 4 and 6 dpl). Dark red shows strong cell enrichment and no color shows absence of cells. **C.** Cells colored by cell cycle phases G1, S, and G2/M phase in blue, green and orange, respectively. **D.** Expression profile of *pcna* (proliferation marker). Legend: logarithm of normalized counts per million. Number of cells in the core dataset: 11.690.

Cells progressed over time from left to right, from the uninjured, to the 44 hpl, the 4 dpl, as well as the 6 dpl samples, paralleling the progression described for cellular identities. Cells belonging to non-reactive MG were found in uninjured as well as lesioned conditions, as expected by the lesion paradigm, which mainly affects the central/dorsal retina and spares the ventral retina[121]. The vast majority of cells of the uninjured sample belonged to cluster 1 as well as cluster 2. However, a small proportion of cells (Figure 11B), aligning in a trajectory from non-reactive MG (left side of the map) through reactive MG (middle part) to RPCs and differentiating progeny (right side), was observed in the uninjured sample. At 44 hpl, cells mapping to non-reactive MG were still observed, although mostly shifted to the right and towards a cluster that represented reactive MG (cluster 3). In contrast, cells mapping to the second cluster of reactive MG (cluster 4) as well as to RPCs (clusters 5-9) were overrepresented at 4 dpl, in line with the reported peak in proliferation at this time point [95,108]. Cells mapping to RPCs were still enriched at 6 dpl. Moreover, cells belonging to regenerated progeny (clusters 10-15), which first appear at 4 dpl, became predominantly enriched at 6 dpl. In addition to the overall progression from left to right, it was observed that cells mapping to reactive MG of the second cluster (cluster 4) and the abutting portion of non-reactive MG (cluster 1) were enriched again at this time point, suggesting a reversed direction of the cell density.

Analysis of the cell cycle state of the identified clusters was performed to further support their annotation. Known cell cycle marker genes (see “Methods”) were used to compute the predicted cell cycle state[189–191], and the correspondent cell cycle phase (G1, S, G2/M) was projected onto the UMAP of the single cell transcriptome (Figure 11C). Differentiating as well as differentiated cells were considered as belonging to the G1 phase[192]. Consistently, most cells of the left side and lower middle part, as well as cells branching from the right side of the map, were in G1, and corresponded to non-reactive MG (clusters 1 and 2), one cluster of reactive MG (cluster 4), one RPC population (cluster 7) and the regenerated progeny (clusters 10-15). Few cells in S phase were also present on the left side of the map, which included non-reactive MG (clusters 1 and 2). However, they were in particular enriched in two domains of the middle part corresponding to reactive MG (cluster 3) and RPCs (clusters 5 and 7). Moreover, two domains on the right side of the map, which include photoreceptor and horizontal cell precursors (clusters 8 and 9), showed an accumulation of cells in S phase. The pattern of cells in G2/M phase complemented the pattern of cells in G1 and

S phase. The pattern of cell proliferation was further confirmed by inspecting *pcna* expression (Figure 11D). Indeed, UMAP profile of *pcna* showed high counts in one population of reactive MG (cluster 3) and in RPCs (clusters 5, 6, 8 and 9) (Figure 11D). In summary, scRNAseq analysis enabled the establishment of a transcriptome map of the regenerating retina, which reveals the progressive emergence of non-reactive MG, reactive MG, MG-derived progenitors and regenerated progeny.

4.3 scRNAseq identifies two populations of non-reactive and two of reactive MG in the light-lesioned retina

MG in the uninjured zebrafish retina express GFAP, as well as other glial markers, like *apoeb*, *glula*, *cahz*, *rlbp1a*[101,106,107,136,193,194]. In the current scRNAseq dataset, *apoeb*, *glula*, *cahz*, *rlbp1a* upregulated as marker genes for clusters 1 and 2 (Figure 12 and Appendix 1).

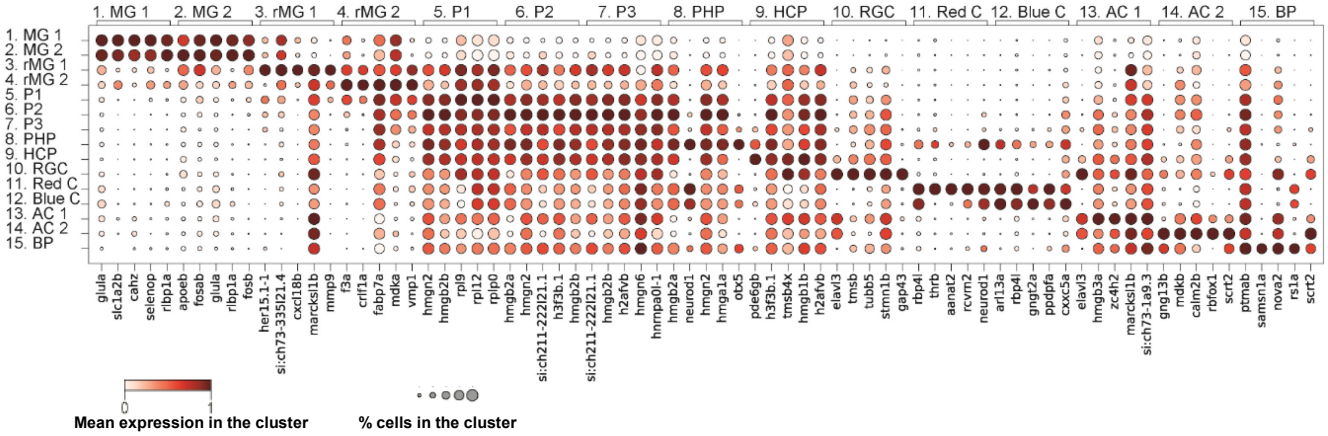

Figure 12. . Dot plot depicting the expression of top 5 marker genes per cluster (see Figure 11A). Dot size scales with a fraction of cells in the cluster expressing the gene (from left to right: 20, 40, 60, 80, 100%), and the dot colour indicates the scaled mean gene expression in the cluster. MG: non-reactive Müller glia; rMG: reactive Müller glia; P1: Müller glia/progenitors 1; P2: progenitors 2; P3: progenitors 3; PHP: photoreceptors precursors; HCP: horizontal cell precursors; RGC: retinal ganglion cells; AC: amacrine cells; BP: bipolar cells. Marker genes per cluster have been calculated using a t-test that compared cells in a cluster versus cells in all the rest of the clusters.

Expression of *apoeb* was plotted on the UMAP and high gene counts were observed in clusters 1 and 2, as well as in clusters 3 and 4, whereas sparse counts were observed in cluster 5 too (Figure 13A). The zebrafish glial marker *gfap* showed a similar pattern, with high counts in clusters 1 to 4, but also high counts in cluster 5 (Figure 13A). Due to the expression pattern of *apoeb* and *gfap*, clusters 1 to 4 were annotated as MG populations. Further analysis indicated clusters 1 and 2 as non-reactive MG (Figure 13B). Indeed, cells belonging to cluster 1 and 2 were mostly in G1 (Figure 11C)

and did not express any injury-specific markers (Figure 12). Next, differentially expressed genes (DEG) between the non-reactive MG clusters 1 and 2 were analysed (Appendix 2). Counts for *mstnb*, which is a ligand of the activin receptor 2[195], were enriched in cluster 1 and 2, with higher expression in cluster 2 (Figure 13B, C). Moreover, the UMAP plot of *inhbaa*, an additional ligand of the activin receptor 2[195], as well as an evolutionarily conserved vertebrate glia marker[134], showed strong transcript expression only in cluster 1, as well as in cluster 3 and 4, but not in cluster 2 (Figure 13B, C). Finally, members of the retinoic acid signalling pathway, like *rdh10a*, *aldh1a3*, *dhrs3a* were enriched mainly in cluster 2[196–198]. (Figure 13C).

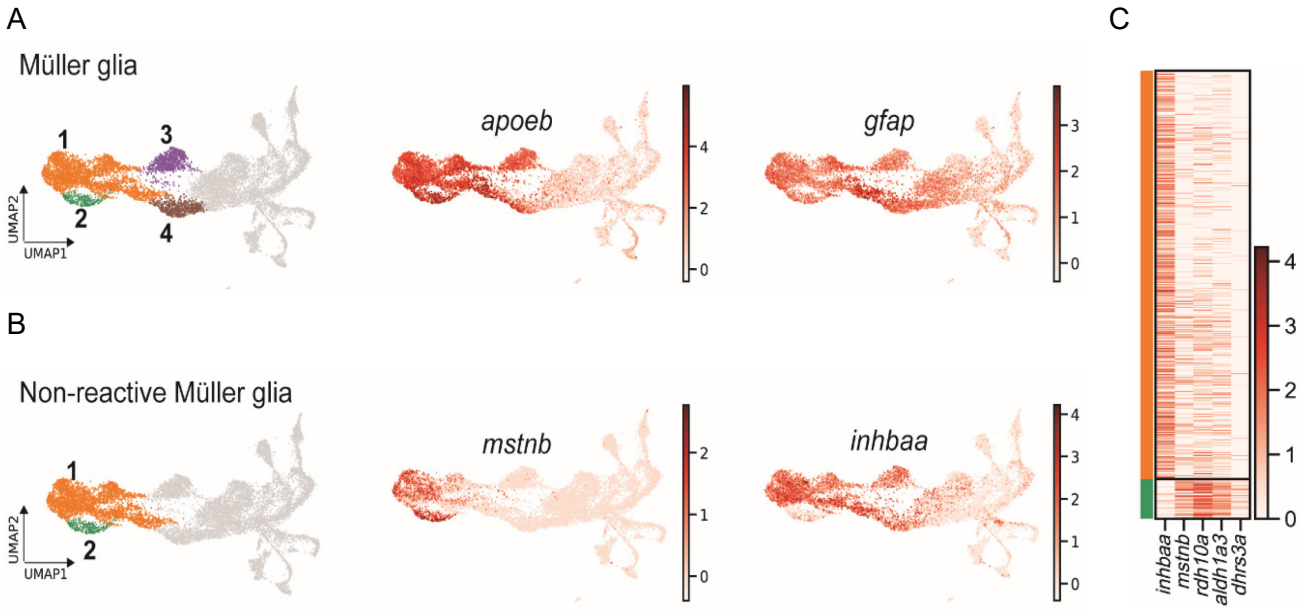

Figure 13. scRNAseq identifies two populations of non-reactive Müller glia in the light-lesioned retina. A. Four Müller glia clusters (cluster 1-4) and expression of *apoeb* and *gfap*. **B.** The two non-reactive Müller glia clusters (cluster 1 and 2) and expression of *mstnb* and *inhbaa*. Cells of both clusters express *mstnb*, but only cells in cluster 1 expresses *inhbaa*. **C.** Heat-map showing differentially expressed genes between the two non-reactive MG clusters 1 (orange) and 2 (green). Note the complementary expression of *inhbaa* and *mstnb* in cluster 1 and 2, respectively, and the enrichment of retinoic acid signalling genes in cluster 2. Differentially expressed gene analysis has been computed using a t-test between cells in cluster 1 (n= 3519) and cells in cluster 2 (n= 343).

Marker gene analysis of MG clusters 3 and 4 revealed that they corresponded to MG that became reactive to the lesion by de-differentiation and upregulation of inflammation-associated markers[6]. Indeed, cells in these clusters downregulated some glial genes, like *glula* and *rlbp1a*, and upregulated inflammatory cytokines, like *crlf1a*[128], matrix metalloproteases, like *mmp9*[125], and growth factors like *hbegfa*[127] in the regenerating retina (Figure 12, Appendix 1). Consistent with that, plotting of *crlf1a* expression onto the UMAP showed high read counts in clusters 3 and 4, as well as in cluster 5 (Figure 14A). Intriguingly, DEG analysis between cluster 3 and 4 showed that cells in cluster 3, but not cells in cluster 4, upregulated *ascl1a*, which is an early marker of MG reprogramming[130,132,140], as well as hairy-related downstream targets of active Notch signalling including *her15.1-1*, *her9* and *her4.1* (Appendix 3 and Figure 14A). Accordingly, UMAP of *ascl1a* expression showed strong enrichment in cluster 3 and fewer transcript counts in the neighbouring cluster 5. Sparse *ascl1a* expression was observed in few cells belonging to cluster 1 of non-reactive MG (Figure 14A). The UMAP plot of *her4.1* showed high gene counts in cluster 3 as well as in cluster 5 (Figure 14A).

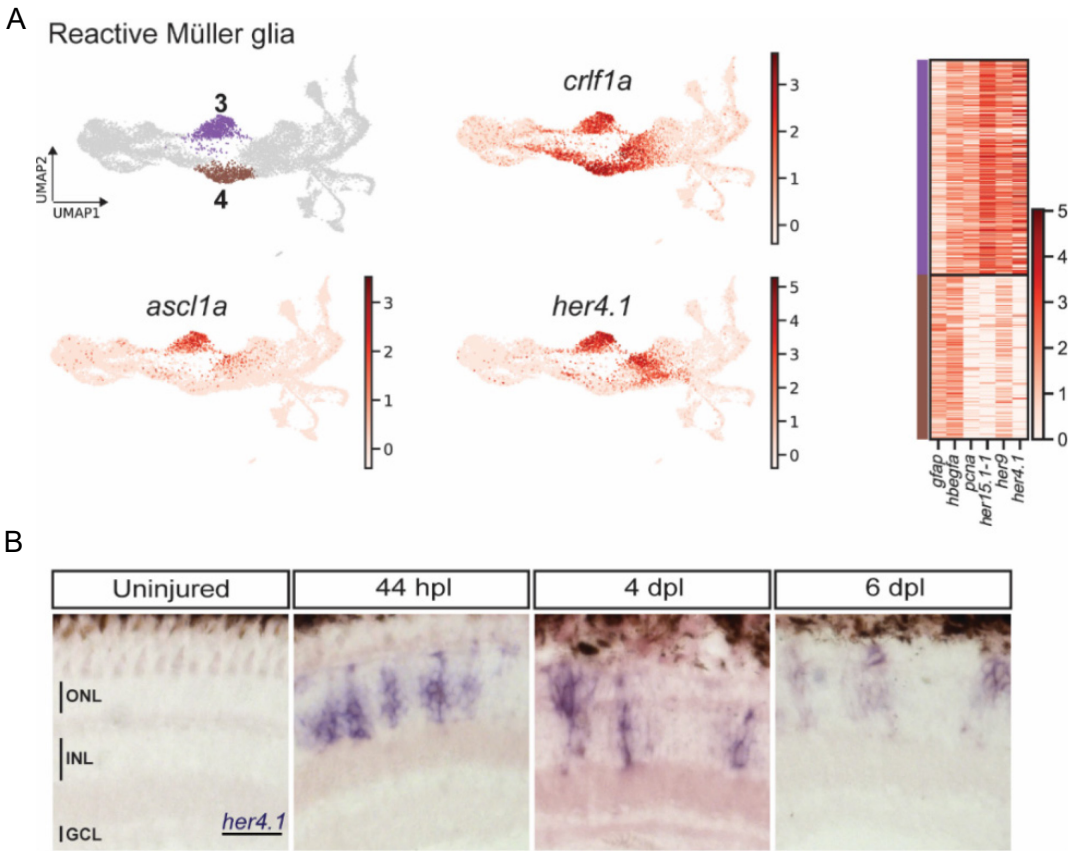

Figure 14. scRNAseq identifies two populations of reactive Müller glia in the light-lesioned retina. A. Left: Visualization of the two reactive Müller glia clusters (cluster 3 and 4) and the relative expression levels of *crlf1a*,

ascl1a and *her4.1* projected onto the main transcriptional UMAP. Cells of both clusters express *crlf1a*, but only cells in cluster 3 express *ascl1a* and *her4.1*. Right: heat-map showing shared marker genes (*gfap*, *hbegfa*) and differentially expressed genes (*pcna*, *her15.1-1*, *her9*, *her4.1*) between cluster 3 (violet) and cluster 4 (brown). Note that cluster 4 has very low counts of *pcna* and hairy-related genes. **B.** Bright field microscopy images of chromogenic *in situ* hybridization detecting *her4.1* on retinal sections of uninjured control animals and at 44 hours post lesion (hpl), 4 days post lesion (dpl) and 6 dpl (N= 3 animals per condition). The position of the outer nuclear layer (ONL), inner nuclear layer (INL) and ganglion cell layer (GCL) is indicated in the uninjured sample. Scale bar: 30 µm. Differentially expressed gene analysis has been computed using a t-test between cells in cluster 3 (n= 913) and cells in cluster 4 (n= 697).

In situ hybridization was used to validate *her4.1* expression in the regenerating tissue. In agreement with the scRNAseq dataset, *her4.1* signal was not present in the uninjured retina, but was upregulated at 44 hpl in the inner nuclear layer of the central retina (Figure 14B). At 4 and 6 dpl, *her4.1* expression remained in the inner nuclear layer and was expressed by cells positioned in the outer nuclear layer too (Figure 14B). Further expression analysis of *crlf1a*, a marker of reactive MG, was done using fluorescent *in situ* hybridization combined with immunohistochemistry against GFAP and the proliferation marker PCNA (Figure 15). As expected from its scRNAseq profile, *crlf1a* in the uninjured, central retina, could not be detected, but the signal was upregulated in Zrf1/PCNA-double positive cells at 44 hpl (Figure 15A, B). At 4 dpl, *crlf1a* signal was still present in Zrf1/PCNA-double positive cells and returned back to undetectable levels at 6 dpl (Figure 15). Taken together, cellular heterogeneity of MG during regeneration was detected, and included two non-reactive and two reactive MG populations that express distinct marker genes.

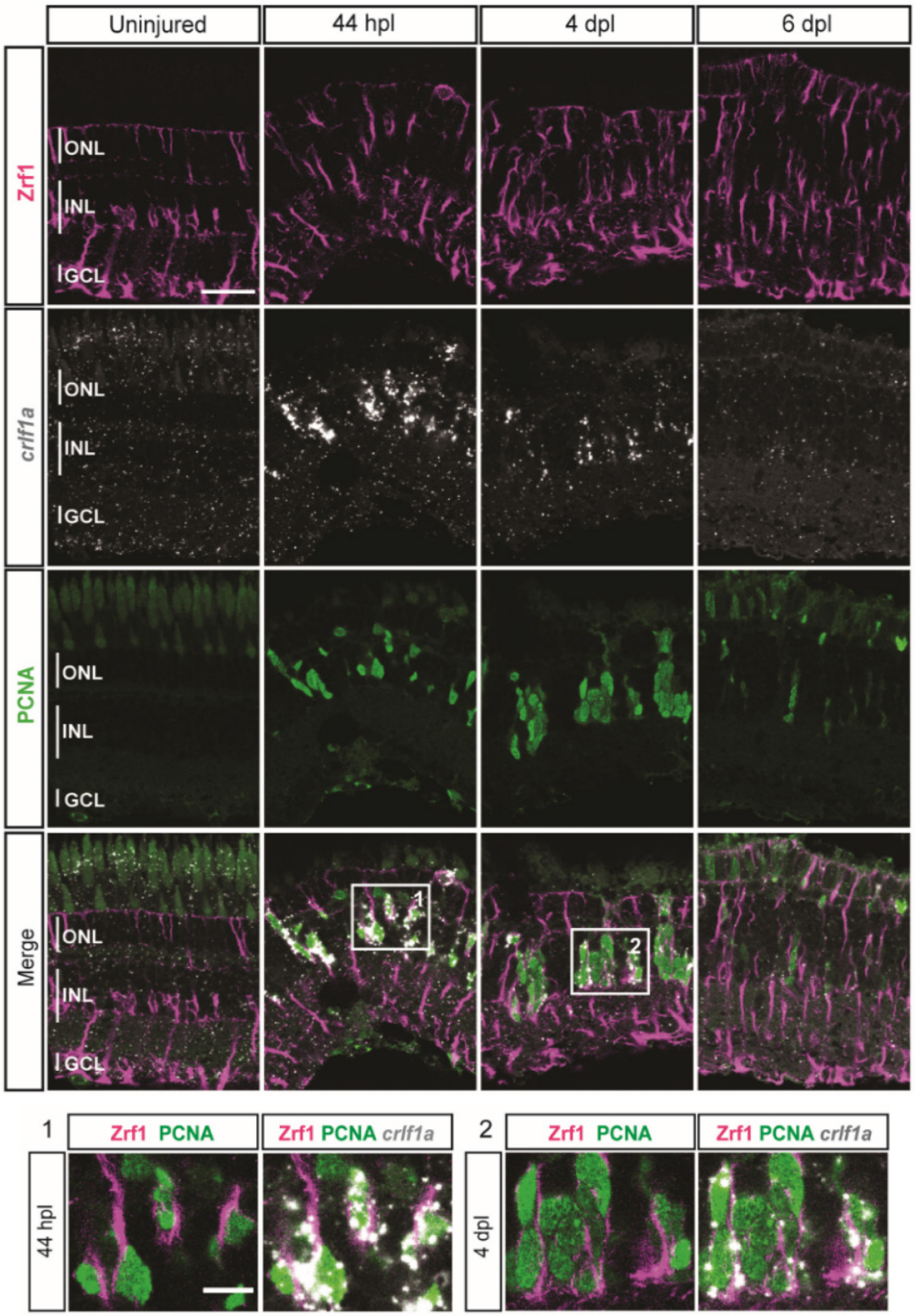

Figure 15. Expression profile of *crlf1a* during retina regeneration. Confocal images of fluorescent *in situ* hybridization for *crlf1a* (grey) and immunohistochemistry detecting Zrf1-positive MG fibers (magenta) and the proliferation marker PCNA (green) on retinal sections of uninjured control animals and at 44 hours post lesion (hpl), 4 days post lesion (dpl) and 6 dpl (N= 3 animals per condition). The position of the outer nuclear layer (ONL), inner nuclear laser (INL) and ganglion cell layer (GCL) is indicated in the uninjured sample. Scale bar: 30 µm. Panels 1 and 2 are magnifications of the areas indicated by the squares 1 and 2. Scale bar: 10 µm.

4.4 scRNAseq identifies a cell population with hybrid characteristics of reactive MG and early RPCs in the light-lesioned retina

As observed above, several MG-related genes, like *gfap* or *crlf1a*, were also expressed in cluster 5, which locates next to the reactive MG (clusters 3 and 4), includes proliferative cells and becomes eminent only at 4 dpl. Further analysis showed expression of several members of the High Mobility Group (Hmg) protein family among the top 100 upregulated marker genes (Appendix 1). Consistent with that, the UMAP expression profile of *hmgb2b* displayed high transcript counts already in cluster 3 (reactive MG), as well as in further downstream RPC and regenerated progeny clusters (Figure 16A).

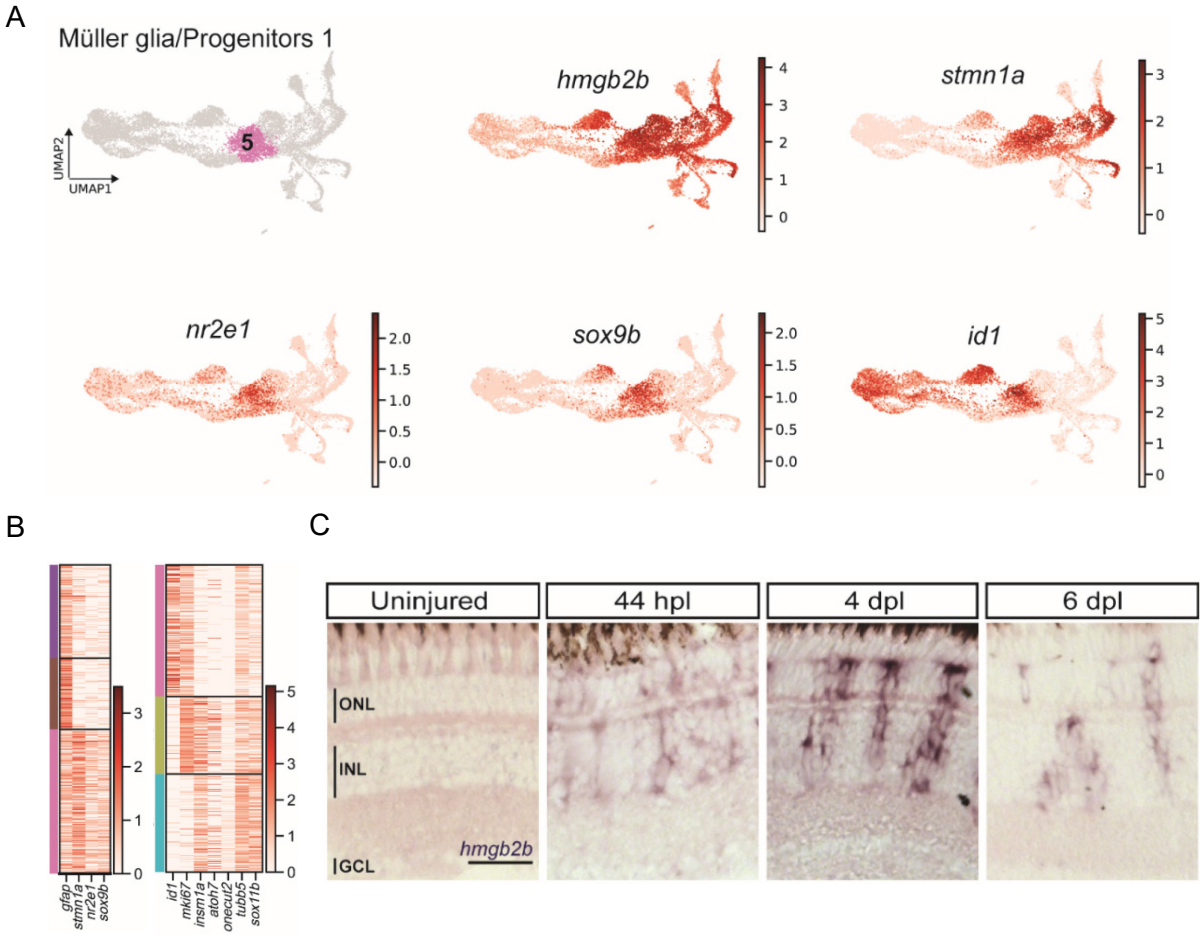

Figure 16. scRNAseq identifies a cell population with hybrid characteristics of reactive Müller glia and early progenitors in the light-lesioned retina. A. UMAP visualization of the Müller glia/progenitor 1 cluster (cluster 5) and the expression levels of *hmgb2b*, *stmn1a*, *nr2e1 sox9b* and *id1*. **B.** Left heat-map: differentially expressed genes between reactive MG clusters (violet and brown, clusters 3 and 4, respectively) and Müller glia/progenitor 1 cluster (pink). Note that cells in cluster 5 express high counts of *stmn1a*, *nr2e1* and *sox9b*. Right heat-map: differentially expressed genes between cluster 5 and downstream progenitor clusters 6 and 7 (green and light blue, respectively). Note that cells in cluster 5 show high counts of *id1*, whereas cells in cluster 6 and 7 show neurogenic (*atoh7*, *onecut1*, *onecut2*) gene counts. **C.** Bright field microscopy images of chromogenic *in situ* hybridization

detecting *hmgb2b* on retinal sections of uninjured control animals and at 44 hours post lesion (hpl), 4 days post lesion (dpl) and 6 dpl (N= 3 animals per condition). The position of the outer nuclear layer (ONL), inner nuclear layer (INL) and ganglion cell layer (GCL) is indicated in the uninjured sample. Scale bar: 30 µm**.** Differentially expressed gene analysis has been computed using a t-test between cells in cluster 5 (n= 1415) and cells in cluster 3 (n= 913), between cells in cluster 5 and cells in cluster 4 (n= 697) and between cells in cluster 5 and cells in cluster 6 (n= 835). Differentially expressed genes between cells in cluster 6 and cells in cluster 7 (n= 1056) has been computed using a t-test.

This suggested a transition from MG to RPC fate and that cells of cluster 5 might have hybrid characteristics of reactive MG and downstream Müller glia-derived RPCs. To analyse its identity more in detail, cluster 5 was compared to reactive MG (clusters 3 and 4), as well as to the neighbouring, downstream RPCs (cluster 6) using DEG analysis. When compared to reactive MG, cells in cluster 5 upregulated several genes, including *stmn1a*, *nr2e1* and *sox9b* (Figure 16A, B and Appendices 4 and 5). Consistently, UMAP expression profile of *stmn1a* showed counts mainly in cluster 5 and in the neighbouring, downstream RPCs that position on the right side of the map. By contrast, *stmn1a* counts were low in the reactive MG cluster 3 and absent in reactive MG cluster 4 as well as in non-reactive MG clusters on the left side (Figure 16A). UMAP expression of *nr2e1* was sparse in all non-reactive and reactive MG, but very strong in cluster 5. Conversely, UMAP expression of *sox9b* showed high counts that were almost exclusively restricted to cluster 5. DEG analysis between cluster 5 and the neighbouring downstream cluster 6 revealed also expression of *nr2e1* and sox9b, but additional expression of transcripts like *id1* (Figure 16B and Appendix 6). Consistently, high *id1* counts were found in cluster 5 and in other reactive or non-reactive MG clusters, but not in downstream RPCs locating on the right side of the map (Figure 16A). The expression of *hmgb2b* and *id1* was analysed in the regenerating retina using chromogenic *in situ* hybridization and fluorescent *in situ* hybridization combined with immunohistochemistry, respectively, to validate the respective scRNAseq expression pattern. Consistently, *hmgb2b* signal was not detectable in the uninjured, central retina, but individual cells residing in the inner nuclear layer initiated signal expression at 44 hpl (Figure 16C). Subsequently, *hmgb2b* transcripts could be detected in clusters of cells that scattered between the inner and outer nuclear layers at 4 and 6 dpl (Figure 16C).

The expression of *id1* in the regenerating tissue matched the scRNAseq data too. *id1* was already detectable in Zrf1-positive but PCNA-negative cells in the inner nuclear layer of the uninjured, central retina (Figure 17A, B). At 44 hpl, the transcript was

strongly upregulated in Zrf1/PCNA-double positive cells in the inner nuclear layer. At 4 and 6 dpl, *id1* expression was still associated with Zrf1/PCNA-double positive cells and, occasionally, with PCNA-only positive cells (Figure 17A, B). To summarize, marker gene analysis reveals that cells in cluster 5 display a transcriptional signature of reactive MG, as well as RPCs, which is the reason why it was assigned a hybrid identity.

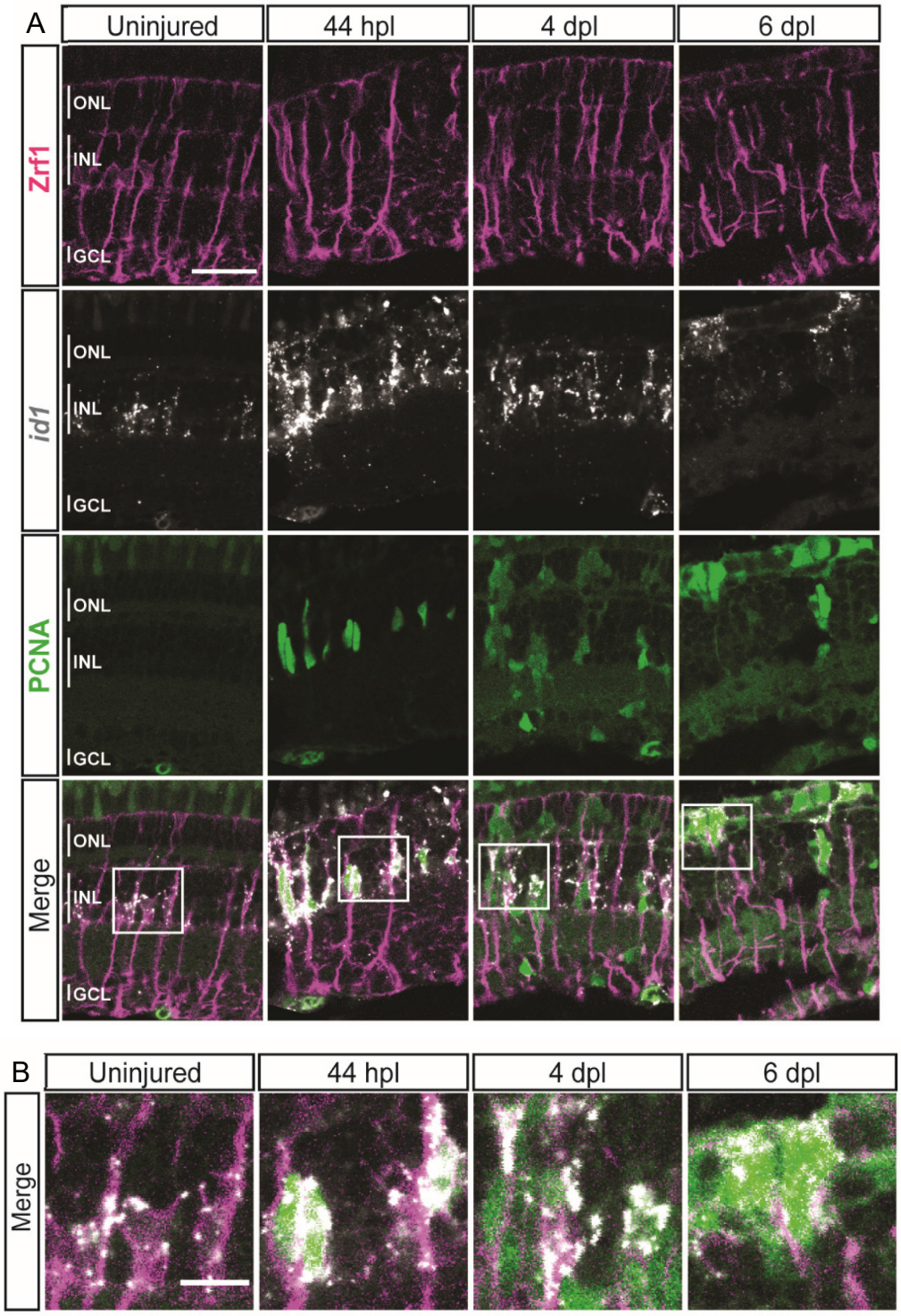

Figure 17. Expression profile of *id1* during retina regeneration. A. Confocal images of fluorescent *in situ* hybridization for *id1* (grey) and immunohistochemistry against Zrf1-positive MG (magenta) and the proliferation marker PCNA (green) on retinal sections of uninjured control animals and at 44 hours post lesion (hpl), 4 and 6 days post lesion (dpl) (N= 3 animals per condition). The position of the outer nuclear layer (ONL), inner nuclear layer (INL) and ganglion cell layer (GCL) is indicated in the uninjured sample. Scale bar: 30 µm. **B.** Magnification of the areas indicated by the squares in panel A. Scale bar: 10 µm.

4.5 scRNAseq identifies two neurogenic progenitor populations in the light-lesioned retina

The DEG-analysis between cluster 5 (cells with hybrid Müller glia/progenitor identity) and cluster 6 (downstream RPCs) also revealed that the latter upregulated *insm1a* (Figure 16B, right heat-map, and Appendix 6), which promotes the exit of RPCs from the cell cycle in the injured fish retina at 4 dpl[188]. Additional differentially expressed genes included *atoh7* and *onecut2*, which were expressed in cluster 6 (Figure 16B, right heat-map, and Appendix 6). The highly redundant gene *onecut1* was also expressed in cluster 6, albeit it did not result from the DEG analysis. The UMAP expression profile of *insm1a* confirmed high read counts in cluster 6 but also in clusters 7, 8 and 10 (Figure 18). The UMAP expression profile of *atoh7* also confirmed expression in cluster 6, as well as in clusters 7 and 10 (Figure 18). Additionally, the UMAP expression profile of *onecut1* and *onecut2* confirmed that both genes were expressed in clusters 6 and 7 and in cluster 9 (Figure 18A). Cluster 7 expressed further neurogenic marker genes like *tubb5* and *sox11b*[4,199–201] (Figure 16B and Appendix 6). Finally, *mki67*, a marker of mitotic cell division, showed transcript counts in cluster 6, but not in cluster 7, in the UMAP plot (Figure 18A and 16B). Hence, it was concluded that cluster 6 and cluster 7 represented neurogenic progenitors, and were named progenitors 2 and progenitors 3, respectively. To validate *atoh7*, *onecut1* and *onecut2* expression in the regenerating retina, *in situ* hybridization was employed. In agreement with the scRNAseq data, *atoh7* signal was absent in the uninjured and 44 hpl retina, but became detectable in the inner and outer nuclear layers at 4 and 6 dpl (Figure 18B). Similarly, *onecut1* and *onecut2* were prominently expressed in the inner and outer nuclear layer at 4 and 6 dpl, in addition to their homeostatic expression in the presumptive horizontal cell layer in the uninjured and 44 hpl retina (Figure 18B, black arrowheads). In summary, scRNAseq showed transcriptional heterogeneity of neurogenic progenitors, which upregulate known markers of developmental retinogenesis in the regenerating zebrafish retina.

A

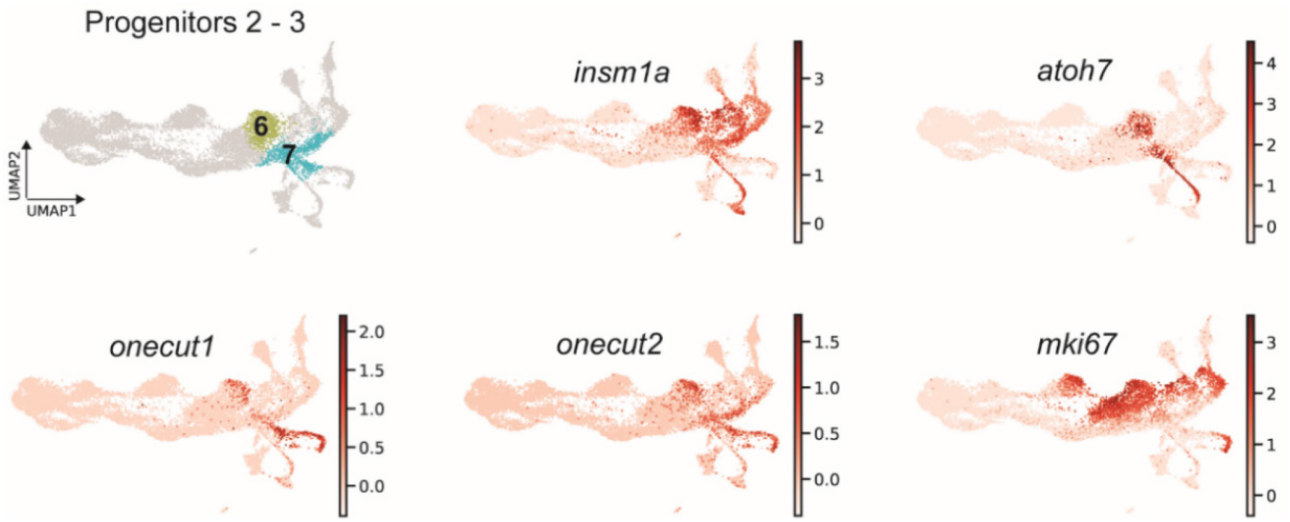

B

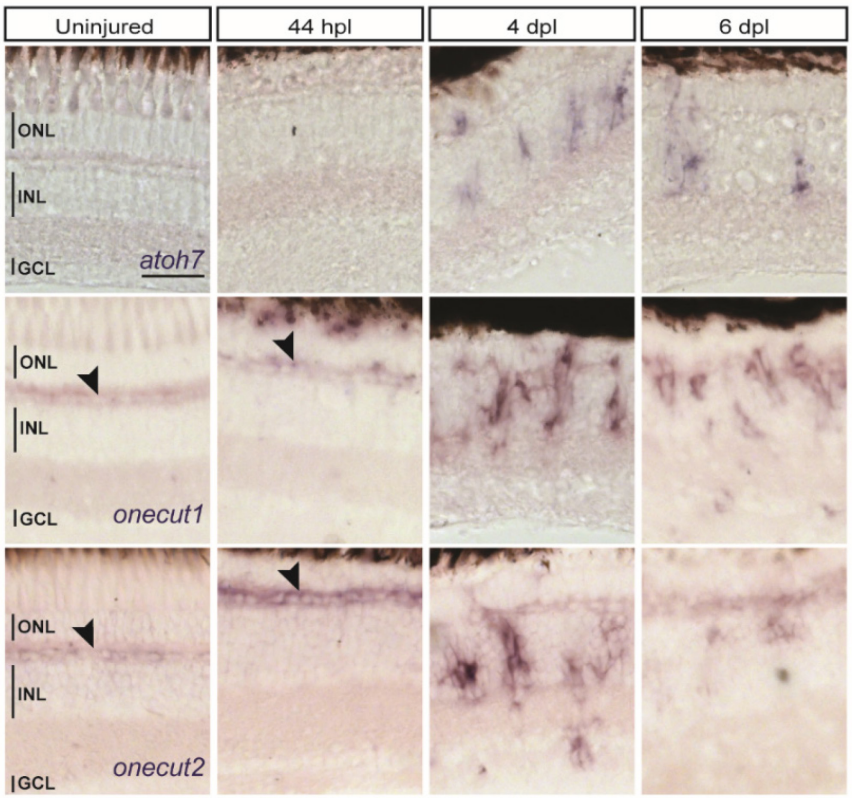

Figure 18. scRNAseq identifies two neurogenic progenitor populations in the light-lesioned retina. A. The two progenitor clusters (cluster 6 and 7) and the relative expression levels of *insm1a*, *atoh7*, *onecut1*, *onecut2* and *mki67*. **B.** Bright field microscopy images of chromogenic *in situ* hybridization detecting *atoh7*, *onecut1* or *onecut2* on retinal sections of uninjured control animals and at 44 hours post lesion (hpl), 4 days post lesion (dpl) and 6 dpl (N= 3 animals per gene and condition). Black arrowheads indicate horizontal cells. The position of the outer nuclear layer (ONL), inner nuclear layer (INL) and ganglion cell layer (GCL) is indicated in the uninjured sample. Scale bar: 30 µm.

4.6 scRNAseq identifies committed precursors in the light-lesioned retina

Marker genes of cluster 8, which locates next to the neurogenic progenitors of clusters 6 and 7, included several well-known photoreceptor precursor genes, like *crx*, *nr2e3*, *otx5* and *thrb* (Appendix 1). Correspondent UMAP plots for all these transcripts revealed high counts in cluster 8 (Figure 19A). Moreover, *crx*, *nr2e3* and *otx5* were highly expressed in clusters 11 and 12, whereas *thrb* expression was restricted to the sole clusters 8 and 11. Further gene expression analysis identified clusters 11 and 12 as differentiating cone photoreceptors arising from cluster 8. Indeed, clusters 11 and 12 represent differentiating blue and red cone photoreceptors, as shown by the UMAP expression for cone-specific opsins *opn1sw2* and *opn1lw2*, respectively (Figure 19B). During zebrafish retinogenesis, rod and cone photoreceptors derive from highly similar precursors, which express *crx* and *nr2e3*[103]. Moreover, differentiating rods and cones that have not yet extended the outer segments are highly similar to each other in the developing zebrafish retina[58]. Hence, the expression of known rod photoreceptor markers *rho* and *gnat1* was plotted on the UMAP to check whether they could be detected in the scRNAseq dataset. However, expression of *rho* and *gnat1* counts was very low and sparse and did not define any specific rod cluster (Figure 19B).

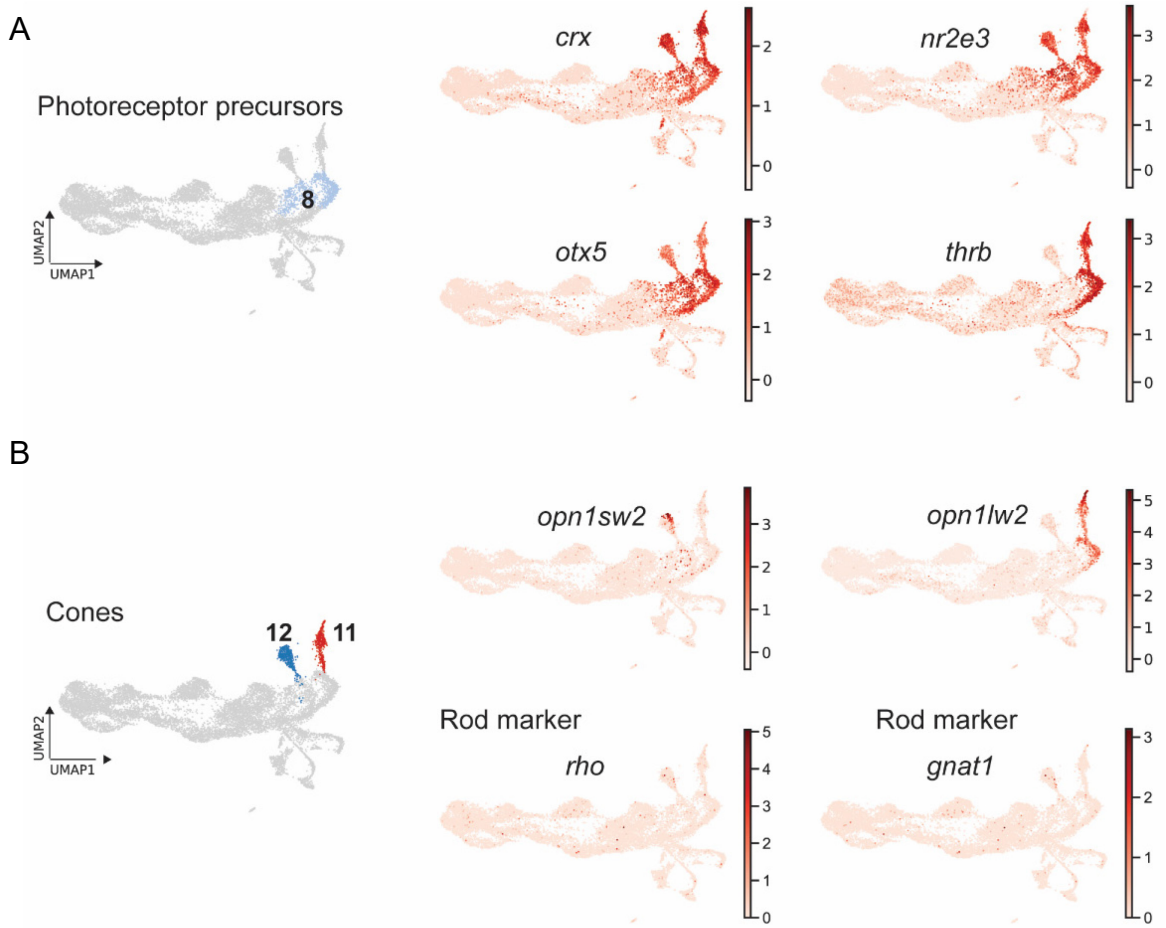

Figure 19. scRNAseq identifies photoreceptor precursors as well as differentiating cone, but not rod, photoreceptors in the light-lesioned retina. A. UMAP expression of the photoreceptor precursor (n= 1010 cells) markers *crx*, *nr2e3*, *otx5* and *thrb*. **B.** The red (n= 425 cells) and blue (n= 419 cells) cone clusters (cluster 11 and 12) express blue cone *opn1sw2* and red cone *opn1lw2*, but do not express rod markers *rho* and *gnat1*.

Cluster 9, which branches from the neurogenic progenitor 3 (cluster 7), expressed developmental markers of horizontal cell precursors like *prox1a* and *rem1* (Appendix 1). Consistently, the UMAP plot for *rem1* showed high expression almost restricted to this cluster specifically (Figure 20). Further analysis revealed that *ptf1a*, which is necessary to start lineage specification of horizontal and amacrine cells in the developing retina[38,69], was expressed in cluster 9. In line with this, the UMAP expression of *ptf1a* confirms high counts in the left part of cluster 9, but such expression was even more pronounced in the upstream part of cluster 7 feeding into cluster 9 (Figure 20). Finally, UMAP expression of *lhx1a*, an additional marker of developing horizontal cells in the zebrafish retina, was plotted[202,203]. Consistently, *lhx1a* transcript counts were located downstream *ptf1a* expression and restricted almost exclusively to cluster 9. In addition, expression of mature markers of horizontal cells in cluster 9 was checked. To this aim, the expression of *gad1b*, which encodes

for the GABA-synthesizing enzyme GAD67, was plotted on the UMAP. However, high *gad1b* counts were found in clusters 13 and 14, which were annotated as amacrine cells (see below and Appendix1), but were not detected in cluster 9. Hence, cells in cluster 9, which expressed developmental markers of horizontal cell precursors and markers of proliferation (Figure 11 C, D), were identified as horizontal cell precursors.

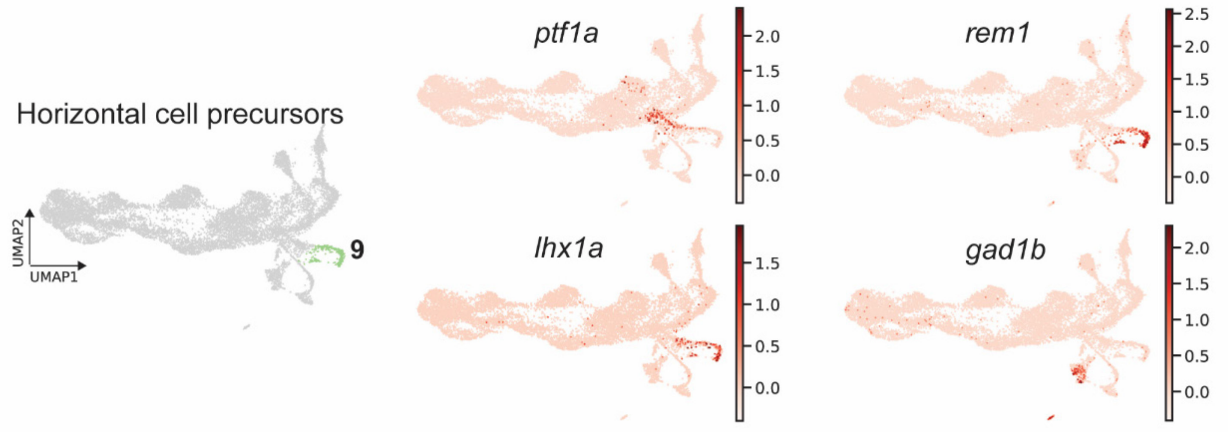

Figure 20. scRNAseq identifies horizontal cell precursors. UMAP visualization of marker genes for cluster 9 (n= 293 cells), which expresses high counts of horizontal cell markers *rem1* and *lhx1a* as well as few *ptf1a* counts. Note that *ptf1a* transcripts are higher in the upstream cluster 7. By contrast, *gad1b*, a marker of mature horizontal cells, is not expressed in cluster 9.

In summary, scRNAseq of the regenerating retina detected committed precursors of photoreceptors as well committed precursors of horizontal cells. Furthermore, while differentiating red and blue cone photoreceptors could be detected among the regenerated progeny, it was not possible to detect neither differentiating rods nor differentiating horizontal cells up to 6 dpl.

4.7 scRNAseq identifies differentiating retinal ganglion, amacrine and bipolar cells in the light-lesioned retina

Gene expression analysis of the remaining clusters 10, 13, 14 and 15 identified them as differentiating, non-photoreceptor, retinal neurons. These clusters corresponded to retinal ganglion cells (cluster 10), amacrine cells (clusters 13 and 14), as well as bipolar cells (cluster 15) (Appendix 1). More specifically, cells in cluster 10 strongly upregulated *gap43* and the more mature retinal ganglion cell marker *isl2b*[49], as shown by the relative UMAP plots (Figure 21A). Cells belonging to clusters 13 and 14, instead, upregulated *stx1b* and *pvalb6*, known marker genes of differentiating and mature amacrine cells (Figure 21B). Moreover, cells in cluster 13 were characterized by

expression of *calb2a* and *calb2b*, two calcium-binding proteins that are additional mature horizontal and amacrine cell markers. Indeed, UMAP visualization of *calb2a* counts showed some expression in cluster 3 (reactive MG) and even stronger expression in cluster 13. Counts for *calb2b* were almost exclusively restricted to cluster 13. By contrast, cells in cluster 14 showed high expression of *chata*, which encodes for the enzyme choline O-acetyltransferase a (Figure 21B). Intriguingly, and in addition to *chata*, cells in cluster 14 upregulated *gad1b* counts too (Figure 20), which identified them as starburst amacrine cells[43].

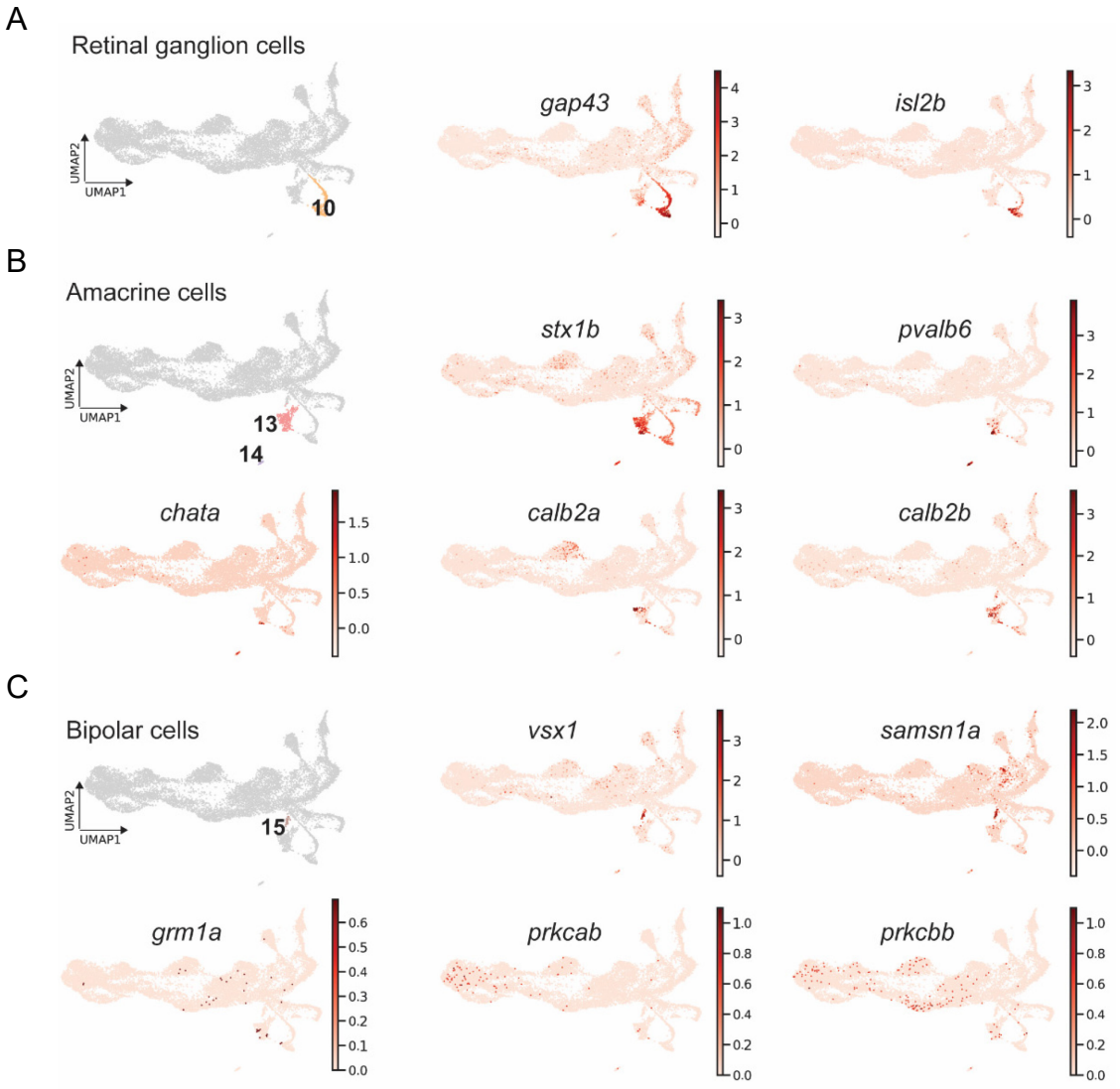

Figure 21. scRNAseq identifies regenerating retinal ganglion, amacrine and bipolar cells in the light-lesioned retina. A. UMAP visualization of *gap43* and the mature retinal ganglion cell marker *isl2b,* both expressed by cells in cluster 10 (n= 330 cells). **B.** UMAP visualization of clusters 13 (n= 344 cells) and 14 (n= 50 cells) and the correspondent expression of *stx1b*, *pvalb6*, *chata, calb2a* and *calb2b*, markers of differentiating and mature amacrine cells. Note *chata* enrichment in cluster 14. **C.** UMAP visualization of cluster 15, which expressed the known bipolar cell marker *vsx1* and the novel bipolar cell marker *samsn1a*. Note that cells in cluster 15 (n= 41 cells) do not express mature marker genes of bipolar cells, like *grm1a*, *prkcab* and *prkcbb*.

Finally, cells in cluster 15 upregulated *vsx1*, which is a known marker of a subset of bipolar cells, as well as the novel marker gene *samsn1a* (Appendix 1 and Figure 21C). The expression of *grm1a*, which encodes for the metabotropic glutamate receptor 1, as well as variants of protein kinase C using *prkcab* and *prkcbb* (protein kinase alpha b, protein kinase beta b) was checked to investigate the presence of mature bipolar cells (Figure 21C). Counts for *prkcab* were sparsely found in some non-reactive and reactive MG (clusters 1-4). *prkcbb*-positive cells were found more frequently in some non-reactive and reactive MG (clusters 1-4), progenitor 1 (cluster 5), as well as in amacrine cells (clusters 13, 14). Importantly, *prkcab* or *prkcbb* were not detected in bipolar cells.

Recently, Lahne and colleagues showed that regenerated progeny arise according to the developmental order of fish neurogenesis in the light-lesioned retina[186]. To check whether regenerated progeny in the scRNAseq dataset recapitulated this order too, the fraction of cells that differentiate into a specific cell fate during the time course of regeneration was plotted (Figure 22). The earliest committed progeny emerged at 4 dpl and corresponded to retinal ganglion cells or red cones. At 6 dpl, the number of retinal ganglion cells and red cones continued to increase. Retinal ganglion cells expressed the mature marker gene *isl2b*, whereas red cones expressed *opn1lw2*, which encodes for one type of red opsin (Figures 19B and 21A). Moreover, a significant number of blue (*opn1sw2*) cones and amacrine cells was observed, as well as a small number of bipolar cells at 6 dpl. Differentiating progeny that generated horizontal cells or rods at this stage was not observed (see above).

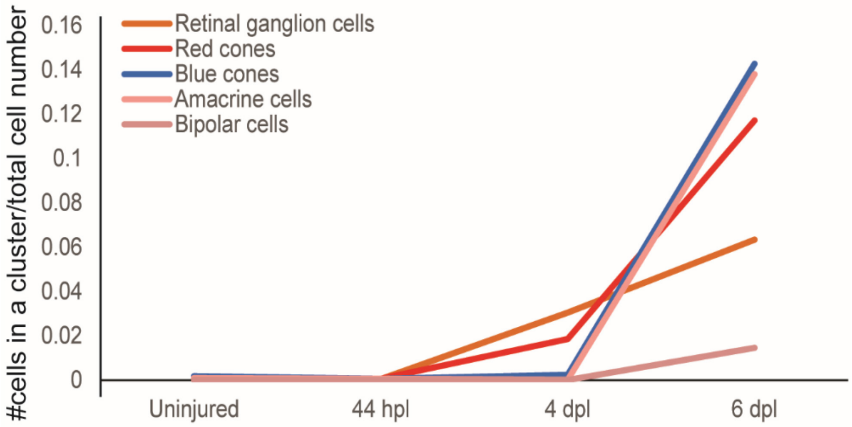

Figure 22. scRNAseq reveals the sequential appearance of the regenerated progeny in the light-lesioned retina. Graph plotting the fraction of cells (y-axis) embarking on a specific retinal cell fate (coloured curves) in relation to a given time point (x-axis). hpl: hours post-lesion; dpl: days post-lesion.

Taken together, the present scRNAseq data reveal the sequential appearance of differentiating progeny in the light-lesioned, adult zebrafish retina. Moreover, the analysis of more mature marker genes shows that the differentiation of retinal ganglion cells and red cones precedes the appearance of blue cone photoreceptors, amacrine and bipolar cells.

PART II

4.8 4-hydroxytamoxifen induces CreER^{T2}-mediated recombination in the *TgBAC(mmp9:CreERt2,cryaa:EGFP);Tg(Olactb:loxP-DsRed2-loxP-EGFP)* line

Previous short-term, lineage tracing studies have found that zebrafish MG-derived RPCs give rise to all retinal neurons independently of the applied lesion paradigm and of the type of affected cells[143,187]. However, it remains unclear whether and how all the regenerated neurons integrate properly in the existing retinal circuitry. In order to lineage trace MG-derived RPCs and regenerated progeny on a long term in the light-lesioned retina, the transgenic line *TgBAC(mmp9:CreERt2,cryaa:EGFP);Tg(Olactb:loxP-DsRed2-loxP-EGFP)* was used[163,204,205]. This double transgenic line carries the Cre-driver *TgBAC(mmp9:CreERt2,cryaa:EGFP)* as well as the Cre dependent reporter *Tg(Olactb:loxP-DsRed2-loxP-EGFP)*. In the Cre-driver, the *mmp9* promoter controls the expression of the Cre-recombinase enzyme fused to the human ligand-binding domain of the estrogen receptor (ER^{T2}), whereas the lens-specific *cryaa* promoter drives the expression of EGFP in the lens, serving as a transgenesis marker. The fusion of Cre to the ER^{T2} receptor allows the **temporal** control of Cre translocation to the cell nucleus upon 4-OHT binding to the receptor. In non-recombined conditions, the medaka (*Oryzias latipes*) broadly expressed promoter *Olactb* controls the expression of DsRed2[163,205]. Upon 4-OHT binding, CreER^{T2} moves to the nucleus and catalyses recombination, which results in the deletion of the loxP-flanked DsRed2 cassette. Subsequently, *Olactb* drives the expression of EGFP in all recombined cells (Figure 23).

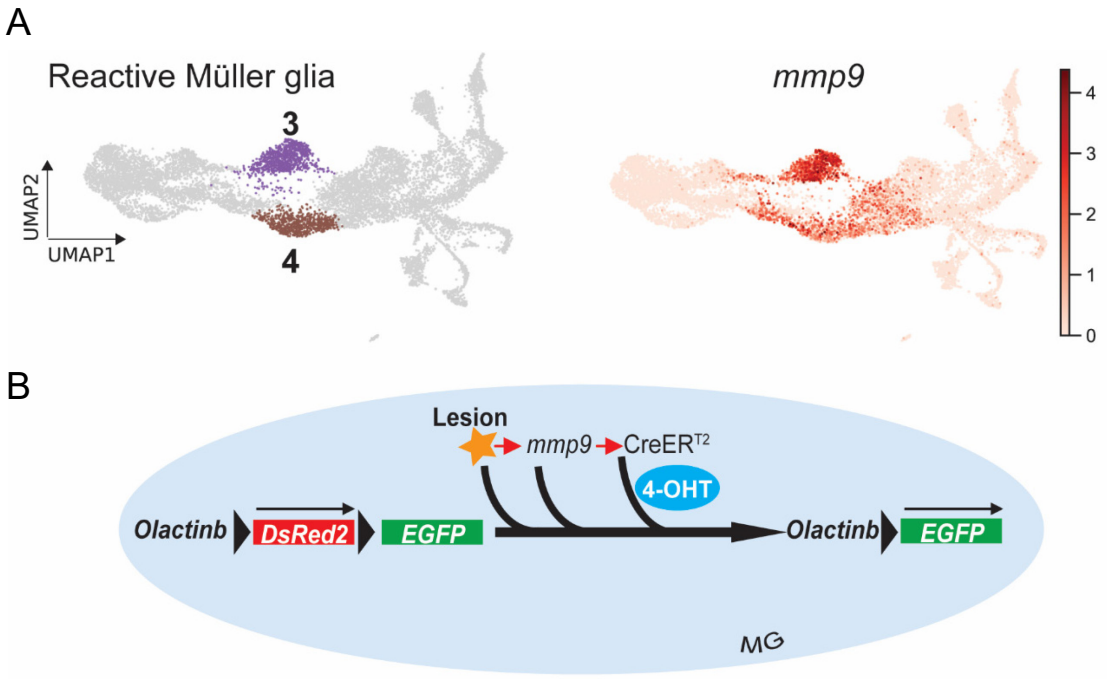

Figure 23. CreER^{T2}-mediated recombination in injury-reactive MG. A. UMAP visualization of *mmp9* expression in the scRNAseq dataset generated in the current thesis. Very high *mmp9* counts are found in reactive MG 1 (cluster 3) that is evident at 44 hpl. High counts are found also in reactive MG 2 (cluster 4), evident at 4 dpl, and in the neighbouring MG/Progenitors 1 cluster 5 at 4 dpl. **B.** In the *TgBAC(mmp9:CreERt2,cryaa:EGFP);Tg(Olactb:loxP-DsRed2-loxP-EGFP)* line, *mmp9* drives CreER^{T2} expression. Upon 4-OHT administration **at 6 or 24 hpl**, the metabolite binds to ER^{T2}, CreER^{T2} enters the MG nucleus and catalyses the excision of DsRed2. Subsequently, *Olactinb* drives EGFP in the recombined MG and MG-derived RPCs and progeny, which will be permanently EGFP-positive. MG: Müller glia. Legend: logarithm of normalized counts per million.

In the light-lesioned retina, *mmp9*, which encodes for the matrix metalloprotease 9, is upregulated as early as 8 hpl in injury-reactive MG[125]. Moreover, *mmp9* is a marker gene for clusters 3 and 4 in the scRNAseq dataset generated in the current PhD thesis (Figure 23). Both clusters correspond to reactive Müller glia, with cluster 3 becoming eminent at 44 hpl, and cluster 4 becoming enriched later, at 4 dpl (see "Results, PART I"). Hence, upon 4-OHT administration in a time frame between 8 hpl (earliest documented *mmp9* upregulation in MG[125]) and 44 hpl, when the first reactive MG is observed in the present scRNAseq, CreER^{T2}-mediated recombination should result in the permanent EGFP-labelling of reactive MG and MG-derived cells in the light-lesioned *TgBAC(mmp9:CreERt2,cryaa:EGFP);Tg(Olactb:loxP-DsRed2-loxP-EGFP)* retinae. First, as a control for lesion-specific induction of CreER^{T2}, uninjured, untreated zebrafish retinae were cryosectioned and immunostained for EGFP and PCNA to check whether any unspecific, EGFP-positive signal was detected in the homeostatic, central retina. No EGFP-positive cells could be observed in the uninjured, untreated retinae. Occasionally, PCNA-positive cells were detected at the base of the outer

nuclear layer in the uninjured, untreated controls, corresponding most likely to rod precursors (Figure 24A). To control for injury-specific CreER^{T2} induction, a second group of uninjured fish underwent intraperitoneal injection of 2.5 mM 4-OHT and their retinae were processed for immunohistochemistry. Again, no EGFP-positive cells could be detected in the central retinae of uninjured, 4-OHT injected fish, and occasional PCNA-positive, most likely rod precursors were observed at the base of the outer nuclear layer (Figure 24A). 4-OHT was then injected in light-lesioned animals at 6 hpl and retinae were harvested and processed for immunohistochemistry against EGFP and PCNA at 4 dpl. Retinae from light-lesioned fish that had been injected with 4-OHT at 6 hpl showed clusters of fusiform, PCNA-positive cells scattered across all the retinal layers at 4 dpl, which is consistent with MG-derived progenitors that peak in proliferation and initiate migration to different layers to regenerate neurons. Moreover, a substantial amount of EGFP-positive cells was observed in the retinae of 6 hpl 4-OHT injected fish. The majority of EGFP-positive cells was also PCNA-positive (Figure 24B). Importantly, retinae from light-lesioned fish that had been injected at 6 hpl with ethanol/phosphate buffer, which was the vehicle for 4-OHT, did not show any EGFP positivity, confirming that recombination occurred because of 4-OHT induced CreER^{t2} nuclear translocation in reactive MG. To improve the efficiency of recombination, injection of 4-OHT was also tested at 24 hpl, that is, 16 hours later than the first *mmp9* expression documented in reactive MG[125]. Ethanol/phosphate buffer was injected in a separate control group and in parallel to 4-OHT injection. Retinae from both vehicle and drug injected fish were harvested at 4 dpl and processed for immunohistochemistry. As expected, PCNA-positive cells were scattered between the inner and the outer nuclear layers of 4 dpl retinae from both ethanol/phosphate buffer as well as 4-OHT injected fish. However, vehicle-treated retinae did not display any EGFP-positive signal in the central, light-lesioned retina. By contrast, numerous EGFP-positive cells were observed in the central retina of light-lesioned and 4-OHT injected fish (Figure 24C). The great majority of EGFP-positive cells expressed PCNA signal too. In summary, injection of 4-OHT either at 6 hpl or at 24 hpl results in conditional recombination in a substantial number of *mmp9:CreER^{T2}*-epressing, reactive MG in *TgBAC(mmp9:CreERt2,cryaa:EGFP);Tg(Olactb:loxP-DsRed2-loxP-EGFP)*, light-lesioned fish.

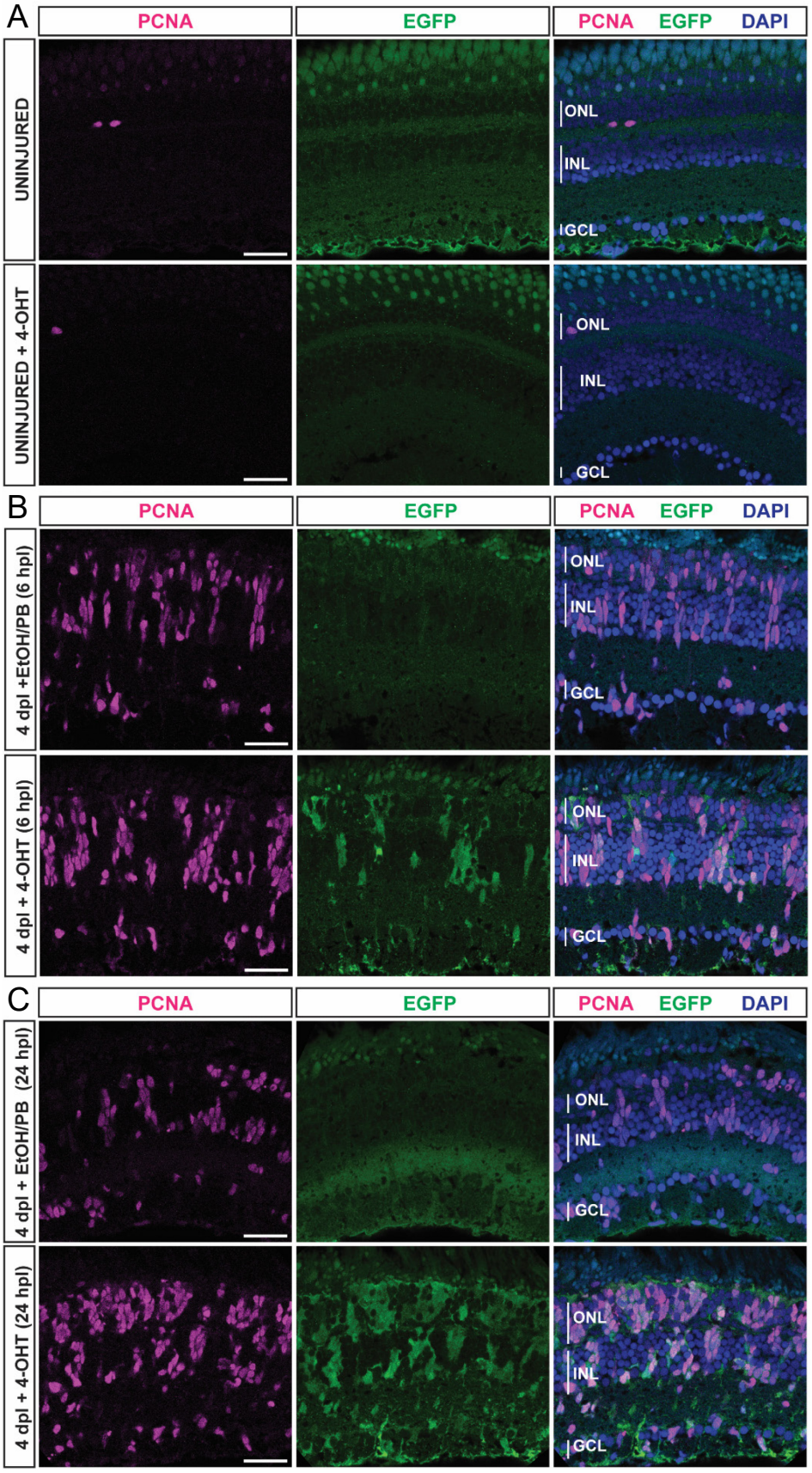

Figure 24. 4-hydroxytamoxifen induced, CreER^{T2}-mediated recombination in *TgBAC(mmp9:CreERt2,cryaa:EGFP);Tg(Olactb:loxP-DsRed2-loxP-EGFP)*. A. Retinae from uninjured,

untreated (N= 3 animals) as well as uninjured, 4-OHT (N= 2 animals) injected fish display rare PCNA-positive cells at the base of the outer nuclear layer (ONL), most likely corresponding to rod precursors, but no EGFP-positive cells. **B.** Retinae from fish (N= 2 animals) injected with ethanol/phosphate buffer (EtOH/PB) at 6 hours post-lesion (hpl) show many PCNA-positive cells, but no EGFP-positive signal at 4 days post-lesion (dpl). Conversely, retinae from fish (N= 3 animals) injected with 4-hydroxytamoxifen (4-OHT) at 6 hpl show many PCNA-, as well as EGFP-positive cells at 4 dpl. **C.** Retinae from fish (N= 2 animals) injected with EtOH/PB at 24 hpl show many PCNA-positive cells, but no EGFP-positive signal at 4 dpl. Conversely, retinae from fish (N= 2 animals) injected with 4-OHT at 24 hpl show many PCNA-, as well as EGFP-positive cells at 4 dpl. ONL: outer nuclear layer; INL: inner nuclear layer; GCL: ganglion cell layer. Scale bar: 30 µm.

5. DISCUSSION

In this study, a short-term lineage tracing strategy enabled the selective enrichment of MG and MG-derived cells for up to six days post light lesion. Subsequent scRNAseq of sorted cells resolved the transcriptome of individual MG, RPCs as well as regenerated progeny, and allowed reconstructing their lineage relationship in the homeostatic and regenerating zebrafish retina (Figures 9, 11). A previous study combined bulk RNA sequencing of sorted MG with scRNAseq of whole retinae from zebrafish upon NMDA as well as light lesions[134]. This work characterized specifically the early reprogramming of MG and progenitor production, covering up to 36 hours post NMDA and light lesion. The authors report that MG go through an activated, non-proliferative state characterized by upregulation of markers of gliosis. However, neither did they find any evidence of MG heterogeneity in uninjured conditions nor did they provide any extensive characterization of MG-derived RPCs[134]. Previously, several RNA sequencing studies of the regenerating zebrafish retina have used microarrays as well as RT-PCR and qRT-PCR to evaluate transcriptional changes at a population level, without providing any MG/RPC single cell resolution[122,126,133,144,206]. Previous immunohistochemistry and *in situ* hybridization experiments provided a morphological description of the population of MG-derived RPCs. Indeed, progenitors are described as fusiform cells that proliferate and express markers of multipotency like Pax6 and Sox2, as well as some neurogenic markers like Atoh7, Ptf1a, Vsx1 and others[95,113,119,130,186,188]. In contrast to these previous results, the current study is the first providing a comprehensive description of the **molecular signature** of MG, MG-derived cells and their lineage relationship up to 6 days post lesion in the zebrafish retina. Due to the selective enrichment of MG and their respective progeny, an adequate **single cell** resolution was obtained to observe substantial heterogeneity in the population of MG in uninjured as well as regenerating conditions. Moreover, an in depth description of RPC molecular identity, cell fate decisions and production of regenerated progeny is provided to cover all key aspects during zebrafish retina regeneration upon light-lesion. This short-term lineage strategy enabled to define two main trajectories in the regenerating zebrafish retina (Figure 25). The first trajectory (solid and dashed red lines) comprises clusters 1 to 5 and describes a closed cycle that both maintains the MG pool and produces the first-born Müller glia-derived RPCs. The second trajectory (solid black lines) involves clusters 6 to 15 and generates all

retinal neurons via the progressive fate-restriction of neurogenic RPCs and committed precursors. I am discussing the two trajectories separately below.

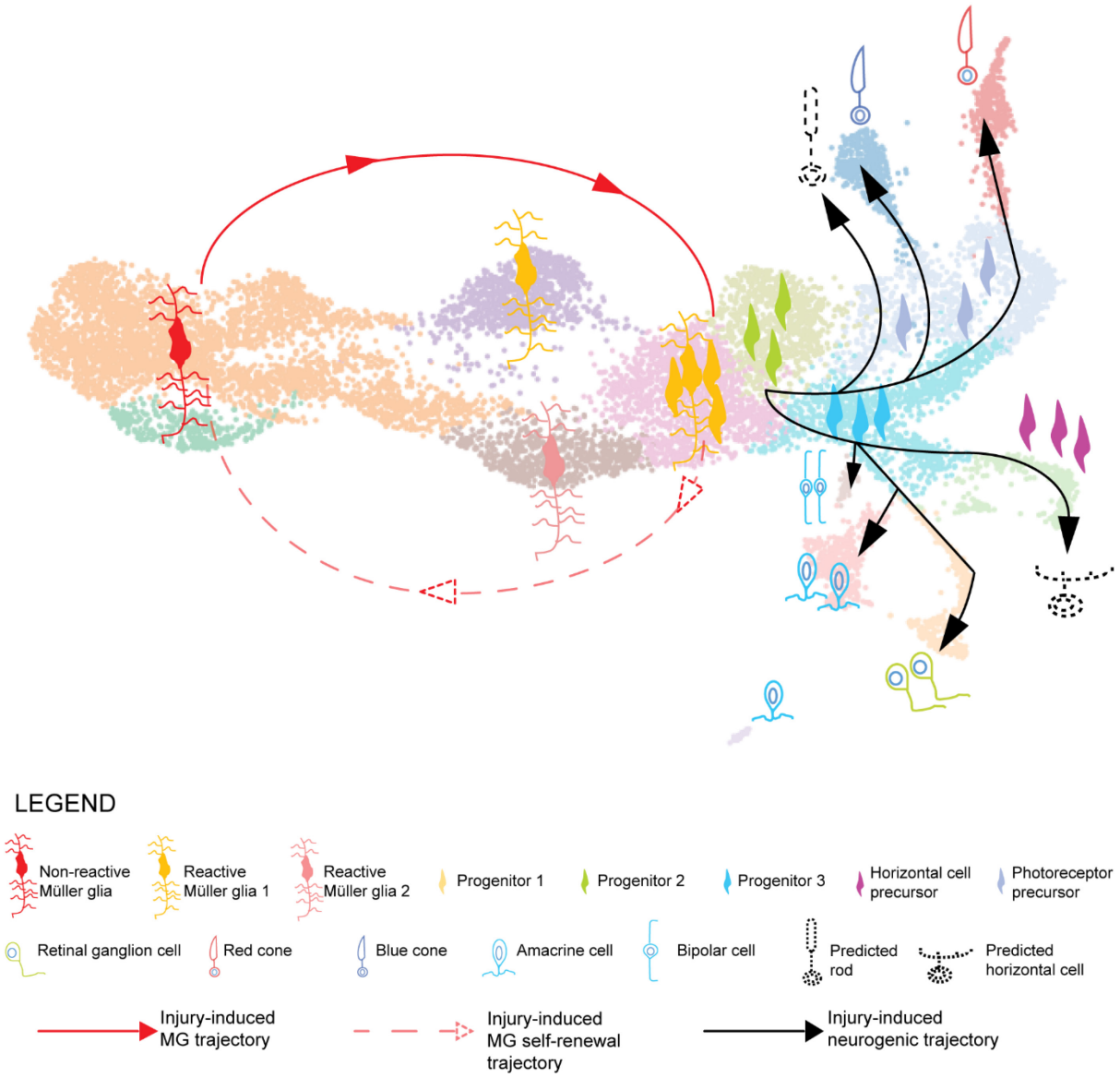

Figure 25. Proposed model describing the cellular events underlying zebrafish retina regeneration. Upon lesion, non-reactive MG on the left side of the UMAP feed into a population with hybrid Müller glia/progenitor identity via reactive Müller glia (solid red line). Based from this hybrid cell population, the existence of a Müller glia trajectory that reverts to the initial starting point is suggested. This trajectory might lead to Müller glia self-renewal (dashed red line). On the other hand, the hybrid cell population might represent also the starting point of the neurogenic trajectory, which results in the generation of neuronal precursors and differentiating neurons (solid black lines). Differentiating rods and horizontal cells, which have not been found in the scRNAseq, are indicated with dashed lines and positioned in the predicted location on the main UMAP.

5.1 Müller glia self-renew and give rise to early, multipotent progenitors

The glial trajectory starts with non-reactive MG (clusters 1 and 2), which express canonical glial marker genes like *gfap*, *apoeb*, *glula*, *rlbp1a* and *cahz* that ensure the

housekeeping function of MG during homeostasis (Figures 12 and 13A, Appendix 1). Most cells belonging to the non-reactive MG clusters are quiescent as shown by the cell cycle analysis, and are found in the uninjured as well as in the lesioned retina at all sampled time points (Figure 11B, C). However, it was noticed that some non-reactive MG are in S or G2/M phases of the cell cycle, and express *pcna*, albeit at a lower level as compared to the expression in injury-induced, proliferating cell clusters (Figures 11C, D). This is consistent with the previous findings that zebrafish MG proliferate occasionally also in the uninjured, central retina and generate rod progenitors that feed the rod precursor pool at the base of the outer nuclear layer[95,104]. Accordingly, immunohistochemistry shows some cells expressing PCNA in the uninjured, central retina (Figure 7A). Furthermore, a small fraction of cells aligns in a trajectory from non-reactive MG on the left through reactive MG in the middle, to photoreceptor precursors on the right side of the UMAP in the uninjured sample (Figure 11B). However, some of those cells end up in the amacrine as well as retinal ganglion cell clusters. This suggests that MG might have the potential to generate not only rod photoreceptors, but also all other retinal neurons in the homeostatic, adult retina of the zebrafish. Indeed, it is known that MG in the uninjured retina express, albeit at a low level, multipotency markers like *pax6*, and share many marker genes with RPCs, thus they are referred to late-stage progenitors[80,95,101]. Nevertheless, MG and injury-induced RPCs are still considered **distinct** cell populations[6]. Upon injury, MG divide only once between 31 and 48 hpl, whereas MG-derived RPCs continue to divide, reaching a peak of proliferation at 4-5 dpl (discussed in [6, 120, 136, 137]). Cells in cluster 3 were isolated at 44 hpl, a time point when MG are about to undergo, or already underwent, their asymmetric cell division[6,95,137,142] and were annotated as *early* reactive MG. Consistent with that, cells in cluster 3 do not only express *gfap* and *apoeb*, but also *pcna* (Figures 11D and 13A). Moreover, the analysis of the predicted cell cycle phase per cluster shows cell cycle progression and supports the reactive state of MG in cluster 3. Indeed, whereas cells in the left part of cluster 3 are mostly in G1, cells in G2/M phase are found in the right part, with cells in S phase overlapping with both domains (Figure 11C). Reactive MG cells in cluster 3 upregulate also genes associated with MG reprogramming, like *ascl1a*[130,132], as well as those involved in the inflammatory response, like *crlf1a*, as well as *mmp9* and *hbegfa* (Figure 14A and Appendix 1), which might make MG behaviour similar to the function of immune cells[125,127,128]. In this context, the population of early reactive MG (cluster 3), identified

mostly at 44 hpl, is similar to the reactive MG cell pool that is described in the regenerating zebrafish retina at 36 hpl[134]. However, while the early reactive MG cluster identified in the present PhD study is proliferative, the one discussed by the mentioned study is not. The presence of a distinct pool of non-proliferative, reactive MG as early as 36 hpl in the earlier study might be explained by the different time points of sample collection, and/or by the lower, total number of cells sequenced in the current scRNAseq experiment (11.690) in comparison to the previous one (45.153)[134]. In summary, MG in the uninjured zebrafish retina might have the potential to behave like multipotent RPCs. Upon injury, reactive MG express inflammation-associated genes, like *crlf1a*, and undergo asymmetric cell division which products most likely map to cluster 5, discussed below.

5.2. A crossroad in the glial trajectory: hybrid cell cluster with MG and RPC characteristics

The close similarity between zebrafish MG and MG-derived RPCs at the level of expressed molecular markers as well as cellular and subcellular morphology has been already discussed in literature[6,108,186]. Thus, I propose that cells in cluster 5, which show a transcriptional hybrid identity between MG and RPCs, are the products of the asymmetric cell division of the *early* reactive MG (cluster 3) that is eminent at 44 hpl. Cells in cluster 5 are still *gfap*-positive, and share the expression of some markers with early reactive MG, like *her4.1* and *crlf1a* (Figures 13A and 14A). On the other hand, many cells in cluster 5 are highly proliferative and become prominent only at 4 dpl, a time point when predominantly RPCs are proliferating[6,95,108,136,137]. Indeed, cluster 5 display high *pcna* counts and the correspondent, predicted cell cycle status indicates that most cells are in S or G2/M phase (Figure 11C, D). Moreover, previous studies have found expression of *her4.1* and *crlf1a* in MG-derived RPCs in the light- as well as stab-lesioned retina, where they regulate RPC proliferation at 4 dpl[127,128,207]. In my performed *in situ* hybridization, *her4.1* signal at 4 and 6 dpl locates to the inner nuclear layer as well as the outer nuclear layer, where presumptive RPCs reside at this time point (Figure 14B)[208]. Additionally, cells in cluster 5 express *sox9b* and *nr2e1* as marker genes, which characterize early, multipotent RPCs of the developing fish, avian and mammalian retinae, as well as RPCs found in late retinogenesis, where they regulate MG production[62,82,84,85,209]. Hence, I propose that cluster 5 represents a crossroad of the glial and neurogenic trajectory, and contains self-renewed MG as well as first-born, MG-derived RPCs as a direct result of the earlier (44 hpl) asymmetric MG cell division.

I further propose that self-renewed MG close the cycle via late (4 dpl) reactive MG (cluster 4) and return into non-reactive MG (clusters 1 and 2, red, dashed line in Figure 25). In this context, it is observed that cells in the lower part of cluster 5 are found in the G1 (differentiating)[192] phase of the cell cycle (Figure 11C), and are contiguous to cells in cluster 4 (late reactive MG), which cells are found in G1 too. In contrast, MG-derived RPCs start the neurogenic trajectory with cells in cluster 6 (solid, black line). In this context, it is interesting to observe that *stmn1a*, coding for a microtubule-associated protein, is a marker gene for cluster 5. It has been previously reported that *stmn1a* is a marker for early neurogenesis in the developing zebrafish retina[66]. Alternatively, I suggest that cells in cluster 5 might represent *only* MG that have upregulated early RPC as well as gliogenic markers like *sox9b* and *nr2e1* and are dividing a *second* time at 4 dpl to generate renewed MG (cluster 4) and neurogenic RPCs (cluster 6). However, MG have been described to divide only once between 30 and 48 hpl and additional and/or asynchronous MG divisions later than 2 dpl have not been investigated[137,142]. BrdU/EdU lineage tracing experiments will be required to address this issue, with the caveat that MG and RPCs are hardly distinguishable from each other in the 4 dpl retina, especially when using the Zrf1 antibody to label GFAP-positive MG[101,108]. Live imaging of the regenerating retina would be the best tool to follow MG and MG-derived progenitors *in vivo*, but the current state of the art is not optimized for long recordings from the intact tissue in the living, adult animal[142]. Either way, the change of cell density over time (Figure 11B) supports the proposed model of self-renewing MG trajectory. Following the cells across the four time points on the UMAP, initially most cells of the uninjured sample map to non-reactive MG (clusters 1 and 2) located at the far left. At 44 hpl, the cell density shifts towards the upper right portion of cluster 1 and towards the early reactive MG (cluster 3) in the upper, middle of the map. At 4 dpl, sampled cells mostly map to RPCs (clusters 5-9) on the right, as well as to late reactive MG (cluster 4) in the lower, middle part. Additionally, cells mapping to the lower right part of non-reactive MG (clusters 1 and 2) are enriched in this sample, indicating a reverse direction from right to left. This population increases further at 6 dpl, when the number of RPCs is less prominent and the differentiating neural progeny at the top and bottom right are predominantly present in the sample. It is predicted that, in agreement with this model, sample collection at even later time points, e.g. 10 or 14 dpl, might show that the initial status has been restored and that non-reactive MG are mostly enriched in the sorted sample. However, it is unlikely that

this experiment could be performed with the short-term labelling strategy employed in the current study.

5.3 The neurogenic trajectory produces regenerated progeny that partially recapitulate the developmental birthdate order of neurogenesis

Neurogenic RPCs map to the right of cluster 5, and include proliferating, neurogenic RPCs (cluster 6) and the downstream, non-proliferating, neurogenic RPCs (cluster 7). Cells in these clusters express *insm1a*, *atoh7* and additional neurogenic genes that are involved in the generation of several neuronal lineages (Figures 16B, 18A and Appendices 1 and 6). Indeed, *atoh7* expression initiates in RPCs on their way to the last cell division generating a retinal ganglion cell and another cell that can be either an amacrine cell, or a precursor of a horizontal or of a cone cell during the development of the zebrafish retina[8,65,68]. Clusters 6 and 7 appear also similar to the transient, neurogenic RPC state that has been reported in the developing mouse retina[192]. I propose that progenitors in clusters 6 and 7 form the roots of the neurogenic trajectory from which committed precursors and regenerated neurons arise at 4 and 6 dpl (solid, black line in Figure 25). Cells in cluster 6, which are *mki67*-positive, express also *insm1a*, which promotes RPC cell cycle exit at 4 dpl in the lesioned retina[188]. Cells in cluster 6 might represent RPCs undergoing their last cell division, as suggested by the expression of *atoh7*. Accordingly, high read counts of *atoh7* are found in cells of cluster 6, to cluster 7 and eventually cluster 10. Cluster 10 represents differentiating retinal ganglion cells that are evident as early as 4 dpl (Figures 18, 21A and 22).

Interestingly, committed precursors of cone and horizontal cells were found in the regenerating retina (Figures 19A, 20 and 25), similarly to what has been described in the developing retina[56,71]. Consistent with the events during development, red cones (cluster 11) arise from *thrb*-positive cells of the photoreceptor RPC cluster (cluster 8). Interestingly, *thrb* transcripts are found in neurogenic RPCs of cluster 7 as well as at the beginning of cluster 9, which contains horizontal cell precursors becoming evident at 4 dpl (Figures 19A, 20). This is in agreement with studies of the developing zebrafish retina, where horizontal and cone cells share a common Thrb-positive progenitor[70]. Mature markers of horizontal cells, like expression of *gad1b*, which encodes for the correspondent GABA synthesizing enzyme, are not detected in cluster 9 (Figure 20 and Appendix 1). Conversely, mature markers of cone photoreceptors, like opsin transcripts, were detected at 4 and 6 dpl (Figure 19B). While it might be that mature

horizontal cells arise later than 6 dpl, their absence from the regenerated progeny could also be due to the used experimental set-up. As mentioned above (sorting gate, Figure 9C), mCherry-only positive and EGFP/mCherry-double positive cells were sorted to obtain MG and MG-derived RPCs and regenerated progeny. While MG actively expresses the mCherry transcript, driven by the *gfap* promoter fragment, the subsequent labelling of MG-derived cells is entirely dependent on the half-life of the fluorophore. Protein turnover and further cell divisions result in a constant depletion of mCherry in MG-derived cells over time. In this context, *pcna* is a marker gene of cluster 9 and points to additional cell divisions that might have diluted the mCherry label to undetectable levels (Figure 20 and Appendix 1). Inclusion of EGFP-positive only cells in the used gating strategy may reveal the pool of mature horizontal cells, which would inherit the fluorophore from their *pcna*:EGFP-positive precursors. Consistently, horizontal cell precursor markers are observed in the dataset. For instance, cells in cluster 9 express *onecut1* and *onecut2*, which encode transcription factors and are upregulated in horizontal cell RPCs in the developing mouse retina, and which regulate horizontal cell maintenance in adult animals[210–212] (Figure 18B). Earlier neurogenic RPCs in clusters 6 and 7 show some *onecut1* and *onecut2* expression too, where they might contribute to the transient state of RPCs together with additional neurogenic markers, like *atoh7*[192]. This resembles again observations in the developing mouse retina, where Onecut1 and Onecut2 redundantly regulate the development of retinal ganglion cells, as well as the development of cones, horizontal cells, and of a subset of amacrine cells, while inhibiting rod specification genes[210,212].

While differentiating cone photoreceptors were detected among the regenerated progeny, rod-specific cluster expressing mature rod markers like *rho* and *gnat1* (Figure 19B) could not be found. It is predicted that mature rods would arise as a third branch from the photoreceptor RPC cluster (Figure 25), which indeed expresses markers like *nr2e3* that in the zebrafish retina identifies precursors of both cone and rod photoreceptors as well mature rods (Figure 19A and Appendix 1). I speculate that rods either become evident only later than 6 dpl, or that they do not survive the isolation procedure, due to their complex morphology characterized by long outer segments. A third possibility might be that rod photoreceptors are replenished by their dedicated rod precursors faster than the triggering of the MG-dependent response to lesion. In this context, rod precursors form a pool of cells at the base of the outer nuclear layer and proliferate as early as 16 hpl[99,136,213]. Since the already available pool of rod precursors

would be *gfap*:mCherry-negative, there is the possibility that the resulting rod progeny have been left out, given the used sorting gate.

To summarize, in the first part of this PhD thesis I provide a comprehensive framework of the transcriptional networks that underlie regeneration in the light-lesioned retina of the zebrafish up to 6 dpl. First, MG go through an inflammatory-like and reprogrammed state before producing hybrid MG/RPCs that eventually feed-back to non-reactive MG as well move forward along the neurogenic trajectory. Neurogenic RPCs exhibit progressively restricted competence markers to regenerate neurons that include retinal ganglion cells and red cones at 4 dpl, followed by blue cone, amacrine and bipolar cells at 6 dpl.

5.4 Devising a long-term lineage tracing strategy of MG-derived cells in the light-lesioned retina

Previous studies have shown that the response of MG to a lesion involves the regeneration of all retinal neurons, independently of the injury paradigm that have been used to selectively ablate different retinal neurons[143,186,187]. Whether and how the excess of cells survives in the regenerated retina and integrates to rewire within the existent circuitry is still unclear. Moreover, even though a previous study[126] has used microarrays and RT-PCR to address long-term transcriptional signatures of the regenerating zebrafish retina, these approaches lack the single cell resolution that can profile rare and intermediate cell states as well as the transcriptional heterogeneity of a broad cell population. In the current PhD work, I sought to establish a long-term lineage tracing strategy of MG-derived cells in the light-lesioned, zebrafish retina using the conditional, CreER^{T2} transgenic line *TgBAC(mmp9:CreERt2,cryaa:EGFP)* in combination with the Cre-dependent reporter *Tg(Olactb:loxP-DsRed2-loxP-EGFP)*. The Cre-driver line takes advantage of the expression of the matrix metalloprotease *mmp9* transcript only in reactive MG as early as 8 hpl[125]. Hence, by choosing an appropriate time of 4-OHT administration, efficient CreER^{T2}-mediated recombination should occur in reactive MG only, which would be permanently expressing EGFP. Moreover, any cell deriving from recombined and proliferating MG should be EGFP-positive too. Intraperitoneal injections of 4-OHT at 6 and 24 hpl and subsequent immunohistochemistry for EGFP on retinal section at 4 dpl showed that efficient recombination occurred substantially in a lesion-specific fashion (Figure 24). It was not possible to quantify the exact number of recombined, EGFP-positive cells of retinae

from 6 and 24 hpl, injected animals for two reasons. First, the outcome of EGFP-positive cells, albeit substantial in both 6 and 24 hpl, 4-OHT injected fish, was highly variable among the animals in a group, due to the variability of the lesion as well as of the injection procedure. Importantly, 4-OHT, freshly diluted to 2.5 mM from an ethanol stock of 25 mM, was precipitating in the vehicle solution, even when the drug stock had been prepared on the same day of injection. Neither heating at 65°C, nor sonication[214] led to the complete dissolution of the drug in the solvent, thus the injected solution was always cloudy and injected concentration could not be kept constant at 2.5 mM. Second, appropriate quantification of EGFP-positive cells was hard to achieve by manual counting on retinal sections, due to the clonal nature of the cytoplasmic, EGFP-signal[215]. Hence, it was not feasible to distinguish the boundaries between EGFP-positive cells in a clone. An appropriate cell segmentation, image analysis pipeline[216], together with an improved 4-OHT injection procedure, are needed to optimize cell counting resulting from successful recombination at 6 ad 24 hpl. Alternatively, FACS of dissociated EGFP-positive, single cells could be used to get an approximate number of recombined cells. Either way, the use of the *TgBAC(mmp9:CreERt2,cryaa:EGFP);Tg(Olactb:loxP-DsRed2-loxP-EGFP)* double transgenic line is promising for long-term lineage tracing of MG-derived RPCs and progeny in the regenerated zebrafish retina. Importantly, this line represents an alternative to the *Tg(pcna:EGFP);Tg(gfap:mCherry)* one used in this work for short-term lineage tracing of MG-derived cells and subsequent scRNAseq. Indeed, the lineage tracing based on the inheritance of the mCherry reporter by RPCs and progeny is dependent on the half-life[4,193] of the fluorophore protein as well as on the proliferation rate of MG and RPCs. Hence, such a strategy allows sampling only regenerative events up to 6-7 dpl, when reporter fluorescence is still detectable via FACS. However, it does not enable long-term sampling, which is especially useful to study the appropriate integration of the regenerated progeny in the existent retinal circuit. Moreover, sampling of MG-derived cells at later time points can be the basis of an additional scRNAseq experiment, which, in turn, would characterize the transcriptional signature of later events in retina regeneration at an unprecedented, single cell detail. Hence, single cells derived from light-lesioned *TgBAC(mmp9:CreERt2,cryaa:EGFP);Tg(Olactb:loxP-DsRed2-loxP-EGFP)* could help to resolve some of the above discussed shortcomings of the present study. Moreover, the use of the Cre-driver line *TgBAC(mmp9:CreERt2,cryaa:EGFP)* is not limited to

genetic lineage tracing, but provides genetic access to reactive MG to employ other Cre-based approaches including gain- and loss-of-function experiments.

LIST OF ABBREVIATIONS

°C= Degrees Celsius

4-OHT= 4-hydroxytamoxifen

AC= Amacrine cell

AP= Alkaline phosphatase

BC= Bipolar cell

cDNA= Complementary deoxyribonucleic acid

CMZ= Ciliary marginal zone

Cre= Causes recombination

DAPI= 4′,6-Diamidin-2-phenylindol

DEG= Differentially expressed gene

DEPC= Diethylpyrocarbonate

DIG= Digoxygenin

dpl= Days post lesion

EBSS= Earle's Balanced Salt Solution

EDTA= Ethylendiaminetetraacetic acid

EGFP= Enhanced green fluorescence protein

FACS= Fluorescent activated cell sorting

FISH= Fluorescent *in situ* hybridization

GABA= Gamma-aminobutyric acid

GAD= Glutamic acid decarboxylase

GCL= Ganglion cell layer

GFAP= Glial fibrillary acidic protein

GS= Glutamine synthetase

HC= Horizontal cell

hpl= Hours post lesion

INL= Inner nuclear layer

IPL= Inner plexiform layer

ISH= *in situ* hybridization

loxP= Locus of crossover (x) in P1

MABT= Maleic acid buffer containing Tween 20 (0.1%)

MG= Müller glia

NBT/BCIP= Nitro blue tetrazolium/5-bromo-4-chloro-indolyl-phosphate

nls= nuclear localization sequence

NMDA= N-Methyl-D-aspartic acid

ONL= Outer nuclear layer

OPL= Outer plexiform layer

PB= Phosphate buffer

PBS= Phosphate buffer saline

PBSTx= Phosphate buffer saline Triton x-100 (0.3%)

PCNA= Proliferating cell nuclear antigen

PKCα= Protein kinase C alpha

PKCβ= Protein kinase C beta

POD= Peroxidase

RGC= Retinal ganglion cell

RNA= Ribonucleic acid

RPC= Retinal progenitor cell

RPE= Retinal pigmented epithelium

RT= Room temperature

RT-PCR= Reverse transcription polymerase chain reaction

scRNAseq= Single cell RNA sequencing

SSC= Saline sodium citrate

TNT= Tris NaCl Tween 20 (0.1%) buffer

t-SNE= t- Distributed stochastic neighbour embedding

UMAP= Uniform manifold approximation projection

UV= ultraviolet

µl= Microliter

µM= Micromolar

PUBLICATIONS

The work described in **RESULTS-PART I** of the present PhD thesis is currently in preparation for submission:

Laura Celotto, Fabian Rost, Juliane Bläsche, Andreas Dahl, Anke Weber, Stefan Hans, and Michael Brand. “scRNAseq unravels the transcriptional network underlying zebrafish retina regeneration”. *In submission.*

ACKNOWLEDGMENTS

This thesis would not exist without the support of Prof. Michael Brand, who proposed me to work on this beautiful project and gave me the freedom to explore my own ideas. Thanks also to my TAC members, Prof. Anne Grapin-Botton and Prof. Mike O. Karl for their support. I am very thankful to Dr. Stefan Hans, for his continuous help and strong encouragement throughout my PhD journey, and for his friendship and assistance in facing the challenges of research. My gratitude goes to Dr. Fabian Rost, who was an incredibly supportive colleague. Thanks for the hilarious and insightful discussions, and thank you for being a terrific partner in crime. Thank you Dr. Volker Kroehne and Dr. Robert Münch for all your insightful advice. Many thanks to the awesome Anja Machate, Michaela Geffarth, Daniela Zöller and Sandra Spiess, the best technicians I could wish. Thanks for all the chats and coffees in the morning. Thank you, Dr. Judith Konantz. You, your hugs and supportive smile were there whenever I needed. Thanks for having been a loyal friend. Big thanks go to Jule, with whom I had the greatest Mexican margarita in the marvellous city of Denver. Thank you for all the times you have reminded me my poster, my umbrella, my sweater and all the tiny things that a cute mom reminds to her kid. Simone, my dear. Thank you for all the coffees, the insightful conversations about the meaning of life, how awesome is the city of Dresden and, seriously, how awesome is “Friends”? Many thanks to Dr. Oliver Bludau, who taught me every secrets about *in situ* hybridizations as well as that “Anderer Benutzer” was NOT a former lab member. Thank you, Dr. Viktoria Bosak. You were the greatest support at the beginning of my PhD. A huge thank you goes to Ecem, Gaya, Sebastian and all the rest of the “Brand Lab”, past and present members. Thank you to our awesome fish caretakers, Marika, Dani, Jitka, Sylvio. Thanks for keeping our fish happy and healthy. Big thanks also to Katja Bernhardt and her invaluable patience in assisting with dozens of cell sortings, while listening to a very chatty Italian girl who was just at the beginning of her PhD. Huge thanks also to Susanne Weiche, for the cryosectioning of some of my retinae, and to the whole Dresden Genome Center for assisting with the sequencing experiment.

Finally, this work would not definitely exist without the amazing support of my friends, Elisa Cicciabella, Ivan, Mandy, Petra, Elisa Nerli, Tommaso, Cecilia, Grazia, Fabrizio, Tullio, Milica and Janko. Neither would it exist without my family. Mamma, papà, Francesca, Marta, zia Rosaria e zio Mario. I love you. Vi amo.

APPENDICES

Appendix 1

Cluster 1-Non-reactive Müller glia 1

GENES	SCORES	LOG FOLD CHANGES
glula	202.4346	5.833523
slc1a2b	183.2414	5.140877
cahz	182.9701	6.424218
selenop	180.7526	5.330976
rlbp1a	172.976	5.283491
aqp1a.1	170.692	6.171694
nfasca	153.0779	4.26958
cdo1	152.254	5.086096
gstp1	151.2817	4.877549
fosab	149.3541	5.282332
fxyd6l	137.2993	3.659705
si:ch211-152c2.3	137.0068	6.22127
ptgdsb.2	136.8515	5.723503
jdp2b	136.2845	5.292197
spock3	134.9536	4.483845
sparc	132.7677	4.232048
fosb	131.2225	4.36926
efhd1	130.836	4.415274
zfp36l1b	130.4942	4.800185
eno1a	128.9211	3.307034
icn	127.1163	4.93367
fosl1a	126.1979	4.024052
mt2	125.033	5.786455
ppp1r14aa	123.0459	4.849192
s100a10b	120.6196	4.40558
rhbg	120.5902	4.047342
atp1a1b	117.981	4.247701
zgc:165604	115.436	3.359636
pik3ip1	112.6725	4.668478
btg2	111.3905	3.15526
aplp2	108.6828	3.532805
mcl1b	108.0181	3.970384
cavin2a	105.313	4.867989
apoeb	104.8825	4.027953
prdx6	103.3325	3.429146
jun	101.6418	3.013286
socs3a	101.591	4.512181
mcl1a	101.506	3.701191
col15a1b	100.4798	5.353168
si:dkey-16p21.8	99.58262	3.89637
mCherry	96.94631	3.514687
slc38a4	95.86198	4.357031
junba	95.83254	3.064757
insig1	95.09448	3.54694
ubb	94.82858	3.61183
dap1b	94.21604	3.266351
atp1b4	94.20795	6.214067
dab2ipa	93.97268	3.3033
atp1b3a	93.81084	3.831694
hsp70l	93.31802	5.357698
epas1b	92.86622	4.177621
hsp70.2	92.45098	5.219596
junbb	92.05714	3.12044
hsp70.3	90.29752	5.169946
mycb	89.90348	3.781744
pfkfb3	89.82876	4.429638
jund	89.80586	3.04676
gulp1a	88.92162	4.50795
dhrs13l1	87.82293	4.125034
tob1b	87.59043	3.636733
gpm6bb	87.52592	4.232352

glulb	86.93468	2.942313
nrgna	86.5343	3.377606
hsp90aa1.2	85.88276	4.621142
itm2ba	85.22511	1.974312
hyal6	84.91393	4.751744
CU929418.2	84.85066	3.718532
tob1a	83.87309	3.637747
si:dkey-56f14.7	82.75861	3.836973
lin7a	82.7543	4.844591
gyg1b	82.66338	4.994621
f3b	82.60305	3.784479
csrp2	82.12587	4.869802
gpd1b	81.33405	5.089283
zgc:153704	80.99913	5.608815
vat1	80.49884	2.980296
gadd45ba	80.35832	2.952224
gapdhs	79.81317	1.740205
tmem176l.1	78.8969	2.263582
zgc:92606	78.59956	2.63212
rtn4a	78.45934	1.951095
cnn3a	78.35567	2.745401
ppp1r15a	77.76933	3.812074
gpm6ab	77.76002	2.387986
zgc:195173	77.67789	4.041749
scarb2a	77.54933	2.747275
espn	77.12132	4.101652
alkbh3-1	76.7421	3.68896
hsd11b2	76.62229	4.310727
CR383676.1	76.35896	1.11812
anks4b	75.93623	4.868054
si:ch1073-303k11.2	75.85842	3.036639
dnajb1b	75.45119	4.250009
clstn1	75.32479	2.615637
cebpd	74.94839	4.392706
map4l	74.88611	3.423485
hmgcs1	74.86773	4.080979
hsp70.1	74.67686	4.99632
slc43a2b	74.32397	4.363461
acbd7	73.97585	2.288586

Cluster 2-Non-reactive Müller glia 2

GENES	SCORES	LOG FOLD CHANGES
apoeb	106.334	4.605008
fosab	68.48776	3.710303
glula	62.38844	3.50148
rlbp1a	62.38046	3.271731
fosb	53.34531	3.0752
nfasca	52.18295	2.641236
slc1a2b	51.11511	2.606746
sparc	50.24355	2.870395
cahz	48.28159	2.865405
mt2	46.54424	4.2352
jdp2b	44.74947	3.268232
btg2	41.3894	2.187959
chrdl2	41.05654	5.588739
rdh10a	40.69147	5.249957
jun	40.10576	2.230065
zfp36l1b	39.33615	2.821576
selenop	38.59664	2.610793
sncga	38.21304	3.161439
atp1a1b	36.81063	2.349395
gstp1	34.9228	2.291466
fxyd6l	34.06401	1.88243
atp1b3a	34.0034	2.600071
aldh1a3	33.464	4.511421
ptgdsb.2	32.2485	2.588565

cdo1	31.22018	2.199245
zgc:195173	29.73603	2.713518
nrgna	28.88848	2.129215
aplp2	28.61648	1.900037
jund	28.43835	1.990542
CU467822.1	28.16533	1.877335
tob1a	28.04329	2.447768
stc2a	27.92295	3.924168
zgc:153704	27.90702	2.947695
si:dkey-164f24.2	27.81779	3.105805
f3b	27.6234	2.782377
eno1a	27.36835	1.494157
ppp1r14aa	27.29414	2.183029
si:ch211-152c2.3	27.2213	2.457709
junbb	27.09918	2.115264
socs3a	27.0586	2.826738
hspb1	26.31068	3.335919
s100a10b	25.6166	1.922733
mcl1a	25.44027	2.156741
efhd1	25.02043	1.881289
junba	24.98672	1.958903
egr1	24.31924	2.771735
clstn1	23.9734	1.831335
mstnb	23.95243	4.543767
fosl1a	23.76232	2.227058
slc38a4	23.59912	2.157702
epas1b	23.56985	2.195223
sik2b	22.82044	2.199272
si:dkey-16p21.8	22.3226	1.94325
rsrp1	21.95772	1.676835
ptmaa	21.81192	1.292658
pik3ip1	21.65113	1.894111
cavin2a	21.4658	2.047475
prdx6	21.35275	1.57737
dab2ipa	21.30005	1.702703
mcl1b	21.23481	1.918085
gyg1b	21.21754	2.125426
gulp1a	20.91881	2.079518
bgnb	20.61047	2.366395
rbpms2b	20.46741	1.680674
dhrs13l1	19.99698	1.883864
insig1	19.91047	1.677845
pfkfb3	19.65537	2.199845
slc4a4a	19.38198	2.02141
dusp2	19.2915	2.530095
mCherry	19.25415	1.687427
hopx	19.24791	2.067633
btg1	18.99416	1.188444
spock3	18.86499	1.408798
cebpd	18.65459	2.186013
mycb	18.38472	2.029505
tob1b	18.14173	1.81266
col15a1b	18.06737	1.744889
gpd1b	17.80615	1.976152
slc43a2b	17.60483	2.067804
ndrg3a	17.5949	2.007047
ivns1abpa	17.35951	1.565198
alkbh3-1	17.25975	1.818648
CU929418.2	17.22066	1.727149
espn	17.01364	1.804711
itm2ba	16.92506	1.058801
map4l	16.77126	1.681954
cav1	16.64918	2.327599
csrp2	16.62286	1.98047
rhbg	16.41214	1.40557
gnai2b	16.38775	2.707526
dap1b	16.18257	1.355489
hsp90aa1.2	16.12121	2.228899
pim1	16.09024	1.191421

nocta	15.97082	1.43132
tmem176l.1	15.77423	1.026698
im:7152348	15.72226	2.020355
rtn4a	15.69392	0.85289
vegfaa	15.52684	1.801396
mdka	15.52096	0.896474
rpz5	15.33037	1.897436

Cluster 3-Reactive Müller glia 1

GENES	SCORES	LOG FOLD CHANGES
her15.1-1	58.02736	4.22501
si:ch73-335l21.4	57.05906	3.122822
cxcl18b	52.75472	4.977983
marcksl1b	52.34999	2.36035
mmp9	50.80667	4.913656
stm	48.47406	8.312149
cdh2	45.71982	1.957092
rplp1	45.05664	1.426795
sox4a-1	44.04139	3.711539
txn	43.90092	3.346036
her9	43.68443	3.637079
si:dkey-151g10.6	42.14235	1.381599
fosab	41.71621	2.003262
si:ch211-222l21.1	41.42971	1.932316
rplp2l	41.2953	1.510434
pim1	41.13966	1.882245
ncl	41.0663	2.076798
id1	39.84898	2.902093
rps11	39.72352	1.308058
hspa5	39.58265	2.044267
hbegfa	39.39593	3.199383
rpl27	39.37078	1.390632
rtn4a	39.29338	1.448977
rps14	39.26819	1.292783
six3b	38.62426	1.994689
rps8a	38.4972	1.238654
rpl23	38.42531	1.288289
rpl9	38.19319	1.35327
rps27a	37.9284	1.250831
rps25	37.88544	1.387265
rps15a	37.86848	1.308765
rps23	37.85899	1.287878
rplp0	37.41143	1.225993
rps26l	37.09454	1.370551
her15.1	36.9349	3.66686
rpl36a	36.76678	1.341036
foxj1a	36.76667	3.513093
uba52	36.4925	1.225246
tomm20a	36.4276	2.381071
zgc:158343	36.32206	2.799567
rps2	36.2913	1.176841
her12	36.14827	4.560903
rps15	35.9535	1.2252
hsp90aa1.2	35.66359	2.108299
myl6	35.63562	2.198964
rps24	35.56178	1.204319
her4.2	35.55307	3.94767
rpl35	35.52575	1.269109
eef2b	35.24443	1.252345
rps19	35.18133	1.196425
rpl17	35.08038	1.169333
rpl32	35.0037	1.212829
her6	34.67548	2.641202
mych	34.61427	2.114997
rps10	34.58969	1.129958
cd63	34.58833	2.145319

TXN	34.55949	1.499873
rpl28	34.5156	1.169592
rps13	34.39772	1.185781
rps7	34.37388	1.129495
rpsa	34.21595	1.146769
rpl19	34.15697	1.127461
sgk1	34.14804	2.012307
rpl7	34.12462	1.149122
rps5	34.07727	1.135283
RPS17	34.06856	1.173175
her4.1	34.03872	4.4916
rps9	33.97892	1.105676
rpl14	33.95321	1.165777
rpl36	33.75732	1.332931
atp1b1a	33.72487	1.963865
rps12	33.72482	1.174201
rpl18a	33.65269	1.162939
krt8	33.58528	2.353866
rpl23a	33.49052	1.208751
ier2b	33.46938	2.473191
hsp70.3	33.42881	2.135173
cirbpa	33.37631	1.243928
si:dkey-7j14.6	33.31284	1.477176
rpl35a	33.18785	1.189859
nme2b.1	33.15488	1.203779
RPL37A	33.13859	1.198282
rpl13	33.09223	1.106846
hsp90ab1	33.00584	0.964442
crlf1a	32.99549	2.786086
eef1a1l1	32.97499	0.900469
tubb4b	32.90364	1.166004
rpl10	32.86886	1.094586
rpl31	32.85209	1.156771
rpl13a	32.73288	1.072018
rpl39	32.71383	1.118949
rps3a	32.60934	1.066306
rpl7a	32.46098	1.091045
her4.2-1	32.34126	4.645434
vmp1	32.28925	2.584382
rpl21	32.22758	1.119827
rpl10a	32.224	1.058583
ppdpfb	32.20901	1.185378
rps4x	32.0587	1.095569
rpl15	31.79554	1.086902

Cluster 4-Reactive Müller glia 2

GENES	SCORES	LOG FOLD CHANGES
f3a	55.36212	3.084531
crlf1a	48.00781	4.067601
fabp7a	45.29711	1.886966
mdka	43.44316	1.95893
vmp1	42.79474	2.970814
marcksl1a	42.75191	2.05885
crabp1a	36.21816	1.700721
clcf1	35.68691	3.765312
myl6	35.67439	2.276099
txn	33.94541	3.097077
hbegfa	33.53465	3.055269
cdh2	31.51853	1.473042
zic2b	31.50673	3.065355
akap12b	31.32176	2.762204
ppdpfb	30.08066	1.160497
flna	29.97908	2.376907
cd82a	29.05429	1.853297
six3b	29.03836	1.834222
dusp5	28.49575	2.876735

cnn2	28.39768	2.20565
acbd7	28.14837	1.591599
rpl12	27.13593	0.97616
gfap	26.47637	1.71114
si:ch211-251b21.1	26.15443	3.095376
CR383676.1	26.15266	0.72878
marcksl1b	26.13877	1.290313
rpl9	25.55742	1.026162
si:dkey-238o13.4	24.85637	2.669304
lepb	24.81931	3.228264
ckbb	24.4378	1.224566
bzw1b	24.03344	1.352009
tgif1	23.72293	1.649937
mvp	23.71933	1.615901
rasgef1bb	23.52336	1.740111
nme2b.1	23.25942	0.99787
rps2	22.98646	0.882616
col18a1a	22.78006	2.001248
elovl1b	22.62617	2.455639
rplp0	22.11063	0.830476
zgc:165604	21.60006	1.371934
mdkb	21.37778	1.696122
tjp2b	21.34831	2.258096
cd81a	20.93864	1.194727
atp1b1a	20.68841	1.644294
krt8	20.54859	1.769301
sgk1	20.44717	1.403936
si:dkey-7j14.6	20.43421	1.045556
myl9b	19.57335	1.285054
rpl19	19.47244	0.725688
rpl7a	19.40669	0.7198
si:ch1073-303k11.2	19.36223	1.230882
sall1b	19.31191	3.526893
rplp1	19.22264	0.731488
mmp9	19.20126	2.362295
rtn4a	19.05221	0.876077
c7b	18.77744	2.77231
fam129bb	18.77638	2.28985
nrp2b	18.6152	1.960113
pim1	18.60892	0.977517
tpt1	18.462	0.72684
gpm6aa	18.2658	0.829823
rps9	18.14201	0.69292
aplp1	18.09368	1.954046
igfbp5b	18.02501	2.394521
yap1	17.98789	1.520969
zgc:86709	17.95627	3.522382
rpl32	17.87215	0.675937
pros1	17.85444	1.84541
zgc:153867	17.84432	0.912853
rps14	17.80692	0.660975
rps3a	17.74341	0.66545
grb10b	17.70638	1.505983
myl12.1	17.66671	0.779661
il11b	17.64211	4.810226
lgals2a	17.63276	2.190257
pprc1	17.50554	1.910522
rack1	17.49477	0.660356
irf2	17.48677	2.837458
tpm4a	17.30012	2.237983
eef1g	17.23352	0.694715
cnn3a	17.06765	1.188983
rps11	17.03423	0.66361
rpl11	17.00854	0.683453
rps10	16.9364	0.657839
rpl36a	16.53119	0.678872
rpl23	16.49108	0.650539
rps8a	16.48499	0.622688
fabp3	16.45695	0.908652

si:dkey-79d12.5	16.39497	1.804925
mych	16.39429	1.198716
klf7b	16.3875	1.336815
actb1	16.37879	0.509623
nat8l	16.33082	1.995871
fosl2	16.27498	1.075387
npdc1b	16.27261	2.002557
rps15a	16.17297	0.677109
kitlgb	16.02795	3.640209
dbn1	15.98582	1.425459
rps12	15.98538	0.65464
rpl8	15.96231	0.584302

Cluster 5-Müller glia/Progenitors 1

NAMES	SCORES	LOG FOLD CHANGES
hmgn2	68.39232	2.729561
hmgb2b	63.28001	2.253686
rpl9	61.13248	1.683426
rpl12	60.21627	1.503011
rplp0	59.62198	1.539669
rplp1	59.1498	1.471201
rps2	56.12161	1.469378
h2afvb	55.04961	1.873374
rps9	54.23639	1.38154
rplp2l	54.04665	1.505197
rps12	53.88076	1.40589
rps3a	53.59622	1.372345
rpl23	53.5159	1.383932
rpl10a	53.37649	1.363327
rps10	52.57711	1.357023
rpl7a	52.35942	1.369403
rpl11	52.08962	1.363908
rpl3	51.9273	1.341997
rps8a	51.79038	1.363578
rpl32	51.48996	1.337257
si:dkey-151g10.6	51.31477	1.310819
rpl15	51.17108	1.409646
rpsa	50.93291	1.367237
rpl10	50.88318	1.302158
hmgb2a	50.71026	2.166219
rpl21	50.68056	1.339956
rps7	50.56798	1.311058
rps19	50.27814	1.334269
ran	49.99977	1.585142
rpl8	49.80364	1.286369
eef1g	49.54037	1.367532
si:ch211-222l21.1	49.48146	2.151709
rps14	49.47591	1.266066
rps6	49.35487	1.386384
rps5	49.35282	1.321284
rps15a	49.28632	1.34652
rps24	49.27847	1.261343
rpl19	49.21072	1.316273
rpl13	49.04952	1.298481
rps23	48.86997	1.293151
rpl18a	48.85421	1.300502
rps4x	48.74708	1.315248
rps27a	48.62541	1.287005
rpl17	48.2268	1.263866
rps16	48.21977	1.255934
rps11	48.07288	1.259169
rpl28	48.00758	1.242783
rps13	47.75944	1.283989
nme2b.1	47.68089	1.425988
rpl18	47.59703	1.262466
rpl13a	47.48776	1.201496

rps25	47.39968	1.329606
rps3	47.33768	1.295441
rps27.1	47.14485	1.247563
rpl7	47.1441	1.279642
eef1b2	47.06527	1.361622
rack1	47.02077	1.274111
fabp3	46.95059	1.628017
tpt1	46.93792	1.252315
eef1a1l1	46.3877	1.03474
rps15	46.00953	1.244218
rpl5a	45.88334	1.392658
eef2b	45.78035	1.255832
si:ch211-288g17.3	45.4481	1.849825
rpl36a	45.25935	1.28327
hmgb1b	45.25665	1.614726
rpl27	45.01738	1.249033
rpl23a	44.91151	1.277434
rpl24	44.5558	1.199122
rpl35	44.42942	1.212393
crabp1a	44.30365	1.685112
cirbpa	44.06984	1.35493
rpl35a	43.63777	1.238346
rpl39	43.45329	1.187108
hmga1a	43.04143	1.828811
ppiaa	42.9143	1.288335
RPS17	42.75465	1.163947
faua	42.63739	1.165847
uba52	42.33688	1.111466
fabp7a	42.30542	1.598577
rpl30	41.64565	1.158921
rpl34	41.45354	1.149295
rpl31	41.24366	1.106784
serbp1a	41.22321	1.21775
RPL37A	40.6989	1.172426
pcna	40.53197	2.519946
cirbpb	40.42265	1.056655
rps26l	40.22673	1.208529
h3f3b.1	40.20798	1.706689
seta	40.18583	1.592276
si:dkey-238o13.4	40.04027	3.349407
snrpd1	40.01326	1.582401
naca	39.92827	1.137398
snrpb	39.54791	1.488209
rpl4	39.33717	1.294696
rpl22l1	39.03199	1.24107
rps17	38.826	1.253697
rpl37-1	38.64377	1.188985
hnrnpabb	38.45846	1.344951
marcksb	38.33159	1.568654

Cluster 6-Progenitors 2

NAMES	SCORES	LOG FOLD CHANGES
hmgb2a	87.25797	3.047537
hmgn2	84.35824	3.128717
si:ch211-222l21.1	74.9759	2.752526
h3f3b.1	71.59824	2.711129
hmgb2b	68.31348	2.523654
hmga1a	67.3632	2.501764
tubb2b	66.21985	2.726396
h2afvb	55.49695	2.118938
mki67	51.94138	3.309106
si:ch73-281n10.2	50.23926	2.130485
stmn1a	49.73759	2.934291
si:ch211-288g17.3	47.28036	2.094867
tuba8l4	46.34163	1.940417
seta	45.18188	1.879339

dek	45.16863	2.623578
hmgb1b	42.74128	1.741089
cirbpa	42.6862	1.440792
ran	42.34833	1.582096
hmgb1a	41.80008	1.640624
ptmab	40.86359	1.430267
cbx3a	40.40691	1.952655
snrpd1	39.98124	1.816248
hnrnpaba	39.28574	1.372293
lbr	38.72216	2.611175
cirbpb	36.51932	1.116987
hnrnpabb	36.44706	1.465348
hnrnpa0l-1	36.42182	1.236985
rpsa	35.40435	1.168694
rplp0	35.37712	1.17237
rplp1	35.33271	1.132003
tubb4b	34.73749	1.308234
snrpb	34.64986	1.570525
stmn1b	34.09365	1.798956
syncrip	34.06445	1.401675
calm2b	33.89594	1.535693
tuba1a	33.82048	1.875162
rps8a	33.55668	1.094731
rpl12	33.51262	1.084751
rpl9	33.36365	1.241927
anp32a	33.29186	1.733923
rps2	33.20897	1.105596
top2a	33.0755	3.056525
ccna2	33.01615	2.93569
rps10	32.88968	1.076673
chd7	32.51994	2.048763
rps3a	32.49846	1.088833
eef1g	32.04942	1.135146
marcksb	31.92685	1.57704
rps9	31.85204	1.059009
rpl21	31.67633	1.063766
rps27.1	31.66462	1.06888
ddx39ab	31.63532	1.542528
rps5	31.55388	1.084018
cenpf	31.54819	3.224763
tuba8l	31.5033	2.619464
atrx	31.48364	1.441904
rps12	31.38468	1.059976
rpl11	31.38432	1.067273
rpl8	31.23812	1.011838
rack1	31.11732	1.068051
si:ch211-156b7.4	31.02056	2.002809
khdrbs1a	30.96933	1.123795
rpl10	30.92304	1.04692
rpl7a	30.8417	1.033722
rplp2l	30.82251	1.149688
rpl17	30.79738	1.031118
rps23	30.77365	1.030158
rps7	30.7561	1.014339
smc1al	30.75104	1.697335
rps4x	30.67778	1.067283
rpl23	30.57838	1.031162
cdk1	30.51452	3.077165
sumo3a	30.51121	1.500948
hnrnpa0b	30.49336	1.282517
rps3	30.45933	1.085661
rps19	30.39997	1.08299
nusap1	30.39967	3.574989
rps16	30.34506	0.992664
rpl15	30.18792	1.100135
ranbp1	30.18565	1.699102
rps6	30.05888	1.113032
rps15a	29.97981	1.014885
rps27a	29.95521	1.010507

rpl7	29.87661	1.020481
rbbp4	29.82339	1.833595
rpl24	29.76094	0.985218
CABZ01058261.1	29.62782	2.826436
sox11a	29.47841	3.320036
rpl32	29.3923	0.991548
rpl18	29.27316	1.010679
rpl10a	29.15111	1.003625
si:ch211-137a8.4	29.10474	1.58495
rpl3	29.00317	1.005699
hdac1	28.81993	1.406099
snrpf	28.79664	1.455658
nono	28.72711	1.620739
rps25	28.72005	1.06541
chaf1a	28.65783	2.064607
ube2c	28.6253	3.317969
rpl23a	28.60292	1.047564

Cluster 7-Progenitors 3

GENES	SCORES	LOG FOLD CHANGES
si:ch211-222l21.1	41.61283	1.779264
hmgb2b	38.623	1.602673
h2afvb	37.9501	1.413876
hmgn6	35.88954	1.159591
hnrnpa0l-1	35.50745	1.024328
rps19	34.65981	0.914957
tubb5	34.61428	1.913021
eef1g	34.50315	0.944486
hmgn2	34.45097	1.665736
cirbpb	33.95919	0.873041
rps10	33.86999	0.886373
rpl23	33.5192	0.87815
rplp0	33.43109	0.853234
rps12	33.38526	0.91177
rplp1	33.13024	0.839943
rpl11	33.08396	0.883605
rpl17	33.00816	0.854162
fabp7a	32.99862	1.321531
rps9	32.12623	0.828431
rps5	31.86653	0.849497
rps3a	31.68187	0.832876
rps27.1	31.66276	0.856041
eef1b2	31.55722	0.932367
rpl15	31.44047	0.882216
rpl21	31.41321	0.838808
rps13	31.09816	0.845566
rpl7a	30.99184	0.810452
rpl8	30.97138	0.794834
rplp2l	30.96316	0.920136
rps7	30.83394	0.78795
rpl13	30.68253	0.80433
rpl12	30.45439	0.809612
rpl28	30.41	0.812544
rps4x	30.4074	0.82514
rpl10	30.38111	0.792707
rps15a	30.33371	0.827185
rpsa	30.12223	0.801591
rpl10a	29.91078	0.779753
si:dkey-151g10.6	29.90657	0.768597
rpl32	29.80276	0.828408
rps8a	29.78196	0.771633
rpl24	29.74594	0.792007
rpl18	29.6037	0.791923
rps25	29.56172	0.856717
rpl3	29.30279	0.778003
rpl35a	29.29649	0.839905

rps16	29.25809	0.781751
fabp3	29.08586	1.149132
rps24	28.81985	0.755633
stmn1b	28.65819	1.45516
faua	28.60137	0.820814
si:ch211-288g17.3	28.44066	1.324968
rps14	28.36089	0.728639
rps6	28.25324	0.825859
rps27a	28.15806	0.75181
sox11b	27.82893	2.157066
rpl7	27.66368	0.753323
rps15	27.65852	0.770884
rps2	27.62746	0.743544
rack1	27.57765	0.769946
rpl19	27.32542	0.712889
ppiaa	27.16442	0.85877
rps11	27.00904	0.743216
rpl18a	26.99198	0.726324
rps3	26.98615	0.789535
hnrnpabb	26.85308	1.010206
rps23	26.71899	0.722134
cirbpa	26.68651	0.857137
rpl27	26.49814	0.747078
rpl23a	26.48748	0.792257
tp53inp2	26.20919	1.926506
khdrbs1a	26.02629	0.786469
rpl39	25.90498	0.765112
cnp	25.84046	1.600691
rpl9	25.76854	0.810308
rpl13a	25.6954	0.666965
rps26l	25.57702	0.781824
ptmab	25.47652	0.82161
hnrnpaba	25.3942	0.783417
rpl36a	24.54305	0.736451
marcksb	24.38404	1.152521
rpl5a	24.31759	0.778607
snrpb	24.28328	1.005743
rps17	24.15112	0.820434
rpl35	23.73368	0.702389
naca	23.6569	0.694909
rpl30	23.61177	0.687989
h3f3b.1	23.56041	0.950644
rpl31	23.53444	0.673664
hdac1	23.37359	1.009632
ddx39ab	23.33385	1.070854
RPS17	23.28409	0.667255
rpl22	23.16479	0.731656
uba52	22.68652	0.617799
snrpd1	22.41313	0.968627
rpl34	22.39778	0.673187
serbp1a	22.22529	0.69851
si:dkey-56m19.5	22.13316	1.587212
rpl14	22.03477	0.628465
insm1a	21.95723	2.050113

Cluster 8-Photoreceptor precursors

GENES	SCORES	LOG FOLD CHANGES
hmgb2a	67.12348	2.779354
neurod1	59.31221	4.457813
hmgn2	56.68037	2.804169
hmga1a	54.15988	2.229558
otx5	53.13665	4.293461
h3f3b.1	52.59372	2.427685
stmn1a	49.46758	3.096511
si:ch73-281n10.2	49.11773	2.244505
hmgb2b	48.6291	2.011792

nr2e3	47.91886	3.9563
pde6gb	44.3974	4.142102
h2afvb	43.6097	1.809594
h2afx	40.63955	3.024345
tuba8l4	40.17926	1.770045
tubb2b	39.5692	2.097799
hmgn6	38.96754	1.345106
stmn1b	38.70943	2.050159
faua	38.42354	1.19576
arl13a	38.16461	3.777628
chaf1a	37.5683	2.378392
crx	37.20008	3.141419
si:ch211-156b7.4	37.1531	2.186158
rps27.1	36.82118	1.130154
si:ch211-288g17.3	36.57405	1.676701
anp32e	35.88087	1.735584
inhbb	35.48219	3.087439
ptmab	35.37823	1.268137
dek	35.36619	2.233665
rplp1	35.1895	1.066069
h2afva	35.14886	1.827295
cirbpa	34.75042	1.185678
si:ch73-28h20.1	34.5794	4.08181
rbbp4	34.35822	1.939522
rps9	34.31971	1.02952
rps5	34.1325	1.087626
rplp2l	34.03513	1.17622
rpl21	33.5185	1.059054
rpsa	33.44976	1.076922
rps10	33.04453	1.010643
rpl10	32.74474	1.043875
cxxc5a	32.58	2.115902
rpl7a	32.43849	1.022391
rpl11	32.37378	1.027662
rps23	32.34606	1.042909
rack1	32.30142	1.076356
insm1a	32.22336	2.895099
rps7	32.1926	1.021976
rps3	32.12946	1.04431
atp1a3b	31.93337	3.332613
rps19	31.84344	1.010192
rpl18a	31.7183	1.01771
rps4x	31.4954	1.038497
ran	31.45869	1.139657
rps3a	31.36823	0.995695
rps25	31.31455	1.067583
rpl28	31.12911	0.963129
msi1	30.95373	1.650295
rpl8	30.82375	0.984677
six7	30.60105	3.94679
lbr	30.58515	2.219437
rpl24	30.45271	0.952076
rpl15	30.40518	1.067016
rps14	30.34067	0.921545
rpl23	30.28661	0.977214
rpl18	30.26096	0.981683
rps16	30.24792	0.964312
pcna	30.1896	2.281074
rps6	30.10794	1.080719
khdrbs1a	30.10605	1.004436
rps12	30.09531	1.02113
rps8a	29.98163	0.976803
rrm2-1	29.90607	2.406019
rpl10a	29.89342	0.939995
rps24	29.74668	0.93827
rbp4l	29.58597	3.060017
rps13	29.55441	0.949156
snrpd1	29.49668	1.342951
thrb	29.49044	3.617176

rpl17	29.48057	0.951196
rpl13	29.37915	0.956986
rps15	29.22549	0.958226
rps27a	28.99521	0.949157
snrpf	28.95937	1.355659
rpl3	28.85182	0.95441
rpl19	28.73604	0.925646
rpl7	28.69171	0.960864
seta	28.57745	1.258389
rps15a	28.40662	0.91184
uba52	28.37418	0.907005
rpl32	28.36332	0.912044
mki67	28.3106	2.186181
rpl30	28.28944	0.941928
ppiab	28.28312	0.947445
si:dkey-151g10.6	28.18334	0.889485
rps2	28.0612	0.917724
eef1g	27.74969	0.959606
slbp	27.74192	2.341869
cct2-1	27.73662	1.251081
mibp	27.68613	2.588896
rxrgb	27.67214	3.21361

Cluster 9-Horizontal cell precursors

GENES	SCORES	LOG FOLD CHANGES
pde6gb	45.31855	5.805341
h3f3b.1	34.27803	2.064032
tmsb4x	34.15756	1.992909
hmgb1b	28.27168	1.809103
h2afvb	27.3001	1.631614
hmgn2	26.91901	2.163399
prox1a	26.91223	3.606124
tubb5	24.92814	2.359227
zeb2a	22.976	2.637862
tubb2b	22.90328	1.908595
si:ch211-288g17.3	22.47307	1.657691
h3f3d	22.46573	0.929173
cotl1	22.42771	1.616795
ywhah	22.39713	2.09093
hmgn6	22.19003	1.086266
rem1	21.49858	8.354462
onecut1	21.43028	5.181398
tfap2b	21.32709	5.268526
hmgb2b	21.25424	1.528168
stmn1a	21.21375	2.578373
ptmab	21.08867	1.104574
fabp3	21.0306	1.377564
eef1g	20.96286	0.913055
rps27.1	20.50296	0.867427
onecutl	20.34417	7.409418
tox	20.27131	2.241893
golga7ba	20.17522	2.910444
CR361564.1	19.95805	7.876082
ndrg4	19.79968	2.136945
stmn1b	19.54752	1.511134
rbfox2	19.02843	3.179933
rpl28	18.7783	0.775095
rps10	18.54901	0.764748
rps9	18.3002	0.718525
rbbp4	18.2825	1.732675
rps5	18.07771	0.736728
rps19	17.97738	0.791886
hnrnpaba	17.93326	0.935697
rps12	17.93323	0.755777
rpl10	17.88057	0.713867
rps4x	17.8334	0.733099

nme2b.1	17.78885	0.871106
seta	17.73796	1.204391
faua	17.69118	0.793982
hmgn7	17.56817	1.301896
rpl7a	17.42317	0.697598
si:ch73-1a9.3	17.15257	1.245742
si:ch211-222l21.1	17.11261	1.312136
atrx	17.06371	1.236733
si:ch73-281n10.2	17.04289	1.513536
rpl32	16.88686	0.71674
sumo3a	16.8608	1.308553
rpl23	16.6083	0.67206
rplp1	16.46432	0.633801
rack1	16.45527	0.720065
six6b	15.97176	2.492325
rpl24	15.96949	0.700263
khdrbs1a	15.95052	0.82304
rpl21	15.85818	0.657527
chd4a	15.79557	1.609508
hnrnpa0l-1	15.71274	0.720775
rps3a	15.69729	0.670446
hmgb2a	15.68408	1.461215
rpsa	15.63609	0.666254
rpl17	15.56202	0.653774
rplp2l	15.5487	0.759737
rpl19	15.45128	0.632404
plekhg4	15.42409	2.689051
cirbpa	15.32252	0.796741
h3f3b.1-1	15.31708	1.084022
si:dkey-28b4.7	15.11673	1.687421
rpl18	15.04653	0.639845
h2afx	15.01055	2.108588
fkbp1aa	14.93795	1.043141
ndufa4l	14.89999	0.926854
rpl11	14.88396	0.668128
tmsb	14.86012	1.917511
zc4h2	14.84985	2.016159
rps3	14.83941	0.708161
rpl13	14.83679	0.597651
rpl8	14.60755	0.605775
rps8a	14.55141	0.602846
rps7	14.49462	0.593028
rpl3	14.48732	0.630447
pclaf	14.42333	2.173115
tmeff1b	14.40351	1.498789
rps27a	14.25091	0.582784
mab21l1	14.21964	1.896145
uba52	14.16737	0.620056
si:ch211-156b7.4	14.12852	1.598427
rps6	14.1061	0.69013
lsm6	14.0396	1.410926
rps14	14.0236	0.589618
pcdh8	14.00961	4.083307
rps25	13.90268	0.687786
chaf1a	13.8414	1.687628
rpl10a	13.80906	0.583319
rrm2-1	13.73925	2.040427
dalrd3	13.65998	3.842135
rps13	13.61701	0.589053

Cluster 10-Retinal ganglion cells

GENES	SCORES	LOG FOLD CHANGES
elavl3	77.99724	6.284737
tmsb	69.54066	4.788538
tubb5	69.38703	5.394479
stmn1b	66.6868	3.850678

gap43	63.14544	8.218997
tuba1c	54.22678	4.222291
mllt11	53.4115	4.735611
stmn2b	52.82681	7.843676
vim	52.47554	4.247157
tmsb4x	47.32957	2.277806
marcksl1b	44.28115	2.224685
rbpms2b	42.33289	3.402827
tuba1a	41.57	2.990813
uchl1	41.34855	4.457408
fabp3	41.18753	2.427572
gng3	39.73628	4.544009
rtn1a	39.29915	3.117471
tmsb2	38.12695	5.780561
cnp	36.78994	3.632299
rtn1b	36.76604	4.318269
stmn2a	35.2411	7.416444
dpysl3	35.18645	4.678086
klf7b	34.3878	2.974934
vdac3	34.21999	2.9019
si:dkey-280e21.3	33.88601	5.158335
alcama	33.70361	4.884744
nova2	33.13497	2.707599
ywhaz	33.05883	3.038552
rbfox2	33.05655	4.428223
inab	32.79713	7.990091
jpt1b	32.71454	2.790272
elavl4	32.17347	7.08375
islr2	32.03269	6.528104
map1b	31.80873	4.402174
si:dkey-276j7.1	31.67456	3.559438
vat1	31.22507	2.382035
stmn4l	30.59625	7.518034
si:dkey-56m19.5	29.84246	2.89128
rab6bb	29.55522	4.517086
gdi1	29.28638	3.562044
stmn4	29.16547	8.488958
tubb4b	29.07067	1.347496
tubb2	28.98465	7.38816
cfl1	28.3221	1.294718
tuba2	27.83016	5.600058
anxa13l	27.74301	6.787529
scrt2	27.62558	4.455796
maptb	27.5245	4.89145
gpm6aa	27.41314	1.519471
tubb2b	27.31199	1.847709
tmeff1b	26.70131	2.429315
eef1g	26.67317	1.298144
zgc:65894	26.34632	5.259031
h2afx1	25.94992	1.579253
marcksb	25.81384	1.759351
ywhag2	25.34646	3.982825
ppp1r14ba	25.03397	4.914696
kif3cb	24.97928	5.973311
dpysl2b	24.6315	3.52029
dbi	24.59581	1.687151
dpysl5a	24.47413	3.198285
ank2b	24.39385	2.932426
alcamb	24.06705	4.352358
kif1aa	23.97997	3.952138
gpm6ab	23.67161	1.628277
nsg2	23.29612	2.445737
syt11a	22.97694	2.690351
epb41a	22.92062	2.399034
zgc:153426	22.86145	4.54161
tuba8l4	22.6835	1.430788
prdx2	22.47492	1.330636
ebf3a-1	22.44803	7.209119
zgc:101840	22.26582	4.986061

ywhah	22.20234	2.360124
map7d2b	22.16343	7.872359
ywhaqa	21.70571	2.025177
csdc2a	21.65125	2.832964
si:dkeyp-75h12.5	21.29547	2.491817
fkbp1aa	21.15021	1.322054
hmgb1b	21.08457	1.360093
si:busm1-57f23.1	21.06547	4.324352
hsp90ab1	20.98585	1.071818
gng5	20.91486	1.871557
dclk1b	20.90953	4.903087
add2	20.89866	5.772412
prph	20.81114	8.07297
si:ch211-284f22.3	20.77369	3.973699
cd99l2	20.75372	4.002909
anxa5b	20.66391	4.878666
si:ch211-195b15.8	20.33169	3.041671
si:dkey-28b4.7	20.18958	2.106191
scg2b	20.14479	6.470963
rps19	19.99676	0.791599
tbcb	19.79526	1.865861
adcyap1b	19.61666	8.515849
coro1cb	19.55775	2.983227
zc4h2	19.47209	2.499441
kif5aa	19.36726	4.668578
eml1	19.28413	3.152325
sox11b	19.26969	2.320665

Cluster 11-Red cones

GENES	SCORES	LOG FOLD CHANGES
rbp4l	69.7916	5.663568
thrb	68.77347	4.534097
aanat2	67.73853	6.975239
rcvrn2	62.65492	5.942515
neurod1	51.49628	3.872108
guk1b	49.40574	6.647086
arl13a	48.37612	4.121648
atp5mc3b	46.36296	2.320497
ppdpfa	43.9301	4.699728
ckmt2a	43.92736	6.408275
si:dkey-72l14.3	42.8831	6.207275
fkbp1b	39.92556	3.357849
crx	39.71903	3.784886
zgc:109965	39.18085	4.470721
atp2b1b	38.81934	4.906697
atp5f1b	37.82442	1.95541
atp5pd	35.82613	2.040931
anp32e	35.72473	2.075331
sypb	35.10272	4.735727
cox4i1	34.78309	1.695577
six7	34.2225	4.38798
elovl4b	33.96679	4.435674
cox6a1	33.06525	1.609958
slc25a5	32.63343	1.301928
atp5mc1	32.58017	1.931897
ndufa4l	32.05808	1.575375
gpx4b	30.99536	2.202867
snap25b	30.96257	3.156217
si:dkey-44g23.5	30.96007	4.700011
si:ch73-28h20.1	30.71418	3.563787
xbp1	30.67335	1.851338
atp6v0cb	30.52959	2.497104
h3f3b.1-2	30.08783	1.688843
atp5po	30.03177	1.895008
cox5aa	30.00272	1.830919
hmgn6	29.99281	1.222049

COX5B	29.74447	1.8362
slc25a3a	29.61564	5.821687
rps27.1	29.42719	1.127909
cox8a	28.84851	1.458173
rps5	28.80428	1.122909
rps7	28.566	1.099829
rpl19	28.1412	1.180483
rps6	28.07899	1.131963
cox4i2	27.99816	2.492439
rxrgb	27.97975	3.893286
cox7a2a	27.63653	1.958717
atp5fa1	27.63401	1.587958
mt-co2	27.30873	1.423971
rps4x	27.05352	1.099805
rs1a	26.95639	4.58965
rpl18a	26.94043	1.020689
rpl17	26.9024	1.017889
unc119b	26.49944	3.737752
ckbb	26.37506	1.418717
ndrg1a	26.36163	4.804291
zgc:153441	26.18509	4.608101
tulp1a	26.04637	4.748461
rpl7a	26.03493	1.007829
selenot1a	25.78408	1.917765
mt-nd1	25.76087	1.508603
mdh2	25.66134	1.89292
rpl15	25.65539	1.094472
rpl3	25.59778	1.012274
rps13	25.45943	0.947067
rpl10	25.42695	0.981639
opn6a	25.41356	4.374789
tmem244	25.32793	4.210473
rack1	25.10625	1.089299
mt-co3	25.00665	1.357063
sall1a	24.9954	3.489039
nr2e3	24.94977	3.0094
faua	24.79133	0.986644
mt-atp6	24.7508	1.446356
rpl13	24.65279	1.021046
uba52	24.62097	0.881376
si:dkey-220f10.4	24.58719	4.560071
rpl8	24.55198	0.955642
atp5f1d	24.37313	1.674707
atp5if1b	24.27318	2.072637
eef1g	24.20253	0.985345
arl3l1	24.16562	5.16978
rps19	24.13347	0.902123
ldhbb	24.12926	4.918907
rpl30	24.08674	1.012763
rpl7	23.84151	0.960257
rps9	23.83957	0.917827
rpl10a	23.79163	0.925878
rps8a	23.76958	0.938959
atp5pf	23.61867	1.753031
naca	23.55142	0.975249
rpl28	23.45271	0.939131
inaa	23.39441	6.496418
zgc:103625	23.17529	5.125855
gngt2a	23.17059	4.153347
rpl32	23.1554	0.911996
slc25a18	23.04619	2.834619
tcima	22.94127	4.042627
rpl13a	22.89417	0.89982
pcdh10a	22.84693	4.186197

Cluster 12-Blue cones

GENES	SCORES	LOG FOLD CHANGES
arl13a	53.44701	4.167643
rbp4l	50.26901	5.163287
gngt2a	46.63506	5.043726
ppdpfa	40.0969	4.248779
cxxc5a	38.50266	2.775964
ckmt2a	37.29204	5.475167
zgc:109965	36.8304	4.480729
neurod1	36.21203	3.369782
atp5mc3b	35.98587	1.439428
fkbp1b	35.94051	2.987205
si:ch73-28h20.1	35.54596	5.054293
crx	34.26119	3.467672
rpl19	33.96902	1.001766
anp32e	31.89721	1.759705
nr2e3	31.62177	3.179869
h3f3b.1-2	31.41482	1.656203
zgc:153441	31.2162	4.905677
syt5b	31.06565	4.943227
rps5	30.94678	0.935383
cox4i2	30.92143	2.457739
rps7	30.71694	0.876183
snap25b	29.92464	3.075304
tmem244	29.14986	4.427743
rpl7a	28.83632	0.843263
rps4x	28.46353	0.889535
gpx4b	28.223	2.046368
rpl8	28.17669	0.76419
atp2b1b	27.91111	3.994917
laptm4b	27.8376	1.921811
atp6v0cb	27.81422	2.232342
ndrg1a	27.62278	4.717072
rpl13	27.513	0.828256
rack1	27.1977	0.849815
rpl17	26.57596	0.806814
sypb	26.56752	3.859398
rpl15	26.52748	0.88169
rps27.1	26.41185	0.897525
hmgn6	26.19894	1.068841
rpl18	26.04649	0.781026
rpl10	26.02632	0.736429
opn6a	25.99137	4.398881
rps8a	25.96126	0.77164
rpl18a	25.87892	0.797071
ckbb	25.84623	1.011829
eef1g	25.27461	0.824545
rpl7	25.19827	0.788658
tmx3a	25.13877	4.646425
ndrg1b	24.68048	3.608685
rpl3	24.63154	0.774188
rpl28	24.57047	0.798833
rps6	24.33335	0.859113
rpl11	23.90525	0.715239
rpl10a	23.88967	0.715115
selenot1a	23.56553	1.665691
aplnra	23.55503	4.454495
rps9	23.5456	0.662601
rpl32	23.46778	0.702767
si:dkey-220f10.4	23.39208	4.439289
rpl13a	23.33629	0.704063
slc25a3a	23.30503	4.471028
ndufa4l	23.14509	1.216362
tmsb2	23.12352	3.023331
atp5f1b	22.79394	1.072304
rps10	22.68702	0.706679
fstl5	22.6635	4.286493
tulp1a	22.5865	4.166075

jun	22.32785	1.050023
slc25a5	22.25247	0.643798
faua	22.06378	0.750688
zgc:112294	21.98085	4.350487
ldhbb	21.93536	4.192356
rps2	21.90655	0.706074
cldn2	21.61791	4.262047
mt-co2	21.54855	0.913247
daam1a	21.53014	2.755152
rps23	21.25978	0.711748
pdcl	21.21949	1.655369
mt-co3	21.14372	0.87874
atp5pd	20.9451	1.225665
rs1a	20.81515	4.391171
ptmab	20.67576	0.784829
prdm1a	20.59002	3.912134
hmga1b	20.27947	3.729669
elovl4b	20.1759	3.143271
rcvrn2	20.09399	3.323274
rpgrb	20.08928	2.939603
rps3a	19.78378	0.59144
rpl21	19.62358	0.611033
rps13	19.59334	0.660726
rps3	19.5315	0.688179
prph2a	19.50964	4.992938
rpl30	19.46901	0.742855
unc119b	19.31224	2.952768
nptna	19.24524	3.834177
rps27a	19.16818	0.580068
uba52	19.08483	0.631839
xbp1	18.98545	1.097527
rpl5b	18.95905	0.868398
zgc:103625	18.7948	4.230989
naca	18.60692	0.707758

Cluster 13-Amacrine cells 1

GENES	SCORES	LOG FOLD CHANGES
elavl3	47.59343	4.885855
hmgb3a	39.8751	2.369703
zc4h2	39.0952	3.821973
marcksl1b	36.37799	2.372142
si:ch73-1a9.3	33.59291	1.881838
snap25b	33.55449	4.011559
stx1b	32.71359	5.640388
ptmab	32.12175	1.364897
nova2	31.29289	2.577271
ywhah	31.12801	2.594067
stmn1b	30.46353	2.355851
gng3	29.19424	4.017313
h2afx1	28.89923	1.801385
ndrg4	28.50275	2.811211
tkta	27.96958	3.454151
ppp1r14c	27.66105	5.043893
slc32a1	26.97668	6.620533
hmgn7	26.25145	1.725022
ptmaa	26.10138	1.471296
syt1a	25.45311	5.426211
gpm6aa	25.39178	1.586852
stxbp1a	24.8139	5.629207
tuba1c	24.06178	2.418559
hmgn6	23.91729	1.214541
rbfox2	23.27165	3.688538
atp6v0cb	23.19559	2.439435
h2afy2	23.18473	2.073512
ywhag2	23.18036	3.996521
ccni	22.97561	1.929035

mdkb	22.81258	1.929415
ppiab	22.71882	1.18006
pax6a	22.39902	3.533085
atp6v1g1	22.28578	2.394785
h3f3d	22.00778	1.025007
kdm6bb	21.434	3.426254
ppp1r14ba	21.39812	3.622981
jpt1b	20.91422	1.77291
atp6v1e1b	20.75832	2.28162
apc	20.70758	3.184223
pax10	20.51826	7.094688
mab21l1	20.42645	2.670468
rtn1b	20.4185	2.917535
calm2b	20.40911	1.88776
hsp90ab1	20.29822	0.873705
si:ch73-290k24.5	20.2575	5.234352
h3f3c	20.25117	1.489621
tfap2a	20.22489	6.172959
si:dkey-280e21.3	20.09857	3.644492
basp1	19.91347	4.168926
sncb	19.70108	4.021834
sumo2b	19.41626	1.408166
gng2	19.25251	5.368484
elmo1	19.24801	2.884595
rbfox1	18.74553	5.295085
vamp2	18.55072	2.290857
dnajc5aa	18.41609	3.033177
csdc2a	18.32683	2.371032
eno2	18.22068	3.144123
si:dkey-81l17.6	18.19662	3.702047
pax6b	17.9009	2.382847
atp1a3a	17.81363	3.531244
gpm6ab	17.69015	1.382048
cspg5a	17.64552	1.714193
fscn1a	17.59551	2.139647
rab11bb	17.48482	3.434072
ndrg2	17.40715	2.38387
cnrip1a	17.22821	2.926808
tuba2	17.21075	4.06776
tmsb4x	17.08338	1.030746
zgc:100920	16.91031	4.65483
scrt2	16.76306	3.020741
tiam1a	16.74403	4.688462
gad2	16.70621	6.308122
fez1	16.56593	1.960237
hp1bp3	16.21523	1.792404
nrxn1a	16.14522	4.830284
map1aa	16.12482	2.401688
vdac3	16.0427	1.638497
hist2h2l	16.0084	1.765643
gpr85	15.94105	2.557376
nsfa	15.93045	3.221651
vdac1	15.88041	1.517518
st8sia5	15.80181	4.730092
cdc42	15.73744	1.58497
calm3a	15.70304	1.509706
itm2ca	15.58153	3.611167
fkbp1aa	15.57737	1.156489
si:ch73-119p20.1	15.39997	4.765376
foxg1b	15.35191	2.092312
si:dkey-276j7.1	15.35012	1.675403
ywhaqb	15.33956	1.094246
sv2a	15.30951	5.490233
fabp3	15.28771	1.174806
marcksl1a	15.25371	1.048944
calm2a	15.20846	1.650956
rnasekb	15.11282	1.556983
hmgn3	15.08429	1.61071
cbx1b	15.01925	2.906498

h3f3b.1-1	15.01093	1.021742
fam49al	14.97274	2.882889

Cluster 14-Amacrine cells 2

GENES	SCORES	LOG FOLD CHANGES
gng13b	45.72647	6.802714
mdkb	38.88173	4.460174
calm2b	28.64004	3.109851
rbfox1	28.00863	7.155849
scrt2	24.92979	5.272262
tiam1a	24.80428	6.726093
gnb1a	24.47663	3.227254
ppp1r14c	23.27609	5.525704
olfm1b	23.01315	5.576355
ndrg4	22.51121	3.057493
pvalb6	21.84878	9.853527
ptmaa	20.86428	1.855204
stx1b	20.52764	5.374101
sox2	20.08649	3.241815
nrxn1a	19.6996	6.766798
CR855337.1	19.32253	6.077991
rcan3	18.9845	6.211946
marcksl1b	18.0022	2.097161
snap25b	17.46151	3.774786
fkbp1b	16.53998	3.229223
stmn1b	16.17747	2.007081
syt1a	15.97197	5.825586
ppdpfb	15.76896	2.269364
elavl3	15.47612	3.887324
pcdh19	14.70898	5.537436
si:dkey-35i13.1	14.35941	7.969619
si:ch73-119p20.1	13.96951	5.74709
tmem178b	13.47456	4.701291
tkta	13.37233	3.268823
slc18a3a	13.14749	8.632327
calm3a	12.85786	2.206824
si:dkey-280e21.3	12.76008	4.117484
mpp6b	12.7557	3.339702
atp6v0cb	12.62214	2.675064
tnc	12.59912	3.75455
tfap2a	12.58726	5.362655
palm1b	12.42765	4.401007
slc32a1	12.21835	5.592228
isl1	11.40429	5.900709
cdh18a	11.33207	4.791257
gnao1b	11.25566	5.799741
st8sia5	11.23325	5.268324
ism1	11.17648	5.51096
gpm6aa	10.93974	1.344212
vamp2	10.87052	2.421702
mfge8b	10.78611	5.282326
pcbp3	10.68497	5.640929
nova2	10.68154	2.111907
gldn	10.64083	6.705519
zgc:92912	10.52051	6.795085
stxbp1a	10.50695	4.687234
ctnna2	10.33344	3.887794
h2afy2	10.27837	1.863886
ywhag2	10.23504	3.325377
gng3	10.04401	2.854667
hmx4	9.906478	3.542741
kif1aa	9.864943	3.869918
ulk2	9.744619	3.450796
myt1b	9.740718	4.443648
si:dkeyp-117h8.2	9.73509	4.334377
foxn3	9.665981	4.806186
atp2b3a	9.658111	6.577282

rnasekb	9.606361	1.709561
gnai2b	9.586996	3.220163
rgs11	9.583486	6.444658
zgc:101840	9.544594	4.547499
si:dkey-81l17.6	9.395407	3.981873
atp6v1e1b	9.331401	2.304917
rab3c	9.250629	5.717923
eno2	9.198894	2.995109
ywhah	9.113813	1.685589
lrrtm2	8.945631	5.791002
apof	8.906734	7.841937
grm6b	8.88651	6.393328
zfhx4	8.799727	3.478366
pcdh7b	8.759848	4.501428
tfap2b	8.524959	4.162265
si:ch211-242b18.1	8.523545	4.035509
khdrbs1b	8.509533	2.889556
rassf4	8.509409	7.211474
atp1a3a	8.389304	3.403485
si:dkey-7j14.5	8.371306	4.97475
tmem59l	8.299499	3.087041
rhocb	8.290924	2.350177
zc4h2	8.25281	2.310899
ctnnbip1	8.197758	2.358332
nhsl2	8.10646	3.857315
rgs9bp	8.101274	9.685951
slc6a1b	8.053	5.351061
pcp4l1	8.019696	5.120007
gad1b	7.989145	6.296114
sox13	7.907565	3.139322
atpv0e2	7.879141	1.909164
calm1b	7.632143	2.284139
mef2d	7.547438	2.751391
nptnb	7.408628	4.454635
gad2	7.342015	4.798161
tpd52l1	7.319592	3.633606
gpr85	7.270275	2.846332
mid1ip1l	7.25369	2.44454

Cluster 15-Bipolar cells

GENES	SCORES	LOG FOLD CHANGES
ptmab	11.40276	1.487681
samsn1a	11.34755	7.161874
nova2	11.23821	2.838592
rs1a	10.40148	5.327133
scrt2	10.1512	4.016829
si:ch73-1a9.3	9.9276	1.661365
gnb3a	9.224526	8.706532
mdkb	8.979985	1.945934
marcksl1b	8.880391	1.312654
gng13b	8.705363	5.436635
tmem178b	8.529777	4.663744
hmgn6	8.497252	1.350293
crx	8.285783	2.663531
vsx1	7.944711	7.747238
myt1b	7.572746	4.166636
neurod4	7.407536	2.815643
prox1a	7.071976	2.751247
golga7ba	6.983426	2.397141
nsg2	6.878228	2.516883
h3f3c	6.7116	1.350272
ddah2	6.698836	2.308382
ndrg4	6.697749	1.982662
pdcl	6.658487	1.699536
atp1a3a	6.653254	3.195421
ppp1r14c	6.585759	3.484623

syt5b	6.347886	3.98757
rorab	6.300248	3.410335
scg3	6.198381	2.738588
smarce1	6.154704	1.374953
lhx4	6.120314	4.274254
eml1	6.114842	2.521654
otx5	6.047013	2.319762
gpm6aa	6.028522	1.10494
atp1b2a	5.843028	2.165402
mpp6b	5.742248	2.704507
zc4h2	5.720346	2.033676
ppp1r1b	5.569129	4.717474
elovl4a	5.536537	2.340507
hnrnpa0a	5.476362	1.125403
vamp1	5.439999	6.211827
sypb	5.40134	2.61771
mid1ip1b	5.35729	0.844224
gfra1a	5.3465	3.234407
pcp4l1	5.155189	4.338975
h3f3b.1-2	5.141631	0.962969
fam107b	5.023374	2.349857
bcl2l10	4.945974	1.558781
h3f3b.1-1	4.919767	0.868025
ndrg1b	4.905591	2.516608
sox4a-1	4.899141	2.362223
ckbb	4.874777	0.909867
celf3a	4.851412	2.779972
si:ch211-260e23.9	4.798407	2.211287
isl1	4.767258	4.190191
jpt1b	4.678518	0.934096
stx3a	4.674256	2.516482
sv2bb	4.625063	4.513708
snap25b	4.59484	1.978399
si:dkey-253i9.4	4.580679	3.151839
hmgb1b	4.519246	0.773527
lmo4b	4.490333	3.536036
mbd3b	4.440171	2.648721
ubl3b	4.43759	2.39006
h2afx1	4.414063	0.966692
sox12	4.368863	3.882088
chn1	4.362575	2.214303
grb2b	4.324765	1.536648
tnnt1	4.290765	6.435362
zgc:77784	4.252775	4.691112
hnrnpaba	4.244096	0.570516
ptmaa	4.234839	0.689352
igsf21b	4.203497	4.630031
ndrg3b	4.196335	1.725933
hmgb3a	4.191482	0.89979
si:dkey-56m19.5	4.142285	1.285764
tp53inp1	4.141752	1.42014
ctbp2a	4.138351	2.247343
pcdh19	4.138004	3.290814
itm2ca	4.115719	2.781084
sesn1	4.09314	1.53416
clstn3	4.08592	3.937091
ucp2	4.075579	1.194929
si:ch211-140m22.7	4.022749	1.520209
jagn1a	4.017736	3.121504
selenow1	3.996627	0.988462
dab1b	3.968604	3.615132
h2afva	3.961214	0.857349
khdrbs1a	3.930096	0.57099
bhlhe23	3.922093	5.273127
ube2e1	3.86386	1.19057
oaz1b	3.858248	0.776799
ssbp3b	3.842726	1.742057
si:dkey-28b4.7	3.83905	1.349461
ppp1r9bb	3.836051	4.274052

si:ch211-242b18.1	3.791735	2.402194
snx8b	3.790955	7.411891
cpe	3.789239	2.022013
cd9a	3.784642	2.48159
calm3a	3.760697	1.569121
si:ch211-222l21.1	3.760572	0.787553

Appendix 2

DEG cluster 1/cluster 2

Cluster 1-Non-reactive Müller glia 1

GENES	SCORES	LOG FOLD CHANGES
inhbaa	37.94407	3.546254
bambia	32.67387	4.58123
gpm6ab	31.56866	2.196494
tbx2a	31.52823	5.262084
crabp2b	30.49274	3.225554
pdgfrl	28.89457	4.525547
lman1	28.74099	4.747096
icn	27.91342	2.361162
hspb8	27.43563	3.687712
cyp26c1	27.23067	7.758151
efnb2a	27.03174	4.6717
prss35	26.8124	5.635471
aqp1a.1	26.73771	1.800045
sncgb	23.87616	3.018137
si:dkey-222f2.1	23.37817	3.701657
ndrg4	22.72685	2.267276
atp1b4	21.74528	1.651861
CR383676.1	20.0594	0.50164
zgc:165604	19.54804	1.182066
fstb	19.43203	3.406087
myl6	18.76356	2.052683
ctsla	18.67946	1.334076
fgf24	18.24792	2.19192
txn	18.07088	3.711958
myl9a	17.80181	2.8738
spock3	17.48943	1.053786
uchl1	17.40828	2.283057
atp1b1a	17.10874	1.693768
syt11a	16.73093	2.431066
tbx2b	16.37122	4.085028
gpm6aa	16.28531	1.206821
slco1c1	16.11231	2.497952
CR936442.1	16.08533	2.014393
gapdhs	15.97316	0.750087
si:ch211-237l4.6	15.72556	3.772513
serpinb1	15.5371	2.348144
wfdc2	15.52593	1.450339
c1qtnf12	15.51172	5.112379
tcima	15.4024	2.973572
cavin1b	15.34797	5.277171
fabp7a	15.11265	1.322055
cadm4	14.82402	1.476937
rasgef1bb	14.75837	1.830831
zgc:77112	14.5573	25.50668
ckbb	14.55208	0.709458
sc5d	14.4588	1.554155
si:ch211-207i1.2	14.44481	2.294787
elovl1b	14.40426	3.347477
hmgcra	14.38713	1.501916
dbn1	14.24266	2.300209
cyp26a1	14.20365	2.13
camk1db	14.13887	1.693756
ucmab	14.02546	25.6962

si:dkey-56f14.7	13.818	1.158595
clu	13.7356	2.478725
mmp2	13.58922	3.158927
qsox1	13.52142	2.430235
lepb	13.42554	3.68281
tbx4	13.13469	4.719082
foxg1d	13.11193	25.21665
AL954322.2	13.0667	3.372154
gsna	13.05477	2.201475
lgals2a	13.01243	5.081233
tbx3a	12.92272	3.672332
sema3fa	12.90078	1.486634
hdac5	12.87001	3.191676
cahz	12.84609	0.660078
mrap2a	12.62787	24.92942
msmo1	12.62267	1.180716
eno1a	12.50841	0.595672
stm	12.48074	26.77746
s100u	12.41863	25.10116
hspbp1	12.40152	2.173261
hsd17b12b	12.34388	1.791157
map4k2	12.31199	3.055575
rhoab	12.29561	1.00698
ccdc85a	12.20654	1.922719
clcf1	12.19888	25.50375
igsf9ba	12.18975	1.403207
anxa2a	12.17908	4.538851
si:ch211-79k12.1	12.10606	24.98734
UBB	12.04449	1.197988
lmo7a	11.9385	2.868409
cyp51	11.84347	1.30994
chst15	11.83229	1.787383
idh1	11.73837	1.821365
cxcl14	11.67784	2.674034
rhbg	11.65844	0.776907
calcr	11.65833	24.70619
tnfsf12	11.6406	24.77231
zic2b	11.58307	2.881771
si:zfos-943e10.1	11.55017	1.356757
hbegfa	11.53205	1.847887
mlip	11.47244	24.6629
kctd12.2	11.41919	2.337013
si:ch73-31d8.2	11.40491	1.436943
ppdpfb	11.4041	0.890761
nupr1a	11.38511	1.673978
cd9a	11.3705	24.68389
dbi	11.35781	0.97066

Cluster 2-Non reactive Müller glia 2

GENES	SCORES	LOG FOLD CHANGES
apoeb	43.90213	1.884749
chrdl2	37.53057	4.166361
rdh10a	35.07629	3.738124
aldh1a3	28.35645	3.093189
mstnb	19.48931	2.769267
sncga	16.32416	1.095174
stc2a	13.51636	1.607256
dhrs3a	13.08953	4.17834
smoc1	13.02685	7.674436
si:dkey-164f24.2	12.8342	1.102459
nr2f5	12.69152	4.196837
si:ch211-222l21.1	10.97201	1.698406
rgmb	10.92153	2.732622
gnai2b	10.88741	1.384488
ackr3b	10.57193	4.320561
rgmd	10.23703	2.516204

cyp1d1	9.944285	3.030126
hspb1	9.882424	1.128903
mt2	9.792654	0.823627
elmod1	8.538007	4.446221
fosb	8.491188	0.434918
tnfaip2a	8.352043	1.93702
bmpr1ba	8.216331	1.899815
egr1	8.163019	0.79383
atp1b3a	8.140251	0.503037
cldn7a	8.026628	4.161813
ptgs2a	7.635228	1.153929
sparc	7.574094	0.374151
leo1	7.426731	0.889044
pnp6	7.362914	1.012174
ednraa	7.147677	1.25887
ephb2b	7.121871	1.141223
brinp3b	7.115801	3.568098
pip5k1bb	6.962028	1.683397
bmp7b	6.868118	1.976043
bmpr1bb	6.73305	4.386249
im:7152348	6.627189	0.705563
sox3	6.623856	1.806533
igfbp1a	6.617581	0.780395
CU467822.1	6.530359	0.394079
six6a	6.162166	2.477043
cib2	6.148203	1.364171
ndrg3a	6.075061	0.556735
pik3r3b	6.064154	0.773879
ponzr5	5.963062	2.685592
irx5a	5.777402	0.979611
pcyt1bb	5.747045	2.039862
mt-co3	5.717512	0.266082
slc16a9a	5.494378	2.257709
BX663503.3	5.427116	1.085738
tob1a	5.382612	0.387688
foxi2	5.289058	3.514132
dhrs13a.1	5.249379	0.997201
abat	5.124996	0.678324
arpp21	5.071553	1.379364
hdac4	5.067826	2.217663
slc38a2	5.007825	1.559681
CR354540.1	4.994704	1.773471
vax1	4.981232	4.074256
esr2a	4.951549	3.530527
serpinf1	4.927566	3.571918
rrh	4.925615	0.660763
zgc:195173	4.882537	0.389117
rcan3	4.87946	1.60707
vegfaa	4.649835	0.446214
ch25h	4.637689	2.428311
cntnap5b	4.634336	3.551419
dusp2	4.613782	0.513045
f3b	4.606153	0.420251
mycn	4.597778	1.000431
cav1	4.592935	0.461518
ip6k2b	4.542986	0.566893
mt-co1	4.494689	0.257469
rlbp1a	4.31893	0.194846
si:ch211-145b13.5	4.237026	1.026897
atp2b3b	4.216623	2.79486
foxg1b	4.211659	0.636182
si:dkey-76d14.2	4.09479	0.947381
hmgb2a	4.073831	0.452234
si:dkey-217l24.1	4.07129	1.555879
bgnb	4.055054	0.343164
si:ch73-141c7.1	3.993604	1.65194
fosab	3.939539	0.197728
si:ch73-46j18.5	3.937312	0.285565
si:dkey-112a7.4	3.933747	0.551066

NPFFR2	3.91013	1.037614
iqca1	3.893461	3.934197
diras1a	3.871813	1.346797
marcksl1a	3.849621	0.36326
slc3a2a	3.825608	0.431125
sik2b	3.822247	0.301151
cyp2p6	3.816729	0.986664
si:ch211-105c13.3	3.791507	3.39775
aspa	3.764535	0.447334
aldh1a2	3.729247	0.519296
rxfp3.3b	3.721139	6.24632
nfasca	3.671763	0.156084
si:ch211-286o17.1	3.655677	2.171005
sh3gl2a	3.641486	1.672081
aldh1l1	3.626436	1.548761

Appendix 3

DEG cluster 3/cluster 4

Cluster 3-Reactive Müller glia 1

GENES	SCORES	LOG FOLD CHANGES
hsp90aa1.2	82.35464	7.280427
hsp70.3	66.28247	7.832823
her15.1-1	60.54194	5.88867
fosab	55.58332	4.124118
hsp70l	49.03855	8.664011
stm	49.01005	10.58326
id1	42.62602	4.362969
hsp70.2	42.19383	7.396928
her6	41.85655	4.554995
si:ch211-222l21.1	41.21204	2.949663
her15.1	39.92948	5.519451
ubb	38.23594	2.612924
dnajb1b	37.08304	4.597067
jdp2b	36.60299	3.446919
cxcl18b	35.82386	3.723559
hsp70.1	34.68315	7.875595
jun	34.63765	2.626043
tubb2b	34.19307	3.273972
si:ch73-281n10.2	33.63424	2.815276
pcna	33.39236	3.553328
her12	33.0239	4.520015
tuba8l4	32.91037	2.326612
UBB	32.78486	2.321974
her4.2-1	32.63203	5.523844
her4.2	32.58655	4.103734
tubb4b	32.01009	1.639407
cirbpa	31.76522	1.853839
her4.1	31.74485	4.691708
foxj1a	31.5159	3.284178
cebpb	31.4061	3.698709
junbb	31.1249	2.515971
si:ch73-335l21.4	31.02646	2.666007
junba	30.98528	2.227041
socs3a	30.86547	3.608342
hmgb2a	30.8064	2.714055
hnrnpa1b	30.73948	2.371784
hmgb2b	30.21128	2.393172
arrdc3b	29.89188	3.526479
cdkn1a	29.63683	4.312913
tomm20a	29.20352	2.382114
hmga1a	28.95779	2.122937
tma7	28.69193	2.332645
hspa5	28.6831	2.147303
ascl1a	28.26748	5.355374

h2afvb	27.82815	2.050335
jund	27.55827	2.139712
si:ch211-156b7.4	27.55638	2.757825
gadd45bb	27.0352	3.03599
tuba8l	26.9602	2.795086
nrarpa	26.88822	2.839094
nap1l1	26.84321	2.251417
klf11b	26.57303	3.741071
rhov	26.558	4.548403
hspb1	26.17954	2.979319
sox4a-1	26.11847	2.454757
tuba1a	25.96273	2.253772
pim2	25.94703	4.804348
khdrbs1a	25.53657	1.588989
anp32b	25.48372	2.679931
rrm2-1	25.3829	4.11149
hsp90b1	25.09717	2.306435
snrpe	25.04205	2.148803
atf3	24.81995	2.228287
cirbpb	24.78739	1.340621
rpa2	24.6018	3.002774
ran	24.45253	1.411974
nutf2l	24.3949	3.412919
dut	23.97212	3.487447
pclaf	23.63413	4.183244
mt-atp6	23.63085	1.458391
TXN	23.55486	1.474241
ivns1abpb	23.53427	4.192891
ier2b	23.34049	2.065435
phlda2	23.32513	2.696411
mcl1a	23.31013	1.716982
odc1	23.30475	1.990248
ube2e2	23.27251	2.631728
hspa4a	23.24728	2.490544
mycb	23.18145	2.375153
hspa8	22.97676	1.025164
pfn2	22.96859	1.791699
rrm1	22.96025	3.213909
hmgn2	22.89884	1.93652
ier5	22.86311	1.70014
rpa3	22.81489	2.850908
ncl	22.77591	1.51615
banf1	22.64566	2.745244
fen1	22.64449	3.099192
rbbp4	22.39164	2.44831
cdca7a	22.35177	4.124371
socs3b	22.27313	2.275953
zfand2a	22.06434	2.736086
seta	22.02438	1.77162
chaf1a	22.01164	2.596084
hnrnpa0b	21.99581	1.414582
kpnb3	21.78032	2.50988
her9	21.71943	2.040117
CABZ01080568.1	21.61807	5.599689
hells	21.575	3.470985
mcm5	21.51358	3.51792

Cluster 4-Reactive Müller glia 2

GENES	SCORES	LOG FOLD CHANGES
ckbb	50.84286	3.734844
acbd7	43.06075	3.538525
fabp7a	35.67048	2.07263
gpm6aa	31.36484	2.181624
fxyd6l	29.00227	2.87733
mdka	24.50395	1.458362
col18a1a	22.96548	2.43918

crabp1a	22.51464	1.357243
CU467822.1	21.8247	1.93651
f3a	21.46131	1.343417
pros1	21.12595	2.928259
klf7b	20.6625	2.281087
zgc:165604	20.61534	1.65198
marcksl1a	20.12578	1.255277
si:dkey-238o13.4	19.63945	2.279248
mdkb	18.74052	1.774334
gfap	17.7655	1.350174
slc1a2b	17.73886	2.154527
zgc:165461	16.79933	7.665141
si:ch211-251b21.1	16.71493	1.814292
rlbp1a	16.04219	2.598093
myl9b	15.97128	1.315761
clcf1	15.64738	1.350377
cotl1	15.10173	1.263876
eml1	15.04819	2.150191
crlf1a	14.53827	1.168107
gstp1	14.52729	1.762205
fads2	14.16714	2.553449
smad3a	14.14918	1.93445
si:ch73-352p4.8	14.01927	3.987175
celf2	13.93621	2.07981
plekhg2	13.88625	3.167043
zgc:109949	13.74708	1.530178
tjp2b	13.68649	1.429958
igfbp5b	13.58487	1.896944
sall1b	13.51111	1.979958
actb1	13.47996	0.658644
itm2ba	13.42153	0.94229
ncam1a	13.34969	1.571761
ccni	13.30744	1.353316
eml2	13.29075	1.394144
mgst3b	13.17489	1.279166
ywhag2	13.15285	2.172872
rhbg	12.90405	1.388805
zgc:153867	12.84802	0.862836
ISCU (1 of many)	12.84055	1.269833
il11b	12.73038	2.290368
igsf9ba	12.72013	2.775603
hmgn6	12.68202	0.950532
zgc:86709	12.64639	2.08753
arhgef4	12.62399	2.43392
fabp3	12.48091	0.832521
gpm6ab	12.39938	1.428881
cnn3a	12.33085	1.018712
si:dkey-28b4.7	12.19304	1.937535
cdo1	12.15533	1.729388
hivep2a	12.14949	2.019537
cbsb	11.97805	1.878662
kitlgb	11.93795	2.118536
akap12b	11.93602	1.003729
tp53inp1	11.93179	1.78446
SMIM18	11.87499	3.085141
flna	11.83472	0.958187
slc1a3b	11.8222	5.071202
efhd1	11.74102	1.481784
elmsan1b	11.69203	1.127771
cygb2	11.67312	6.660601
ttyh3b	11.57314	2.330539
s1pr1	11.56586	1.060814
h3f3c	11.54668	1.392057
appa	11.48259	0.975472
FP102018.1	11.47569	2.04702
dusp5	11.42468	1.124017
col2a1a	11.24889	1.526601
atf5b	11.19322	1.664455
slc7a3a	11.05061	1.270786

mvp	10.92912	0.836193
zgc:162780	10.90802	1.421466
zgc:100829	10.8524	1.647323
ndrg4	10.70748	2.193386
ndrg2	10.61652	2.331969
acaca	10.59206	1.66623
swap70b	10.28239	1.954082
enpp6	10.26681	1.985156
ephb2b	10.16133	1.490687
sparc	10.15438	0.888877
myl9a	10.09955	1.868022
chn1	10.07059	1.783767
CR855337.1	10.0666	2.216947
myo1ea	10.06554	1.22503
opcml	9.885158	1.766567
lepb	9.792505	1.081988
anxa4	9.78717	1.525179
zic2b	9.774028	0.915013
dbn1	9.659241	0.945812
nupr1b	9.644771	2.35317
lrrc4.1	9.626767	3.760903
zgc:110182	9.54512	2.229369
ca14	9.416307	1.495686
appb	9.374798	1.406201

Appendix 4

DEG cluster 5/cluster 3

Cluster 5-Müller glia/Progenitors 1

GENES	SCORES	LOG FOLD CHANGES
hmgn6	39.57415	2.131894
ckbb	36.08776	2.636459
h3f3b.1-1	30.95333	2.008455
fabp7a	30.82239	1.702253
gpm6aa	30.8102	2.006668
h3f3c	30.08421	2.430396
hmgn2	29.66204	1.723821
stmn1a	28.7132	2.589657
acbd7	28.15553	2.370024
fabp3	27.85391	1.38769
si:dkey-238o13.4	27.16729	2.512182
si:ch73-1a9.3	27.11039	1.595444
hmgb1b	25.72023	1.373406
GFP	25.22922	3.153699
cadm3	23.78748	1.586514
h3f3b.1	23.68885	1.421848
crabp1a	22.68151	1.223907
si:ch211-288g17.3	22.52918	1.243466
mdkb	22.33049	1.663777
hmgb1a	22.25559	1.19846
hmgb2a	21.26914	1.317965
tdh	20.94719	1.739386
nr2e1	20.64315	2.291473
ptmab	20.28705	0.838802
tspan7	20.16095	1.419095
tmsb	19.9558	1.716845
cbsb	19.62659	2.234595
marcksb	19.60996	1.083264
hmgb2b	19.49424	0.92587
dek	19.21368	1.444203
CU467822.1	18.43581	1.455707
tuba1c	17.86642	1.410547
sox9b	17.68629	1.859356
si:dkey-28b4.7	17.62914	2.130151
adh5	17.57185	1.542553

rcor2	17.48	3.061096
ankrd12	17.23396	1.494664
sesn2	17.20127	1.955557
crabp2a	17.02717	1.986029
psat1	16.95135	1.092075
smc1al	16.65961	1.145084
klf7b	16.64874	1.638218
hmgb3a	16.52694	1.26806
marcksa	16.49779	1.599452
apex1	16.48928	1.374166
h2afvb	16.45271	0.720244
rcc2	16.30293	1.532215
sod1	16.26657	1.188362
slc7a3a	16.21495	1.498661
rpl12	16.15476	0.574338
celf2	16.04774	1.949821
top2b	15.60833	1.320457
tp53inp1	15.2565	1.763965
rab39ba	15.23841	3.177597
h1f0	15.2238	1.353938
ptprz1a	15.19141	2.721706
tp53inp2	15.0532	1.484326
nova2	15.0495	1.107543
seta	14.97295	0.802234
ubtf	14.81291	1.303163
prdx2	14.73677	0.803641
fads2	14.67992	2.178926
si:ch211-137a8.4	14.45589	1.096811
lbr	14.42498	1.253205
pou3f1	14.19874	4.809452
creb1a	14.10757	1.335473
atf5b	14.02652	1.596843
smarca4a	13.69398	1.074636
sept4a	13.54579	1.694413
nucks1a	13.25495	0.945909
phc2a	13.16774	1.356101
acin1a	13.07517	0.839773
nfyba	12.89905	1.45151
atrx	12.86515	0.781367
si:ch73-215f7.1	12.86413	2.224107
tnrc6c2	12.84728	2.21801
snrpd1	12.8338	0.702585
si:ch73-46j18.5	12.8279	0.922019
hmga1a	12.82499	0.682489
baz2ba	12.82041	1.115893
gpm6ab	12.79813	1.261795
slc6a15	12.78617	4.334434
csdc2a	12.52681	1.596228
anp32a	12.512	0.839898
cebpg	12.50603	1.050131
si:dkey-108k21.10	12.50057	1.631147
polb	12.32132	1.647772
hdac1	12.27381	0.751042
ddx39ab	12.24022	0.691922
h3f3d	12.20215	0.499157
znf1035	12.1861	1.370622
slc1a4	12.17181	1.805157
actl6a	12.15832	0.940167
selenow2a	12.13408	1.186491
klf7a	12.12547	2.643582
zgc:153867	12.12113	0.730896
pacsin1b	12.09484	2.469278
ap1s2	11.9897	1.187903
nudt21	11.98962	1.141472
ncam1a	11.92678	1.204929

Cluster 3-Reactive Müller glia 1

GENES	SCORES	LOG FOLD CHANGES
hsp90aa1.2	78.96281	6.156524
hsp70.3	67.37897	7.598966
fosab	60.32014	3.864515
cxcl18b	54.41115	6.127927
si:ch73-335l21.4	54.25473	3.799618
apoeb	50.15687	4.115772
hsp70l	49.6275	9.198058
stm	49.15161	11.48878
ubb	48.80151	2.940044
hspa5	48.58926	3.129906
fosl1a	47.78948	3.239794
sox4a-1	43.41177	4.170949
hsp70.2	42.73847	7.744448
jdp2b	40.42208	3.47695
jund	39.82693	2.880288
jun	38.33742	2.379801
her6	37.62339	3.614906
mmp9	37.06501	3.245725
hspb1	37.02354	5.577278
dnajb1b	36.90395	4.200686
socs3a	35.88629	4.15243
hsp70.1	34.8815	8.202497
mcl1a	34.03123	2.240658
cebpb	33.66378	3.929009
zgc:158343	33.49094	2.860631
rtn4a	33.158	1.535396
UBB	33.15166	2.019451
krt8	33.09382	2.681905
mych	32.59881	2.416787
phlda2	32.40475	3.691947
ier2b	32.13038	2.724097
sgk1	31.57028	2.193032
junba	31.5586	2.038267
atp1b1a	31.22713	2.143112
mycb	30.67942	3.167697
junbb	30.32054	2.22112
s100a10b	29.84934	4.043632
gadd45bb	29.53768	3.263278
foxj1a	29.46652	2.682248
her15.1-1	29.25406	2.393085
hsp90b1	29.07632	2.43212
spry4	28.70327	2.905028
klf6a	28.34971	2.063534
angptl4	27.8325	1.892593
atp1a1b	27.82399	2.743519
arrdc3b	27.66318	2.762813
cdkn1a	27.33998	3.319271
nocta	26.73047	2.115593
zfand2a	26.63722	3.617677
txn	26.63174	2.05768
socs3b	26.47211	2.586601
eno1a	26.30534	1.911909
hbegfa	26.1929	2.144311
cd99	26.18384	3.46875
krt18a.1	26.10007	4.836473
klf11b	26.01771	3.258551
fosb	25.87888	2.240446
irs2b	25.44503	3.124726
atf3	25.40961	1.901364
rhov	25.17624	3.698608
brd2a	25.13917	1.458679
gapdhs	24.98846	1.267286
cd63	24.68965	1.635312
hspb8	24.66699	3.826962
STMP1	24.27877	1.955182
mCherry	24.09944	2.188792

mcl1b	23.96723	2.348563
pim3	23.68014	1.853738
CR383676.1	23.60384	0.715097
ascl1a	23.57243	3.162641
pdgfrb	22.91039	3.372953
dusp1	22.77743	2.231638
tob1b	22.76532	2.983663
marcksl1b	22.72348	1.133145
pgam1a	22.70318	2.1958
c7b	22.6899	3.574649
rasgef1ba	22.67658	1.824629
si:dkey-7j14.6	22.38213	1.169267
tomm20a	22.37193	1.532643
CABZ01080568.1	22.34726	7.764894
tcima	22.30956	3.769706
anxa11a	22.27368	2.720237
fkbp5	22.25666	3.941752
adgrg1-1	22.09657	3.025898
alkbh3-1	22.04471	3.283715
glula	21.9769	2.318345
pim2	21.8734	2.943209
prdx6	21.48656	1.887133
cdh2	21.46231	1.062956
rgs5b	21.31656	5.723075
oaz1a	21.25925	1.020348
dab2ipb	21.25077	2.017103
pgk1	21.23523	1.918073
tuft1a	21.14848	2.924801
ppp1r15a	20.97945	2.838792
hspa4a	20.92429	1.903325
rtn3	20.85957	1.949776
bsg	20.82198	1.313603
MYO1D	20.70807	3.313413
rpz5	20.3744	4.09142

Appendix 5

DEG cluster 5/cluster 4

Cluster 5- Müller glia/Progenitors 1

GENES	SCORES	LOG FOLD CHANGES
hmgb2a	59.88311	4.032021
hmgn2	53.28411	3.660341
hmgb2b	48.89518	3.319043
h3f3b.1	46.57986	2.922519
tubb2b	45.28305	3.779763
si:ch211-222l21.1	44.287	3.044553
hmga1a	42.31578	2.805426
si:ch73-281n10.2	42.1779	3.147583
h2afvb	42.16171	2.770579
pcna	41.41436	3.794421
seta	39.36641	2.573854
si:ch211-288g17.3	39.03107	2.786086
si:ch211-156b7.4	38.83523	3.283548
dek	38.75076	3.699343
hmgb1b	37.81065	2.306587
hmgb1a	37.6093	2.512171
stmn1a	36.73283	3.838214
mki67	36.10389	4.584386
cirbpa	35.11591	1.893434
rrm1	33.81368	3.679839
rbbp4	33.75729	2.964739
ptmab	32.60604	1.622533
lbr	32.29927	3.835795
rrm2-1	32.17185	4.305764
cbx3a	32.10963	2.287667

snrpd1	31.98677	2.024103
stmn1b	31.88383	2.816718
khdrbs1a	31.86275	1.816367
rpa2	31.80771	3.262814
hnrnpaba	31.73182	1.63493
ran	31.64779	1.646397
anp32b	31.6227	2.787544
chaf1a	31.33116	2.990514
snrpe	30.55038	2.304834
pclaf	30.1753	4.3443
snrpb	30.16121	1.93357
hnrnpa0b	29.80031	1.673349
cirbpb	29.76588	1.492201
hnrnpabb	29.56882	1.67234
tuba8l4	29.51319	1.99999
slbp	29.4879	4.300787
banf1	29.38215	3.000735
ahcy	28.97365	2.334974
sumo3a	28.87215	2.109611
snrpf	28.60287	1.968837
tuba1a	28.25925	2.26164
hnrnpa1b	28.16135	2.113005
CABZ01005379.1	28.06565	4.081108
rpa3	27.86267	3.011049
ccna2	27.85132	5.193193
calm2b	27.76758	2.044608
smc2	27.57939	4.493328
abhd6a	27.46467	3.580729
si:ch73-1a9.3	27.4144	1.864256
lig1	27.32397	3.173058
sumo3b	27.30627	2.56958
ddx39ab	27.13763	1.86255
her15.1-1	27.03404	3.495585
top2a	27.01279	4.967511
ppm1g	26.82956	2.378648
ranbp1	26.72907	1.870457
si:ch211-137a8.4	26.31446	2.234992
anp32a	26.25086	1.995782
cks1b	26.14723	4.261715
mibp	26.05821	4.348235
anp32e	25.97471	1.896247
fen1	25.95778	3.096474
zgc:110540	25.95219	4.499549
h2afx	25.71205	2.896785
id1	25.69344	3.157252
baz1b	25.62452	2.442529
cbx5	25.46941	2.536277
tuba1c	25.10795	2.305203
CABZ01058261.1	25.01974	4.617057
her4.1	24.99796	3.359631
hdac1	24.89681	1.754298
setb	24.74794	1.799618
nutf2l	24.6904	3.120162
smc1al	24.66069	1.887412
magoh	24.58812	1.993139
cdk1	24.54513	4.643316
hnrnpa0l-1	24.51803	1.106165
ncapg	24.48101	4.886285
smc4	24.46729	3.825938
syncrip	24.43125	1.531151
snrpd2	24.40524	1.759107
taf15	24.2833	1.957806
dhfr	24.23506	3.964293
cenpf	24.17227	4.719339
actl6a	24.06294	2.28343
dut	23.99543	3.155126
h2afva	23.85158	1.949114
mad2l1	23.68154	4.588408
nasp	23.63137	3.372168

marcksb	23.56229	1.464284
tpx2	23.27903	5.679986
srsf2a	23.27819	1.755616
lmnb2	23.11164	2.727296
aurkb	23.02791	4.603858
si:ch73-21g5.7	23.00684	3.866025

Cluster 4-Reactive Müller glia 2

GENES	SCORES	LOG FOLD CHANGES
marcksl1a	28.45223	1.566915
slc1a2b	27.86047	4.331185
fxyd6l	27.35475	2.33426
zgc:165604	26.48078	2.034056
crlf1a	26.27136	2.145043
dusp5	25.35421	2.675038
sparc	24.78819	2.376524
f3a	24.01298	1.541462
hbegfa	23.4558	2.121441
cnn2	23.029	1.925941
mdka	22.80873	1.142256
cnn3a	22.71172	1.9504
CR383676.1	22.37306	0.709742
krt8	22.35656	2.22081
mvp	21.91733	1.678019
selenop	21.82425	3.010912
txn	21.76608	1.946497
si:ch1073-303k11.2	21.71447	1.689989
gfap	21.41233	1.51608
icn	21.24722	3.998539
atp1b1a	21.22201	1.900651
sgk1	21.03592	1.685408
rhbg	21.01989	2.394857
col18a1a	20.84691	1.998223
myl6	20.33518	1.381881
c7b	20.18061	3.56112
clcf1	20.05112	1.709903
alkbh3-1	19.66386	3.396779
rlbp1a	19.22552	3.395124
cd99	19.18551	2.994941
grb10b	18.90202	1.879711
rtn4a	18.87692	1.032174
anxa13	18.84404	1.88663
apoeb	18.75928	2.621199
aplp2	18.69975	2.014312
gstp1	18.67665	2.208734
mych	18.4314	1.633397
cdo1	18.30334	3.025169
pros1	18.17524	2.132115
myl9b	18.01382	1.368224
spock3	17.80174	3.213433
acbd7	17.78956	1.168501
ckbb	17.64818	1.098385
eml2	17.47475	1.844926
efhd1	17.42809	2.391088
flna	17.09739	1.316083
zfand5a	16.94324	1.677537
tob1b	16.61486	2.226043
vmp1	16.4526	1.2454
bzw1b	16.2472	1.006034
lepb	16.06698	1.834574
irs2b	16.03065	2.343751
kitlgb	15.9755	3.882472
errfi1a	15.63933	1.828523
zic2b	15.62195	1.328985
fosl1a	15.59316	1.633912
epas1b	15.58087	2.754812

s100a10b	15.4264	2.781081
il11b	15.40082	3.16239
ca14	15.34694	3.267858
vim	15.3415	1.479634
klf6a	15.33034	1.333795
cadm4	15.29171	1.475499
ppdpfb	15.23914	0.702868
elovl1b	15.10914	1.502002
ywhag2	14.81845	2.544953
col2a1a	14.76239	2.119178
igfbp5b	14.7455	1.94826
hsd11b2	14.58801	3.330843
pygl	14.56145	2.348547
chmp4ba	14.19309	1.743988
sall1b	14.10458	1.989616
dhrs13l1	14.09953	3.333695
wfdc2	14.05942	3.250407
si:dkey-7j14.6	13.72148	0.804625
dab2ipb	13.60768	1.515479
spry4	13.53919	1.860927
tnfrsf21	13.41025	1.682223
akap12b	13.40001	1.028598
cotl1	13.07852	0.965142
zgc:162780	13.02275	1.687155
midn	13.00825	0.977434
ctsla	13.00383	0.776681
ecm1b	12.93636	3.175005
zgc:165461	12.84795	2.513815
ahnak	12.78009	3.018579
ptgdsb.2	12.69268	3.252967
gsna	12.68134	2.104524
irf2	12.64866	1.73926
lygl1	12.64654	2.54683
igsf9ba	12.58847	2.519939
fam129bb	12.57495	1.397485
myl9a	12.53734	2.643761
cdh2	12.519	0.663453
cd82a	12.50103	0.81131
inhbaa	12.4466	2.094908
zgc:174888	12.35362	3.044917
nocta	12.29703	1.160973
nfkbiaa	12.17441	2.496166
slc12a4	12.134	1.54915

Appendix 6

DEG cluster 5/cluster 6

Cluster 5-Müller glia/Progenitors 1

GENES	SCORES	LOG FOLD CHANGES
id1	33.20395	4.413954
si:dkey-238o13.4	30.18699	2.934452
f3a	29.49284	2.489398
crlf1a	29.26157	3.758567
pim1	28.90828	2.224119
si:ch1073-303k11.2	27.48717	4.214794
acbd7	26.48776	2.14128
her4.1	26.04419	3.313039
nrarpa	25.8404	2.959989
her12	25.70443	4.233252
akap12b	24.70734	2.195335
notch3	23.9893	2.590406
six3b	23.81036	1.779216
ppdpfb	23.02896	1.329558
myl6	22.7005	2.129922
ckbb	22.66209	1.653146

her4.2	22.06587	2.839705
s1pr1	21.78406	2.389015
crabp1a	21.38036	1.167667
abhd6a	21.29357	2.585157
mdka	21.22327	1.112773
clcf1	21.19512	2.955191
lfng	21.14992	2.12735
zgc:165604	20.9498	2.277418
sgk1	20.57258	2.153961
cnn2	20.57133	2.75284
flna	20.52126	2.272692
tjp2b	19.55174	2.835801
CU467822.1	19.54188	1.55237
rtn4a	19.51699	1.212571
zgc:158343	19.33073	2.217154
mmp9	19.04083	3.244989
marcksl1b	18.82026	1.074507
nr2e1	18.09925	2.058403
yap1	18.01408	1.959832
gfap	17.93883	1.542437
si:ch211-251b21.1	17.4214	1.659508
tpm4a	17.3204	3.76093
her9	17.23831	1.610291
sox9b	17.1651	1.834976
f3b	16.94719	2.167219
btg2	16.88596	1.013803
errfi1a	16.83897	3.918623
zgc:109949	16.77024	1.863626
midn	16.36706	1.434379
si:ch73-21g5.7	16.01612	2.18496
nrarpb	15.56761	2.93793
cspg5a	15.4924	2.866997
her4.2-1	15.35021	2.399409
si:dkey-7j14.6	15.33142	1.080294
sox2	15.09371	1.383063
slc12a4	15.05737	3.736255
lgals2a	14.99862	1.881001
sparc	14.86773	2.276907
BX465834.1	14.79454	1.472261
igfbp5b	14.72426	2.648566
txn	14.70218	1.46299
myl9b	14.54179	1.42346
qkia	14.47649	1.297585
bzw1b	14.4581	0.966614
dab2ipb	14.29183	2.518966
her15.1-1	14.10235	1.568661
fxyd6l	14.07612	1.640133
notch1b	13.86108	2.19294
cdh2	13.75786	0.834817
cnn3a	13.69488	1.521155
her4.4	13.66234	2.617347
angptl4	13.35335	1.231126
rasgef1bb	13.24782	1.089429
mCherry	13.21127	1.574851
tmsb4x	13.05165	0.654317
LO018196.1	12.83982	2.251035
dusp5	12.81894	1.963021
her15.1	12.81567	1.637445
fosab	12.7846	1.466152
nocta	12.73726	1.494959
jdp2b	12.71978	1.816286
gpm6aa	12.50174	0.740196
col18a1a	12.48219	1.596507
fhl3b	12.38253	2.873164
fosl1a	12.37457	1.60726
emilin1a	12.23998	4.578283
rbpms2b	12.17257	1.659263
BX284638.1	12.12708	1.292871
slmapb	12.12079	1.791363

atp1b1a	12.07991	1.148278
zic2b	11.99187	1.104104
si:ch73-335l21.4	11.95505	1.246984
nrp2b	11.8913	1.182369
eml1	11.88188	1.89407
sb:cb81	11.86705	3.127805
rhbg	11.85136	2.234928
ccdc80	11.84705	5.136307
cxcl14	11.83785	1.708183
crip3	11.83164	3.947635
CR848047.1	11.81629	1.902241
efhd1	11.80226	3.130786
bcar1	11.7913	3.947092
cited4a	11.71951	0.827467
eif4ebp3l	11.7086	1.782539

Cluster 6-Progenitors 2

GENES	SCORES	LOG FOLD CHANGES
insm1a	29.74285	4.062833
pou2f2a-1	25.10969	3.679822
rbpjb	22.31904	2.437201
si:dkey-56m19.5	22.09177	1.844333
h3f3b.1	21.74553	1.01019
tubb2b	21.56813	1.212005
stmn1a	21.35702	1.334183
hmgb2a	21.26676	0.923674
im:7152348	20.84255	2.880055
tent5ba	20.08026	3.247291
mex3b	20.07191	2.23393
neurod4	19.89341	4.068521
stmn1b	19.65258	1.195198
sox11a	19.12948	1.846146
hes6	18.84141	1.76742
nusap1	18.2124	1.839676
golga7ba	18.13729	2.684294
mycla	17.77845	2.757133
ndrg1b	17.5824	4.818793
mki67	17.57771	1.183244
foxn4	17.39317	2.271308
cdkn1ca	17.2424	3.572549
itm2cb	17.06698	1.813652
nsg2	17.01987	2.492872
chd7	16.56265	1.074339
cenpf	16.49356	1.502182
sox11b	16.28317	1.535938
hmga1a	15.71892	0.713749
top2a	15.68546	1.314869
atoh7	15.63489	3.633435
si:ch211-137a8.4	15.55755	0.957719
zswim5	15.55344	1.320711
tuba8l4	15.51112	0.796337
ccna2	15.48092	1.218246
ube2c	15.25562	1.485815
si:ch211-255i3.4	15.19922	1.938495
cdk1	15.18764	1.3556
histh1l	15.01661	1.247156
si:ch211-222l21.1	14.71231	0.667203
h3f3b.1-2	14.68723	0.852724
si:ch73-281n10.2	14.63193	0.750805
dhx32b	14.50244	1.764132
CABZ01058261.1	14.49623	1.203344
otx2b	14.43487	3.108238
tubb4b	14.4129	0.701844
onecut2	14.3852	3.557531
znrf1	14.34256	1.800946
tuba8l	14.25486	1.170438

tuba1a	14.23932	0.852048
tfap2d	14.04352	5.688826
pou2f2a	13.93332	3.183808
aurkb	13.92913	1.201517
alcamb	13.89505	1.827475
lbr	13.81296	0.898885
birc5a	13.66098	1.532849
cnp	13.48519	1.0663
dek	13.32753	0.782037
h1f0	13.20192	1.047552
dclk1a	13.09317	1.696277
pif1	13.01037	2.443202
bhlhe22	12.95476	3.421463
tpx2	12.83766	1.256716
mad2l1	12.75631	1.149626
cited4b	12.75119	2.145798
tuba1c	12.72924	0.816479
cdc20	12.69682	1.61456
neurod1	12.6789	2.726301
tp53inp2	12.57528	1.101815
lepr	12.56878	1.283785
hmgn2	12.3784	0.51289
tsc22d1	12.32308	0.95009
cep55l	12.26544	1.510048
kifc1	12.26017	1.36743
srrm4	12.2442	1.469047
ncapg	12.21664	1.06696
rimkla	12.10791	1.129551
kif22	12.04421	1.292234
barhl2	11.87954	3.747174
tfap2c	11.84417	2.713201
dlgap5	11.83674	1.166193
robo3	11.82311	2.34776
cxxc5a	11.78868	1.03148
prdm1b	11.64075	3.057979
scml2	11.63646	2.17736
calm2b	11.62686	0.624698
si:dkey-28b4.8	11.61454	1.312385
si:ch211-69g19.2	11.59842	1.706728
arpp19b	11.58961	0.917289
anp32a	11.58766	0.658562
plcxd3	11.55526	2.793504
hmgb3a	11.35004	0.783461
myt1a	11.34812	1.462109
pik3r3b	11.2848	1.710145
hes2.2	11.24021	1.975387
kif11	11.21864	1.493881
lrrfip1a	11.02948	2.591687
h2afva	11.0211	0.676323
plk1	10.98766	1.178637
si:ch211-207i1.2	10.97547	1.301732
kmt5ab	10.92091	1.76093

BIBLIOGRAPHY

1. Streisinger, G., Walker, C., Dower, N., Knauber, D., and Singer, F. (1981). Production of clones of homozygous diploid zebra fish (Brachydanio rerio). Nature *291*, 293–296. 10.1038/291293a0.

2. Grandel, H., Kaslin, J., Ganz, J., Wenzel, I., and Brand, M. (2006). Neural stem cells and neurogenesis in the adult zebrafish brain: origin, proliferation dynamics, migration and cell fate. Dev. Biol. *295*, 263–277. 10.1016/j.ydbio.2006.03.040.

3. Kroehne, V., Freudenreich, D., Hans, S., Kaslin, J., and Brand, M. (2011). Regeneration of the adult zebrafish brain from neurogenic radial glia-type progenitors. Dev. Camb. Engl. *138*, 4831–4841. 10.1242/dev.072587.

4. Lange, C., Rost, F., Machate, A., Reinhardt, S., Lesche, M., Weber, A., Kuscha, V., Dahl, A., Rulands, S., and Brand, M. (2020). Single cell sequencing of radial glia progeny reveals diversity of newborn neurons in the adult zebrafish brain. Development, 1855951. 10.1242/dev.185595.

5. Gemberling, M., Bailey, T.J., Hyde, D.R., and Poss, K.D. (2013). The zebrafish as a model for complex tissue regeneration. Trends Genet. *29*, 611–620. 10.1016/j.tig.2013.07.003.

6. Lenkowski, J.R., and Raymond, P.A. (2014). Müller glia: Stem cells for generation and regeneration of retinal neurons in teleost fish. Prog. Retin. Eye Res. *40*, 94–123. 10.1016/j.preteyeres.2013.12.007.

7. Dowling, J.E. (1987). The Retina: An Approachable Part of the Brain (Harvard University Press).

8. Amini, R., Rocha-Martins, M., and Norden, C. (2018). Neuronal Migration and Lamination in the Vertebrate Retina. Front. Neurosci. *11*, 742. 10.3389/fnins.2017.00742.

9. Hoon, M., Okawa, H., Santina, L.D., and Wong, R.O.L. (2014). Functional Architecture of the Retina: Development and Disease. Prog. Retin. Eye Res. *42*, 44–84. 10.1016/j.preteyeres.2014.06.003.

10. Stenkamp, D.L. (2015). Development of the Vertebrate Eye and Retina. Prog. Mol. Biol. Transl. Sci. *134*, 397–414. 10.1016/bs.pmbts.2015.06.006.

11. Sanes, J.R., and Zipursky, S.L. (2010). Design Principles of Insect and Vertebrate Visual Systems. Neuron *66*, 15–36. 10.1016/j.neuron.2010.01.018.

12. Meier, A., Nelson, R., and Connaughton, V.P. (2018). Color Processing in Zebrafish Retina. Front. Cell. Neurosci. *12*.

13. Baden, T., and Osorio, D. (2019). The Retinal Basis of Vertebrate Color Vision. Annu. Rev. Vis. Sci. *5*, 177–200. 10.1146/annurev-vision-091718-014926.

14. Bringmann, A., Pannicke, T., Grosche, J., Francke, M., Wiedemann, P., Skatchkov, S.N., Osborne, N.N., and Reichenbach, A. (2006). Müller cells in the

healthy and diseased retina. Prog. Retin. Eye Res. *25*, 397–424. 10.1016/j.preteyeres.2006.05.003.

15. Luo, D.-G., Xue, T., and Yau, K.-W. (2008). How vision begins: An odyssey. Proc. Natl. Acad. Sci. *105*, 9855–9862. 10.1073/pnas.0708405105.

16. Molday, R.S., and Moritz, O.L. (2015). Photoreceptors at a glance. J. Cell Sci. *128*, 4039–4045. 10.1242/jcs.175687.

17. Chinen, A., Hamaoka, T., Yamada, Y., and Kawamura, S. (2003). Gene duplication and spectral diversification of cone visual pigments of zebrafish. Genetics *163*, 663–675. 10.1093/genetics/163.2.663.

18. Raymond, P.A., Barthel, L.K., Rounsifer, M.E., Sullivan, S.A., and Knight, J.K. (1993). Expression of rod and cone visual pigments in goldfish and zebrafish: a rhodopsin-like gene is expressed in cones. Neuron *10*, 1161–1174. 10.1016/0896-6273(93)90064-x.

19. Robinson, J., Schmitt, E.A., Hárosi, F.I., Reece, R.J., and Dowling, J.E. (1993). Zebrafish ultraviolet visual pigment: absorption spectrum, sequence, and localization. Proc. Natl. Acad. Sci. U. S. A. *90*, 6009–6012.

20. Cameron, D.A. (2002). Mapping absorbance spectra, cone fractions, and neuronal mechanisms to photopic spectral sensitivity in the zebrafish. Vis. Neurosci. *19*, 365–372. 10.1017/s0952523802192121.

21. Allison, W.T., Haimberger, T.J., Hawryshyn, C.W., and Temple, S.E. (2004). Visual pigment composition in zebrafish: Evidence for a rhodopsin-porphyropsin interchange system. Vis. Neurosci. *21*, 945–952. 10.1017/S0952523804216145.

22. Endeman, D., Klaassen, L.J., and Kamermans, M. (2013). Action Spectra of Zebrafish Cone Photoreceptors. PLOS ONE *8*, e68540. 10.1371/journal.pone.0068540.

23. Allison, W.T., Barthel, L.K., Skebo, K.M., Takechi, M., Kawamura, S., and Raymond, P.A. (2010). Ontogeny of cone photoreceptor mosaics in zebrafish. J. Comp. Neurol. *518*, 4182–4195. 10.1002/cne.22447.

24. Cone Types and Cone Arrangement in the Retina of Some Cyprinids - ENGSTRÖM - 1960 - Acta Zoologica - Wiley Online Library https://onlinelibrary.wiley.com/doi/10.1111/j.1463-6395.1960.tb00481.x.

25. Fadool, J.M. (2003). Development of a rod photoreceptor mosaic revealed in transgenic zebrafish. Dev. Biol. *258*, 277–290. 10.1016/s0012-1606(03)00125-8.

26. Kennedy, B., and Malicki, J. (2009). What drives cell morphogenesis: A look inside the vertebrate photoreceptor. Dev. Dyn. *238*, 2115–2138. 10.1002/dvdy.22010.

27. Arikawa, K., Molday, L.L., Molday, R.S., and Williams, D.S. (1992). Localization of peripherin/rds in the disk membranes of cone and rod photoreceptors: relationship to disk membrane morphogenesis and retinal degeneration. J. Cell Biol. *116*, 659–667. 10.1083/jcb.116.3.659.

28. Steinberg, R.H., Fisher, S.K., and Anderson, D.H. (1980). Disc morphogenesis in vertebrate photoreceptors. J. Comp. Neurol. *190*, 501–508. 10.1002/cne.901900307.

29. Grant, G.B., and Dowling, J.E. (1995). A glutamate-activated chloride current in cone-driven ON bipolar cells of the white perch retina. J. Neurosci. Off. J. Soc. Neurosci. *15*, 3852–3862.

30. Connaughton, V.P., Graham, D., and Nelson, R. (2004). Identification and morphological classification of horizontal, bipolar, and amacrine cells within the zebrafish retina. J. Comp. Neurol. *477*, 371–385. 10.1002/cne.20261.

31. Connaughton, V.P., and Nelson, R. (2000). Axonal stratification patterns and glutamate-gated conductance mechanisms in zebrafish retinal bipolar cells. J. Physiol. *524 Pt 1*, 135–146. 10.1111/j.1469-7793.2000.t01-1-00135.x.

32. Connaughton, V.P. (2011). Bipolar cells in the zebrafish retina. Vis. Neurosci. *28*, 77–93. 10.1017/S0952523810000295.

33. Li, Y.N., Tsujimura, T., Kawamura, S., and Dowling, J.E. (2012). Bipolar cell–photoreceptor connectivity in the zebrafish (Danio rerio) retina. J. Comp. Neurol. *520*, 3786–3802. 10.1002/cne.23168.

34. Connaughton, V.P., Behar, T.N., Liu, W.L., and Massey, S.C. (1999). Immunocytochemical localization of excitatory and inhibitory neurotransmitters in the zebrafish retina. Vis. Neurosci. *16*, 483–490. 10.1017/s0952523899163090.

35. Yazulla, S., and Studholme, K.M. (2001). Neurochemical anatomy of the zebrafish retina as determined by immunocytochemistry. J. Neurocytol. *30*, 551–592. 10.1023/A:1016512617484.

36. Li, Y.N., Matsui, J.I., and Dowling, J.E. (2009). Specificity of the Horizontal Cell-Photoreceptor Connections in the Zebrafish (Danio rerio) Retina. J. Comp. Neurol. *516*, 442–453. 10.1002/cne.22135.

37. SONG, P.I., MATSUI, J.I., and DOWLING, J.E. (2008). Morphological Types and Connectivity of Horizontal Cells Found in the Adult Zebrafish (Danio rerio) Retina. J. Comp. Neurol. *506*, 328–338. 10.1002/cne.21549.

38. Jusuf, P.R., and Harris, W.A. (2009). Ptf1a is expressed transiently in all types of amacrine cells in the embryonic zebrafish retina. Neural Develop. *4*, 34. 10.1186/1749-8104-4-34.

39. Dudczig, S., Currie, P.D., and Jusuf, P.R. (2017). Developmental and adult characterization of secretagogin expressing amacrine cells in zebrafish retina. PLOS ONE *12*, e0185107. 10.1371/journal.pone.0185107.

40. Arenzana, F.J., Arévalo, R., Sánchez-González, R., Clemente, D., Aijón, J., and Porteros, A. (2006). Tyrosine hydroxylase immunoreactivity in the developing visual pathway of the zebrafish. Anat. Embryol. (Berl.) *211*, 323–334. 10.1007/s00429-006-0084-2.

41. Donato, V.D., Auer, T.O., Duroure, K., and Bene, F.D. (2013). Characterization of the Calcium Binding Protein Family in Zebrafish. PLOS ONE *8*, e53299. 10.1371/journal.pone.0053299.

42. Yeo, J.-Y., Lee, E.-S., and Jeon, C.-J. (2009). Parvalbumin-immunoreactive neurons in the inner nuclear layer of zebrafish retina. Exp. Eye Res. *88*, 553–560. 10.1016/j.exer.2008.11.014.

43. O'Malley, D.M., Sandell, J.H., and Masland, R.H. (1992). Co-release of acetylcholine and GABA by the starburst amacrine cells. J. Neurosci. Off. J. Soc. Neurosci. *12*, 1394–1408.

44. Moyano, M., Porteros, Á., and Dowling, J.E. (2013). The effects of nicotine on cone and rod b-wave responses in larval zebrafish. Vis. Neurosci. *30*, 141–145. 10.1017/S0952523813000187.

45. Sanes, J.R., and Masland, R.H. (2015). The types of retinal ganglion cells: current status and implications for neuronal classification. Annu. Rev. Neurosci. *38*, 221–246. 10.1146/annurev-neuro-071714-034120.

46. Burrill, J.D., and Easter Jr., S.S. (1994). Development of the retinofugal projections in the embryonic and larval zebrafish (Brachydanio rerio). J. Comp. Neurol. *346*, 583–600. 10.1002/cne.903460410.

47. Robles, E., Filosa, A., and Baier, H. (2013). Precise Lamination of Retinal Axons Generates Multiple Parallel Input Pathways in the Tectum. J. Neurosci. *33*, 5027–5039. 10.1523/JNEUROSCI.4990-12.2013.

48. E, R., E, L., and H, B. (2014). The retinal projectome reveals brain-area-specific visual representations generated by ganglion cell diversity. Curr. Biol. CB *24*. 10.1016/j.cub.2014.07.080.

49. Kölsch, Y., Hahn, J., Sappington, A., Stemmer, M., Fernandes, A.M., Helmbrecht, T.O., Lele, S., Butrus, S., Laurell, E., Arnold-Ammer, I., et al. (2021). Molecular classification of zebrafish retinal ganglion cells links genes to cell types to behavior. Neuron *109*, 645-662.e9. 10.1016/j.neuron.2020.12.003.

50. Turner, D.L., and Cepko, C.L. (1987). A common progenitor for neurons and glia persists in rat retina late in development. Nature *328*, 131–136. 10.1038/328131a0.

51. Turner, D.L., Snyder, E.Y., and Cepko, C.L. (1990). Lineage-independent determination of cell type in the embryonic mouse retina. Neuron *4*, 833–845. 10.1016/0896-6273(90)90136-4.

52. Wetts, R., and Fraser, S.E. (1988). Multipotent precursors can give rise to all major cell types of the frog retina. Science *239*, 1142–1145. 10.1126/science.2449732.

53. Agathocleous, M., and Harris, W.A. (2009). From progenitors to differentiated cells in the vertebrate retina. Annu. Rev. Cell Dev. Biol. *25*, 45–69. 10.1146/annurev.cellbio.042308.113259.

54. Livesey, F.J., and Cepko, C.L. (2001). Vertebrate neural cell-fate determination: lessons from the retina. Nat. Rev. Neurosci. *2*, 109–118. 10.1038/35053522.

55. Cepko, C.L., Austin, C.P., Yang, X., Alexiades, M., and Ezzeddine, D. (1996). Cell fate determination in the vertebrate retina. Proc. Natl. Acad. Sci. *93*, 589–595. 10.1073/pnas.93.2.589.

56. Weber, I.P., Ramos, A.P., Strzyz, P.J., Leung, L.C., Young, S., and Norden, C. (2014). Mitotic Position and Morphology of Committed Precursor Cells in the Zebrafish Retina Adapt to Architectural Changes upon Tissue Maturation. Cell Rep. *7*, 386–397. 10.1016/j.celrep.2014.03.014.

57. Young, R.W. (1985). Cell differentiation in the retina of the mouse. Anat. Rec. *212*, 199–205. 10.1002/ar.1092120215.

58. Schmitt, E.A., and Dowling, J.E. (1999). Early retinal development in the zebrafish, Danio rerio: Light and electron microscopic analyses. J. Comp. Neurol. *404*, 515–536. 10.1002/(SICI)1096-9861(19990222)404:4<515::AID-CNE8>3.0.CO;2-A.

59. Marquardt, T., Ashery-Padan, R., Andrejewski, N., Scardigli, R., Guillemot, F., and Gruss, P. (2001). Pax6 is required for the multipotent state of retinal progenitor cells. Cell *105*, 43–55. 10.1016/s0092-8674(01)00295-1.

60. Vitorino, M., Jusuf, P.R., Maurus, D., Kimura, Y., Higashijima, S., and Harris, W.A. (2009). Vsx2 in the zebrafish retina: restricted lineages through derepression. Neural Develop. *4*, 14. 10.1186/1749-8104-4-14.

61. Passini, M.A., Levine, E.M., Canger, A.K., Raymond, P.A., and Schechter, N. (1997). Vsx-1 and Vsx-2: differential expression of two paired-like homeobox genes during zebrafish and goldfish retinogenesis. J. Comp. Neurol. *388*, 495–505. 10.1002/(sici)1096-9861(19971124)388:3<495::aid-cne11>3.0.co;2-l.

62. Kitambi, S.S., and Hauptmann, G. (2007). The zebrafish orphan nuclear receptor genes nr2e1 and nr2e3 are expressed in developing eye and forebrain. Gene Expr. Patterns *7*, 521–528. 10.1016/j.modgep.2006.10.006.

63. Gestri, G., Carl, M., Appolloni, I., Wilson, S.W., Barsacchi, G., and Andreazzoli, M. (2005). Six3 functions in anterior neural plate specification by promoting cell proliferation and inhibiting Bmp4 expression. Dev. Camb. Engl. *132*, 2401–2413. 10.1242/dev.01814.

64. Hu, M., and Easter, S.S. (1999). Retinal Neurogenesis: The Formation of the Initial Central Patch of Postmitotic Cells. Dev. Biol. *207*, 309–321. 10.1006/dbio.1998.9031.

65. Poggi, L., Vitorino, M., Masai, I., and Harris, W.A. (2005). Influences on neural lineage and mode of division in the zebrafish retina in vivo. J. Cell Biol. *171*, 991–999. 10.1083/jcb.200509098.

66. Nerli, E., Rocha-Martins, M., and Norden, C. (2020). Asymmetric neurogenic commitment of retinal progenitors involves Notch through the endocytic pathway. eLife *9*, e60462. 10.7554/eLife.60462.

67. Masai, I., Stemple, D.L., Okamoto, H., and Wilson, S.W. (2000). Midline Signals Regulate Retinal Neurogenesis in Zebrafish. Neuron *27*, 251–263. 10.1016/S0896-6273(00)00034-9.

68. Nerli, E., Kretzschmar, J., Bianucci, T., Rocha-Martins, M., Zechner, C., and Norden, C. (2022). Deterministic and probabilistic fate decisions co-exist in a single retinal lineage. 2022.08.11.503564. 10.1101/2022.08.11.503564.

69. Jusuf, P.R., Almeida, A.D., Randlett, O., Joubin, K., Poggi, L., and Harris, W.A. (2011). Origin and Determination of Inhibitory Cell Lineages in the Vertebrate Retina. J. Neurosci. *31*, 2549–2562. 10.1523/JNEUROSCI.4713-10.2011.

70. Suzuki, S.C., Bleckert, A., Williams, P.R., Takechi, M., Kawamura, S., and Wong, R.O.L. (2013). Cone photoreceptor types in zebrafish are generated by symmetric terminal divisions of dedicated precursors. Proc. Natl. Acad. Sci. *110*, 15109–15114. 10.1073/pnas.1303551110.

71. Godinho, L., Williams, P.R., Claassen, Y., Provost, E., Leach, S.D., Kamermans, M., and Wong, R.O.L. (2007). Nonapical Symmetric Divisions Underlie Horizontal Cell Layer Formation in the Developing Retina In Vivo. Neuron *56*, 597–603. 10.1016/j.neuron.2007.09.036.

72. Newman, E., and Reichenbach, A. (1996). The Müller cell: a functional element of the retina. Trends Neurosci. *19*, 307–312. 10.1016/0166-2236(96)10040-0.

73. Reichenbach, A., Stolzenburg, J.U., Eberhardt, W., Chao, T.I., Dettmer, D., and Hertz, L. (1993). What do retinal müller (glial) cells do for their neuronal “small siblings”? J. Chem. Neuroanat. *6*, 201–213. 10.1016/0891-0618(93)90042-3.

74. Reichenbach, A., and Robinson, S.R. (1995). Phylogenetic constraints on retinal organisation and development. Prog. Retin. Eye Res. *15*, 139–171. 10.1016/1350-9462(95)00008-9.

75. Sarthy, V.P., Pignataro, L., Pannicke, T., Weick, M., Reichenbach, A., Harada, T., Tanaka, K., and Marc, R. (2005). Glutamate transport by retinal Muller cells in glutamate/aspartate transporter-knockout mice. Glia *49*, 184–196. 10.1002/glia.20097.

76. Sarthy, P.V. (1982). The uptake of [3H]gamma-aminobutyric acid by isolated glial (Müller) cells from the mouse retina. J. Neurosci. Methods *5*, 77–82. 10.1016/0165-0270(82)90054-1.

77. Matsui, K., Hosoi, N., and Tachibana, M. (1999). Active role of glutamate uptake in the synaptic transmission from retinal nonspiking neurons. J. Neurosci. Off. J. Soc. Neurosci. *19*, 6755–6766.

78. Das, S.R., Bhardwaj, N., Kjeldbye, H., and Gouras, P. (1992). Muller cells of chicken retina synthesize 11-cis-retinol. Biochem. J. *285 (Pt 3)*, 907–913. 10.1042/bj2850907.

79. Franze, K., Grosche, J., Skatchkov, S.N., Schinkinger, S., Foja, C., Schild, D., Uckermann, O., Travis, K., Reichenbach, A., and Guck, J. (2007). Muller cells are living optical fibers in the vertebrate retina. Proc. Natl. Acad. Sci. U. S. A. *104*, 8287–8292. 10.1073/pnas.0611180104.

80. Blackshaw, S., Harpavat, S., Trimarchi, J., Cai, L., Huang, H., Kuo, W.P., Weber, G., Lee, K., Fraioli, R.E., Cho, S.-H., et al. (2004). Genomic analysis of mouse retinal development. PLoS Biol. *2*, E247. 10.1371/journal.pbio.0020247.

81. Reichenbach, A., and Reichelt, W. (1986). Postnatal development of radial glial (Müller) cells of the rabbit retina. Neurosci. Lett. *71*, 125–130. 10.1016/0304-3940(86)90545-8.

82. Corso-Díaz, X., and Simpson, E.M. (2015). Nr2e1 regulates retinal lamination and the development of Müller glia, S-cones, and glycineric amacrine cells during retinogenesis. Mol. Brain *8*, 37. 10.1186/s13041-015-0126-x.

83. Yokoi, H., Yan, Y.-L., Miller, M.R., BreMiller, R.A., Catchen, J.M., Johnson, E.A., and Postlethwait, J.H. (2009). Expression profiling of zebrafish sox9 mutants reveals that Sox9 is required for retinal differentiation. Dev. Biol. *329*, 1–15. 10.1016/j.ydbio.2009.01.002.

84. Poché, R.A., Furuta, Y., Chaboissier, M.-C., Schedl, A., and Behringer, R.R. (2008). Sox9 is expressed in mouse multipotent retinal progenitor cells and functions in Müller Glial cell development. J. Comp. Neurol. *510*, 237–250. 10.1002/cne.21746.

85. Muto, A., Iida, A., Satoh, S., and Watanabe, S. (2009). The group E Sox genes Sox8 and Sox9 are regulated by Notch signaling and are required for Müller glial cell development in mouse retina. Exp. Eye Res. *89*, 549–558. 10.1016/j.exer.2009.05.006.

86. Gorsuch, R.A., Lahne, M., Yarka, C.E., Petravick, M.E., Li, J., and Hyde, D.R. (2017). Sox2 regulates Müller glia reprogramming and proliferation in the regenerating zebrafish retina via Lin28 and Ascl1a. Exp. Eye Res. *161*, 174–192. 10.1016/j.exer.2017.05.012.

87. Graham, V., Khudyakov, J., Ellis, P., and Pevny, L. (2003). SOX2 functions to maintain neural progenitor identity. Neuron *39*, 749–765. 10.1016/s0896-6273(03)00497-5.

88. Taranova, O.V., Magness, S.T., Fagan, B.M., Wu, Y., Surzenko, N., Hutton, S.R., and Pevny, L.H. (2006). SOX2 is a dose-dependent regulator of retinal neural progenitor competence. Genes Dev. *20*, 1187–1202. 10.1101/gad.1407906.

89. Agathocleous, M., Iordanova, I., Willardsen, M.I., Xue, X.Y., Vetter, M.L., Harris, W.A., and Moore, K.B. (2009). A directional Wnt/β-catenin-Sox2-proneural pathway regulates the transition from proliferation to differentiation in the Xenopusretina. Development *136*, 3289–3299. 10.1242/dev.040451.

90. Heavner, W.E., Andoniadou, C.L., and Pevny, L.H. (2014). Establishment of the neurogenic boundary of the mouse retina requires cooperation of SOX2 and WNT signaling. Neural Develop. *9*, 27. 10.1186/1749-8104-9-27.

91. Germer, A., Jahnke, C., Mack, A., Enzmann, V., and Reichenbach, A. (1997). Modification of glutamine synthetase expression by mammalian Müller (glial) cells in retinal organ cultures. Neuroreport *8*, 3067–3072. 10.1097/00001756-199709290-00012.

92. Bringmann, A., Biedermann, B., and Reichenbach, A. (1999). Expression of potassium channels during postnatal differentiation of rabbit Müller glial cells. Eur. J. Neurosci. *11*, 2883–2896. 10.1046/j.1460-9568.1999.00706.x.

93. Felmy, F., Pannicke, T., Richt, J.A., Reichenbach, A., and Guenther, E. (2001). Electrophysiological properties of rat retinal Müller (glial) cells in postnatally developing and in pathologically altered retinae. Glia *34*, 190–199. 10.1002/glia.1053.

94. T, P., A, B., and A, R. (2002). Electrophysiological characterization of retinal Müller glial cells from mouse during postnatal development: comparison with rabbit cells. Glia *38*. 10.1002/glia.10068.

95. Bernardos, R.L., Barthel, L.K., Meyers, J.R., and Raymond, P.A. (2007). Late-Stage Neuronal Progenitors in the Retina Are Radial Muller Glia That Function as Retinal Stem Cells. J. Neurosci. *27*, 7028–7040. 10.1523/JNEUROSCI.1624-07.2007.

96. Hitchcock, P., Ochocinska, M., Sieh, A., and Otteson, D. (2004). Persistent and injury-induced neurogenesis in the vertebrate retina. Prog. Retin. Eye Res. *23*, 183–194. 10.1016/j.preteyeres.2004.01.001.

97. Otteson, D.C., and Hitchcock, P.F. (2003). Stem cells in the teleost retina: persistent neurogenesis and injury-induced regeneration. Vision Res. *43*, 927–936. 10.1016/s0042-6989(02)00400-5.

98. Hitchcock, P.F., and Raymond, P.A. (2004). The teleost retina as a model for developmental and regeneration biology. Zebrafish *1*, 257–271. 10.1089/zeb.2004.1.257.

99. Stenkamp, D.L. (2011). The rod photoreceptor lineage of teleost fish. Prog. Retin. Eye Res. *30*, 395–404. 10.1016/j.preteyeres.2011.06.004.

100. Harris, W.A., and Perron, M. (1998). Molecular recapitulation: the growth of the vertebrate retina. Int. J. Dev. Biol. *42*, 299–304.

101. Raymond, P.A., Barthel, L.K., Bernardos, R.L., and Perkowski, J.J. (2006). Molecular characterization of retinal stem cells and their niches in adult zebrafish. BMC Dev. Biol. *6*, 36. 10.1186/1471-213X-6-36.

102. Raymond, P.A., and Rivlin, P.K. (1987). Germinal cells in the goldfish retina that produce rod photoreceptors. Dev. Biol. *122*, 120–138. 10.1016/0012-1606(87)90338-1.

103. Nelson, S.M., Frey, R.A., Wardwell, S.L., and Stenkamp, D.L. (2008). The developmental sequence of gene expression within the rod photoreceptor lineage in embryonic zebrafish. Dev. Dyn. Off. Publ. Am. Assoc. Anat. *237*, 2903–2917. 10.1002/dvdy.21721.

104. Stenkamp, D.L. (2007). Neurogenesis in the fish retina. Int. Rev. Cytol. *259*, 173–224. 10.1016/S0074-7696(06)59005-9.

105. Chen, J., Rattner, A., and Nathans, J. (2005). The Rod Photoreceptor-Specific Nuclear Receptor Nr2e3 Represses Transcription of Multiple Cone-Specific Genes. J. Neurosci. *25*, 118–129. 10.1523/JNEUROSCI.3571-04.2005.

106. Vihtelic, T.S., and Hyde, D.R. (2000). Light-induced rod and cone cell death and regeneration in the adult albino zebrafish (Danio rerio) retina. J. Neurobiol. *44*, 289–307. 10.1002/1097-4695(20000905)44:3<289::aid-neu1>3.0.co;2-h.

107. Yurco, P., and Cameron, D.A. (2005). Responses of Müller glia to retinal injury in adult zebrafish. Vision Res. *45*, 991–1002. 10.1016/j.visres.2004.10.022.

108. Fausett, B.V., and Goldman, D. (2006). A Role for 1 Tubulin-Expressing Muller Glia in Regeneration of the Injured Zebrafish Retina. J. Neurosci. *26*, 6303–6313. 10.1523/JNEUROSCI.0332-06.2006.

109. Senut, M.-C., Gulati-Leekha, A., and Goldman, D. (2004). An element in the alpha1-tubulin promoter is necessary for retinal expression during optic nerve regeneration but not after eye injury in the adult zebrafish. J. Neurosci. Off. J. Soc. Neurosci. *24*, 7663–7673. 10.1523/JNEUROSCI.2281-04.2004.

110. Hieber, V., Dai, X., Foreman, M., and Goldman, D. (1998). Induction of alpha1-tubulin gene expression during development and regeneration of the fish central nervous system. J. Neurobiol. *37*, 429–440. 10.1002/(sici)1097-4695(19981115)37:3<429::aid-neu8>3.0.co;2-n.

111. Raymond, P.A., Reifler, M.J., and Rivlin, P.K. (1988). Regeneration of goldfish retina: rod precursors are a likely source of regenerated cells. J. Neurobiol. *19*, 431–463. 10.1002/neu.480190504.

112. Faillace, M.P., Julian, D., and Korenbrot, J.I. (2002). Mitotic activation of proliferative cells in the inner nuclear layer of the mature fish retina: regulatory signals and molecular markers. J. Comp. Neurol. *451*, 127–141. 10.1002/cne.10333.

113. Fimbel, S.M., Montgomery, J.E., Burket, C.T., and Hyde, D.R. (2007). Regeneration of Inner Retinal Neurons after Intravitreal Injection of Ouabain in Zebrafish. J. Neurosci. *27*, 1712–1724. 10.1523/JNEUROSCI.5317-06.2007.

114. Maier, W., and Wolburg, H. (1979). Regeneration of the goldfish retina after exposure to different doses of ouabain. Cell Tissue Res. *202*, 99–118. 10.1007/BF00239223.

115. Braisted, J.E., and Raymond, P.A. (1992). Regeneration of dopaminergic neurons in goldfish retina. Dev. Camb. Engl. *114*, 913–919. 10.1242/dev.114.4.913.

116. Shin, J., Park, H.-C., Topczewska, J.M., Mawdsley, D.J., and Appel, B. (2003). Neural cell fate analysis in zebrafish using olig2 BAC transgenics. Methods Cell Sci. Off. J. Soc. Vitro Biol. *25*, 7–14. 10.1023/B:MICS.0000006847.09037.3a.

117. Neuhauss, S.C., Biehlmaier, O., Seeliger, M.W., Das, T., Kohler, K., Harris, W.A., and Baier, H. (1999). Genetic disorders of vision revealed by a behavioral screen of 400 essential loci in zebrafish. J. Neurosci. Off. J. Soc. Neurosci. *19*, 8603–8615.

118. Wan, J., and Goldman, D. (2016). Retina regeneration in zebrafish. Curr. Opin. Genet. Dev. *40*, 41–47. 10.1016/j.gde.2016.05.009.

119. Gorsuch, R.A., and Hyde, D.R. (2014). Regulation of Müller glial dependent neuronal regeneration in the damaged adult zebrafish retina. Exp. Eye Res. *123*, 131–140. 10.1016/j.exer.2013.07.012.

120. Lahne, M., Nagashima, M., Hyde, D.R., and Hitchcock, P.F. (2020). Reprogramming Müller Glia to Regenerate Retinal Neurons. Annu. Rev. Vis. Sci. *6*, 171–193. 10.1146/annurev-vision-121219-081808.

121. Weber, A., Hochmann, S., Cimalla, P., Gärtner, M., Kuscha, V., Hans, S., Geffarth, M., Kaslin, J., Koch, E., and Brand, M. (2013). Characterization of light lesion paradigms and optical coherence tomography as tools to study adult retina regeneration in zebrafish. PloS One *8*, e80483. 10.1371/journal.pone.0080483.

122. Kassen, S.C., Ramanan, V., Montgomery, J.E., T. Burket, C., Liu, C.-G., Vihtelic, T.S., and Hyde, D.R. (2007). Time course analysis of gene expression during light-induced photoreceptor cell death and regeneration in *albino* zebrafish. Dev. Neurobiol. *67*, 1009–1031. 10.1002/dneu.20362.

123. Nelson, C.M., Ackerman, K.M., O'Hayer, P., Bailey, T.J., Gorsuch, R.A., and Hyde, D.R. (2013). Tumor Necrosis Factor-Alpha Is Produced by Dying Retinal Neurons and Is Required for Muller Glia Proliferation during Zebrafish Retinal Regeneration. J. Neurosci. *33*, 6524–6539. 10.1523/JNEUROSCI.3838-12.2013.

124. Bailey, T.J., Fossum, S.L., Fimbel, S.M., Montgomery, J.E., and Hyde, D.R. (2010). The inhibitor of phagocytosis, O-phospho-L-serine, suppresses Müller glia proliferation and cone cell regeneration in the light-damaged zebrafish retina. Exp. Eye Res. *91*, 601–612. 10.1016/j.exer.2010.07.017.

125. Silva, N.J., Nagashima, M., Li, J., Kakuk-Atkins, L., Ashrafzadeh, M., Hyde, D.R., and Hitchcock, P.F. (2020). Inflammation and matrix metalloproteinase 9 (Mmp-9) regulate photoreceptor regeneration in adult zebrafish. Glia *68*, 1445–1465. 10.1002/glia.23792.

126. Cameron, D.A., Gentile, K.L., Middleton, F.A., and Yurco, P. (2005). Gene expression profiles of intact and regenerating zebrafish retina. Mol. Vis. *11*, 775–791.

127. Wan, J., Ramachandran, R., and Goldman, D. (2012). HB-EGF Is Necessary and Sufficient for Müller Glia Dedifferentiation and Retina Regeneration. Dev. Cell *22*, 334–347. 10.1016/j.devcel.2011.11.020.

128. Zhao, X.-F., Wan, J., Powell, C., Ramachandran, R., Myers, M.G., and Goldman, D. (2014). Leptin and IL-6 family cytokines synergize to stimulate Müller glia reprogramming and retina regeneration. Cell Rep. *9*, 272–284. 10.1016/j.celrep.2014.08.047.

129. Conner, C., Ackerman, K.M., Lahne, M., Hobgood, J.S., and Hyde, D.R. (2014). Repressing Notch Signaling and Expressing TNFα Are Sufficient to Mimic Retinal Regeneration by Inducing Müller Glial Proliferation to Generate Committed Progenitor Cells. J. Neurosci. *34*, 14403–14419. 10.1523/JNEUROSCI.0498-14.2014.

130. Fausett, B.V., Gumerson, J.D., and Goldman, D. (2008). The Proneural Basic Helix-Loop-Helix Gene Ascl1a Is Required for Retina Regeneration. J. Neurosci. *28*, 1109–1117. 10.1523/JNEUROSCI.4853-07.2008.

131. Ramachandran, R., Reifler, A., Parent, J.M., and Goldman, D. (2010). Conditional gene expression and lineage tracing of tuba1a expressing cells during zebrafish development and retina regeneration. J. Comp. Neurol. *518*, 4196–4212. 10.1002/cne.22448.

132. Ramachandran, R., Fausett, B.V., and Goldman, D. (2010). Ascl1a regulates Müller glia dedifferentiation and retinal regeneration through a Lin-28-dependent, let-7 microRNA signalling pathway. Nat. Cell Biol. *12*, 1101–1107. 10.1038/ncb2115.

133. Qin, Z., Barthel, L.K., and Raymond, P.A. (2009). Genetic evidence for shared mechanisms of epimorphic regeneration in zebrafish. Proc. Natl. Acad. Sci. U. S. A. *106*, 9310–9315. 10.1073/pnas.0811186106.

134. Hoang, T., Wang, J., Boyd, P., Wang, F., Santiago, C., Jiang, L., Yoo, S., Lahne, M., Todd, L.J., Jia, M., et al. (2020). Gene regulatory networks controlling vertebrate retinal regeneration. Science *370*, eabb8598. 10.1126/science.abb8598.

135. Thummel, R., Enright, J.M., Kassen, S.C., Montgomery, J.E., Bailey, T.J., and Hyde, D.R. (2010). Pax6a and Pax6b are required at different points in neuronal progenitor cell proliferation during zebrafish photoreceptor regeneration. Exp. Eye Res. *90*, 572–582. 10.1016/j.exer.2010.02.001.

136. Thummel, R., Kassen, S.C., Enright, J.M., Nelson, C.M., Montgomery, J.E., and Hyde, D.R. (2008). Characterization of Müller glia and neuronal progenitors during adult zebrafish retinal regeneration. Exp. Eye Res. *87*, 433–444. 10.1016/j.exer.2008.07.009.

137. Nagashima, M., Barthel, L.K., and Raymond, P.A. (2013). A self-renewing division of zebrafish Müller glial cells generates neuronal progenitors that require N-cadherin to regenerate retinal neurons. Development *140*, 4510–4521. 10.1242/dev.090738.

138. Lenkowski, J.R., Qin, Z., Sifuentes, C.J., Thummel, R., Soto, C.M., Moens, C.B., and Raymond, P.A. (2013). Retinal regeneration in adult zebrafish requires regulation of TGFβ signaling. Glia *61*, 1687–1697. 10.1002/glia.22549.

139. Vihtelic, T.S., Soverly, J.E., Kassen, S.C., and Hyde, D.R. (2006). Retinal regional differences in photoreceptor cell death and regeneration in light-lesioned albino zebrafish. Exp. Eye Res. *82*, 558–575. 10.1016/j.exer.2005.08.015.

140. Ramachandran, R., Zhao, X.-F., and Goldman, D. (2011). Ascl1a/Dkk/ -catenin signaling pathway is necessary and glycogen synthase kinase-3 inhibition is sufficient for zebrafish retina regeneration. Proc. Natl. Acad. Sci. *108*, 15858–15863. 10.1073/pnas.1107220108.

141. Thummel, R., Kassen, S.C., Montgomery, J.E., Enright, J.M., and Hyde, D.R. (2008). Inhibition of Müller glial cell division blocks regeneration of the light-damaged zebrafish retina. Dev. Neurobiol. *68*, 392–408. 10.1002/dneu.20596.

142. Lahne, M., Li, J., Marton, R.M., and Hyde, D.R. (2015). Actin-Cytoskeleton- and Rock-Mediated INM Are Required for Photoreceptor Regeneration in the Adult Zebrafish Retina. J. Neurosci. *35*, 15612–15634. 10.1523/JNEUROSCI.5005-14.2015.

143. Powell, C., Cornblath, E., Elsaeidi, F., Wan, J., and Goldman, D. (2016). Zebrafish Müller glia-derived progenitors are multipotent, exhibit proliferative biases and regenerate excess neurons. Sci. Rep. *6*, 24851. 10.1038/srep24851.

144. Craig, S.E.L., Calinescu, A.-A., and Hitchcock, P.F. (2008). Identification of the molecular signatures integral to regenerating photoreceptors in the retina of the zebra fish. J. Ocul. Biol. Dis. Infor. *1*, 73–84. 10.1007/s12177-008-9011-5.

145. Sifuentes, C.J., Kim, J.-W., Swaroop, A., and Raymond, P.A. (2016). Rapid, Dynamic Activation of Müller Glial Stem Cell Responses in Zebrafish. Invest. Ophthalmol. Vis. Sci. *57*, 5148–5160. 10.1167/iovs.16-19973.

146. Haque, A., Engel, J., Teichmann, S.A., and Lönnberg, T. (2017). A practical guide to single-cell RNA-sequencing for biomedical research and clinical applications. Genome Med. *9*, 75. 10.1186/s13073-017-0467-4.

147. Herring, C.A., Chen, B., McKinley, E.T., and Lau, K.S. (2018). Single-Cell Computational Strategies for Lineage Reconstruction in Tissue Systems. Cell. Mol. Gastroenterol. Hepatol. *5*, 539–548. 10.1016/j.jcmgh.2018.01.023.

148. Stegle, O., Teichmann, S.A., and Marioni, J.C. (2015). Computational and analytical challenges in single-cell transcriptomics. Nat. Rev. Genet. *16*, 133–145. 10.1038/nrg3833.

149. Deng, Q., Ramsköld, D., Reinius, B., and Sandberg, R. (2014). Single-cell RNA-seq reveals dynamic, random monoallelic gene expression in mammalian cells. Science *343*, 193–196. 10.1126/science.1245316.

150. Luecken, M.D., and Theis, F.J. (2019). Current best practices in single-cell RNA-seq analysis: a tutorial. Mol. Syst. Biol. *15*, e8746. 10.15252/msb.20188746.

151. Trapnell, C., Cacchiarelli, D., Grimsby, J., Pokharel, P., Li, S., Morse, M., Lennon, N.J., Livak, K.J., Mikkelsen, T.S., and Rinn, J.L. (2014). The dynamics and regulators of cell fate decisions are revealed by pseudotemporal ordering of single cells. Nat. Biotechnol. *32*, 381–386. 10.1038/nbt.2859.

152. Zheng, G.X.Y., Terry, J.M., Belgrader, P., Ryvkin, P., Bent, Z.W., Wilson, R., Ziraldo, S.B., Wheeler, T.D., McDermott, G.P., Zhu, J., et al. (2017). Massively parallel digital transcriptional profiling of single cells. Nat. Commun. *8*, 14049. 10.1038/ncomms14049.

153. Brennecke, P., Anders, S., Kim, J.K., Kołodziejczyk, A.A., Zhang, X., Proserpio, V., Baying, B., Benes, V., Teichmann, S.A., Marioni, J.C., et al. (2013). Accounting for technical noise in single-cell RNA-seq experiments. Nat. Methods *10*, 1093–1095. 10.1038/nmeth.2645.

154. LIII. On lines and planes of closest fit to systems of points in space: The London, Edinburgh, and Dublin Philosophical Magazine and Journal of Science: Vol 2, No 11 https://www.tandfonline.com/doi/abs/10.1080/14786440109462720.

155. van der Maaten, L., and Hinton, G. (2008). Visualizing Data using t-SNE. J. Mach. Learn. Res. *9*, 2579–2605.

156. McInnes, L., Healy, J., Saul, N., and Großberger, L. (2018). UMAP: Uniform Manifold Approximation and Projection. J. Open Source Softw. *3*, 861. 10.21105/joss.00861.

157. Hirano, N., Muroi, T., Takahashi, H., and Haruki, M. (2011). Site-specific recombinases as tools for heterologous gene integration. Appl. Microbiol. Biotechnol. *92*, 227–239. 10.1007/s00253-011-3519-5.

158. Branda, C.S., and Dymecki, S.M. (2004). Talking about a revolution: The impact of site-specific recombinases on genetic analyses in mice. Dev. Cell *6*, 7–28. 10.1016/s1534-5807(03)00399-x.

159. Metzger, D., and Chambon, P. (2001). Site- and time-specific gene targeting in the mouse. Methods San Diego Calif *24*, 71–80. 10.1006/meth.2001.1159.

160. Feil, R., Wagner, J., Metzger, D., and Chambon, P. (1997). Regulation of Cre recombinase activity by mutated estrogen receptor ligand-binding domains. Biochem. Biophys. Res. Commun. *237*, 752–757. 10.1006/bbrc.1997.7124.

161. Indra, A.K., Warot, X., Brocard, J., Bornert, J.M., Xiao, J.H., Chambon, P., and Metzger, D. (1999). Temporally-controlled site-specific mutagenesis in the basal layer of the epidermis: comparison of the recombinase activity of the tamoxifen-inducible Cre-ER(T) and Cre-ER(T2) recombinases. Nucleic Acids Res. *27*, 4324–4327. 10.1093/nar/27.22.4324.

162. Knopf, F., Hammond, C., Chekuru, A., Kurth, T., Hans, S., Weber, C.W., Mahatma, G., Fisher, S., Brand, M., Schulte-Merker, S., et al. (2011). Bone regenerates via dedifferentiation of osteoblasts in the zebrafish fin. Dev. Cell *20*, 713–724. 10.1016/j.devcel.2011.04.014.

163. Ando, K., Shibata, E., Hans, S., Brand, M., and Kawakami, A. (2017). Osteoblast Production by Reserved Progenitor Cells in Zebrafish Bone Regeneration and Maintenance. Dev. Cell *43*, 643-650.e3. 10.1016/j.devcel.2017.10.015.

164. Hans, S., Kaslin, J., Freudenreich, D., and Brand, M. (2009). Temporally-Controlled Site-Specific Recombination in Zebrafish. PLOS ONE *4*, e4640. 10.1371/journal.pone.0004640.

165. Vision impairment and blindness https://www.who.int/news-room/fact-sheets/detail/blindness-and-visual-impairment.

166. Bull, N.D., and Martin, K.R. (2011). Concise review: toward stem cell-based therapies for retinal neurodegenerative diseases. Stem Cells Dayt. Ohio *29*, 1170–1175. 10.1002/stem.676.

167. Song, D.-J., Bao, X.-L., Fan, B., and Li, G.-Y. (2022). Mechanism of Cone Degeneration in Retinitis Pigmentosa. Cell. Mol. Neurobiol. 10.1007/s10571-022-01243-2.

168. Roska, B., and Sahel, J.-A. (2018). Restoring vision. Nature *557*, 359–367. 10.1038/s41586-018-0076-4.

169. Sahel, J.-A., Boulanger-Scemama, E., Pagot, C., Arleo, A., Galluppi, F., Martel, J.N., Esposti, S.D., Delaux, A., de Saint Aubert, J.-B., de Montleau, C., et al. (2021). Partial recovery of visual function in a blind patient after optogenetic therapy. Nat. Med. *27*, 1223–1229. 10.1038/s41591-021-01351-4.

170. Javed, A., and Cayouette, M. (2017). Temporal Progression of Retinal Progenitor Cell Identity: Implications in Cell Replacement Therapies. Front. Neural Circuits *11*.

171. Völkner, M., Wagner, F., Steinheuer, L.M., Carido, M., Kurth, T., Yazbeck, A., Schor, J., Wieneke, S., Ebner, L.J.A., Del Toro Runzer, C., et al. (2022). HBEGF-TNF induce a complex outer retinal pathology with photoreceptor cell extrusion in human organoids. Nat. Commun. *13*, 6183. 10.1038/s41467-022-33848-y.

172. Gasparini, S.J., Tessmer, K., Reh, M., Wieneke, S., Carido, M., Völkner, M., Borsch, O., Swiersy, A., Zuzic, M., Goureau, O., et al. (2022). Transplanted human cones incorporate into the retina and function in a murine cone degeneration model. J. Clin. Invest. *132*, e154619. 10.1172/JCI154619.

173. Karl, M.O., Hayes, S., Nelson, B.R., Tan, K., Buckingham, B., and Reh, T.A. (2008). Stimulation of neural regeneration in the mouse retina. Proc. Natl. Acad. Sci. U. S. A. *105*, 19508–19513. 10.1073/pnas.0807453105.

174. Karl, M.O., and Reh, T.A. (2012). Studying the generation of regenerated retinal neuron from Müller glia in the mouse eye. Methods Mol. Biol. Clifton NJ *884*, 213–227. 10.1007/978-1-61779-848-1_15.

175. Löffler, K., Schäfer, P., Völkner, M., Holdt, T., and Karl, M.O. (2015). Age-dependent Müller glia neurogenic competence in the mouse retina. Glia *63*, 1809–1824. 10.1002/glia.22846.

176. Fischer, A.J., McGuire, C.R., Dierks, B.D., and Reh, T.A. (2002). Insulin and fibroblast growth factor 2 activate a neurogenic program in Müller glia of the chicken retina. J. Neurosci. Off. J. Soc. Neurosci. *22*, 9387–9398.

177. Fischer, A.J., and Reh, T.A. (2003). Potential of Müller glia to become neurogenic retinal progenitor cells. Glia *43*, 70–76. 10.1002/glia.10218.

178. Glass, R., Synowitz, M., Kronenberg, G., Walzlein, J.-H., Markovic, D.S., Wang, L.-P., Gast, D., Kiwit, J., Kempermann, G., and Kettenmann, H. (2005). Glioblastoma-Induced Attraction of Endogenous Neural Precursor Cells Is Associated with Improved Survival. J. Neurosci. *25*, 2637–2646. 10.1523/JNEUROSCI.5118-04.2005.

179. Leinninger, G.M., Jo, Y.-H., Leshan, R.L., Louis, G.W., Yang, H., Barrera, J.G., Wilson, H., Opland, D.M., Faouzi, M.A., Gong, Y., et al. (2009). Leptin acts via leptin receptor-expressing lateral hypothalamic neurons to modulate the mesolimbic dopamine system and suppress feeding. Cell Metab. *10*, 89–98. 10.1016/j.cmet.2009.06.011.

180. Nusslein-Volhard, C., Dahm, R., Nusslein-Volhard, C., and Dahm, R. (2002). Zebrafish (Oxford University Press).

181. Aleström, P., D'Angelo, L., Midtlyng, P.J., Schorderet, D.F., Schulte-Merker, S., Sohm, F., and Warner, S. (2020). Zebrafish: Housing and husbandry recommendations. Lab. Anim. *54*, 213–224. 10.1177/0023677219869037.

182. Zhang, Y., Buchholz, F., Muyrers, J.P.P., and Stewart, A.F. (1998). A new logic for DNA engineering using recombination in Escherichia coli. Nat. Genet. *20*, 123–128. 10.1038/2417.

183. ZFIN Publication: Nüsslein-Volhard et al., 2002 https://zfin.org/ZDB-PUB-021017-11.

184. Lun, A.T.L., McCarthy, D.J., and Marioni, J.C. (2016). A step-by-step workflow for low-level analysis of single-cell RNA-seq data with Bioconductor. 10.12688/f1000research.9501.2.

185. Schindelin, J., Arganda-Carreras, I., Frise, E., Kaynig, V., Longair, M., Pietzsch, T., Preibisch, S., Rueden, C., Saalfeld, S., Schmid, B., et al. (2012). Fiji: an open-source platform for biological-image analysis. Nat. Methods *9*, 676–682. 10.1038/nmeth.2019.

186. Lahne, M., Brecker, M., Jones, S.E., and Hyde, D.R. (2020). The Regenerating Adult Zebrafish Retina Recapitulates Developmental Fate Specification Programs. Front. Cell Dev. Biol. *8*, 617923. 10.3389/fcell.2020.617923.

187. Ng Chi Kei, J., Currie, P.D., and Jusuf, P.R. (2017). Fate bias during neural regeneration adjusts dynamically without recapitulating developmental fate progression. Neural Develop. *12*, 12. 10.1186/s13064-017-0089-y.

188. Ramachandran, R., Zhao, X.-F., and Goldman, D. (2012). Insm1a-mediated gene repression is essential for the formation and differentiation of Müller glia-derived progenitors in the injured retina. Nat. Cell Biol. *14*, 1013–1023. 10.1038/ncb2586.

189. Macosko, E.Z., Basu, A., Satija, R., Nemesh, J., Shekhar, K., Goldman, M., Tirosh, I., Bialas, A.R., Kamitaki, N., Martersteck, E.M., et al. (2015). Highly Parallel Genome-wide Expression Profiling of Individual Cells Using Nanoliter Droplets. Cell *161*, 1202–1214. 10.1016/j.cell.2015.05.002.

190. Tirosh, I., Izar, B., Prakadan, S.M., Wadsworth, M.H., Treacy, D., Trombetta, J.J., Rotem, A., Rodman, C., Lian, C., Murphy, G., et al. (2016). Dissecting the multicellular ecosystem of metastatic melanoma by single-cell RNA-seq. Science *352*, 189–196. 10.1126/science.aad0501.

191. Whitfield, M.L., Sherlock, G., Saldanha, A.J., Murray, J.I., Ball, C.A., Alexander, K.E., Matese, J.C., Perou, C.M., Hurt, M.M., Brown, P.O., et al. (2002). Identification of genes periodically expressed in the human cell cycle and their expression in tumors. Mol. Biol. Cell *13*, 1977–2000. 10.1091/mbc.02-02-0030.

192. Wu, F., Bard, J.E., Kann, J., Yergeau, D., Sapkota, D., Ge, Y., Hu, Z., Wang, J., Liu, T., and Mu, X. (2021). Single cell transcriptomics reveals lineage trajectory of retinal ganglion cells in wild-type and Atoh7-null retinas. Nat. Commun. *12*, 1465. 10.1038/s41467-021-21704-4.

193. Bernardos, R.L., and Raymond, P.A. (2006). GFAP transgenic zebrafish. Gene Expr. Patterns GEP *6*, 1007–1013. 10.1016/j.modgep.2006.04.006.

194. Peterson, R.E., Fadool, J.M., McClintock, J., and Linser, P.J. (2001). Müller cell differentiation in the zebrafish neural retina: evidence of distinct early and late stages

in cell maturation. J. Comp. Neurol. *429*, 530–540. 10.1002/1096-9861(20010122)429:4<530::aid-cne2>3.0.co;2-c.

195. Dogra, D., Ahuja, S., Kim, H.-T., Rasouli, S.J., Stainier, D.Y.R., and Reischauer, S. (2017). Opposite effects of Activin type 2 receptor ligands on cardiomyocyte proliferation during development and repair. Nat. Commun. *8*, 1902. 10.1038/s41467-017-01950-1.

196. Feng, L., Hernandez, R.E., Waxman, J.S., Yelon, D., and Moens, C.B. (2010). Dhrs3a regulates retinoic acid biosynthesis through a feedback inhibition mechanism. Dev. Biol. *338*, 1–14. 10.1016/j.ydbio.2009.10.029.

197. Holmes, R.S., and Hempel, J. (2011). Comparative studies of vertebrate aldehyde dehydrogenase 3: sequences, structures, phylogeny and evolution. Evidence for a mammalian origin for the ALDH3A1 gene. Chem. Biol. Interact. *191*, 113–121. 10.1016/j.cbi.2011.01.014.

198. D'Aniello, E., Ravisankar, P., and Waxman, J.S. (2015). Rdh10a Provides a Conserved Critical Step in the Synthesis of Retinoic Acid during Zebrafish Embryogenesis. PloS One *10*, e0138588. 10.1371/journal.pone.0138588.

199. Baraban, M., Anselme, I., Schneider-Maunoury, S., and Giudicelli, F. (2013). Zebrafish embryonic neurons transport messenger RNA to axons and growth cones in vivo. J. Neurosci. Off. J. Soc. Neurosci. *33*, 15726–15734. 10.1523/JNEUROSCI.1510-13.2013.

200. Song, K., Lin, Z., Cao, L., Lu, B., Chen, Y., Zhang, S., Lu, J., and Xu, H. (2023). Sox11b regulates the migration and fate determination of Müller glia-derived progenitors during retina regeneration in zebrafish. Neural Regen. Res. *18*, 445–450. 10.4103/1673-5374.346550.

201. Mu, Z., Zhang, S., He, C., Hou, H., Liu, D., Hu, N., and Xu, H. (2017). Expression of SoxC Transcription Factors during Zebrafish Retinal and Optic Nerve Regeneration. Neurosci. Bull. *33*, 53–61. 10.1007/s12264-016-0073-2.

202. Poché, R.A., Kwan, K.M., Raven, M.A., Furuta, Y., Reese, B.E., and Behringer, R.R. (2007). Lim1 Is Essential for the Correct Laminar Positioning of Retinal Horizontal Cells. J. Neurosci. *27*, 14099–14107. 10.1523/JNEUROSCI.4046-07.2007.

203. Amini, R., Bhatnagar, A., Schlüßler, R., Möllmert, S., Guck, J., and Norden, C. (2022). Amoeboid-like migration ensures correct horizontal cell layer formation in the developing vertebrate retina. eLife *11*, e76408. 10.7554/eLife.76408.

204. Hans, S., Freudenreich, D., Geffarth, M., Kaslin, J., Machate, A., and Brand, M. (2011). Generation of a non-leaky heat shock-inducible Cre line for conditional Cre/lox strategies in zebrafish. Dev. Dyn. Off. Publ. Am. Assoc. Anat. *240*, 108–115. 10.1002/dvdy.22497.

205. Yoshinari, N., Ando, K., Kudo, A., Kinoshita, M., and Kawakami, A. (2012). Colored medaka and zebrafish: transgenics with ubiquitous and strong transgene expression driven by the medaka β-actin promoter. Dev. Growth Differ. *54*, 818–828. 10.1111/dgd.12013.

206. Morris, A.C., Forbes-Osborne, M.A., Pillai, L.S., and Fadool, J.M. (2011). Microarray Analysis of XOPS-mCFP Zebrafish Retina Identifies Genes Associated with Rod Photoreceptor Degeneration and Regeneration. Invest. Ophthalmol. Vis. Sci. *52*, 2255–2266. 10.1167/iovs.10-6022.

207. Wilson, S.G., Wen, W., Pillai-Kastoori, L., and Morris, A.C. (2016). Tracking the fate of her4 expressing cells in the regenerating retina using her4:Kaede zebrafish. Exp. Eye Res. *145*, 75–87. 10.1016/j.exer.2015.11.002.

208. Campbell, L.J., Levendusky, J.L., Steines, S.A., and Hyde, D.R. (2022). Retinal regeneration requires dynamic Notch signaling. Neural Regen. Res. *17*, 1199–1209. 10.4103/1673-5374.327326.

209. Buenaventura, D.F., Ghinia-Tegla, M.G., and Emerson, M.M. (2018). Fate-restricted retinal progenitor cells adopt a molecular profile and spatial position distinct from multipotent progenitor cells. Dev. Biol. *443*, 35–49. 10.1016/j.ydbio.2018.06.023.

210. Emerson, M.M., Surzenko, N., Goetz, J.J., Trimarchi, J., and Cepko, C.L. (2013). Otx2 and Onecut1 promote the fates of cone photoreceptors and horizontal cells and repress rod photoreceptors. Dev. Cell *26*, 59–72. 10.1016/j.devcel.2013.06.005.

211. Klimova, L., Antosova, B., Kuzelova, A., Strnad, H., and Kozmik, Z. (2015). Onecut1 and Onecut2 transcription factors operate downstream of Pax6 to regulate horizontal cell development. Dev. Biol. *402*, 48–60. 10.1016/j.ydbio.2015.02.023.

212. Sapkota, D., Chintala, H., Wu, F., Fliesler, S.J., Hu, Z., and Mu, X. (2014). Onecut1 and Onecut2 redundantly regulate early retinal cell fates during development. Proc. Natl. Acad. Sci. *111*, E4086–E4095. 10.1073/pnas.1405354111.

213. Morris, A.C., and Fadool, J.M. (2005). Studying rod photoreceptor development in zebrafish. Physiol. Behav. *86*, 306–313. 10.1016/j.physbeh.2005.08.020.

214. Felker, A., Nieuwenhuize, S., Dolbois, A., Blazkova, K., Hess, C., Low, L.W.L., Burger, S., Samson, N., Carney, T.J., Bartunek, P., et al. (2016). In Vivo Performance and Properties of Tamoxifen Metabolites for CreERT2 Control. PLOS ONE *11*, e0152989. 10.1371/journal.pone.0152989.

215. Pan, Y.A., Freundlich, T., Weissman, T.A., Schoppik, D., Wang, X.C., Zimmerman, S., Ciruna, B., Sanes, J.R., Lichtman, J.W., and Schier, A.F. (2013). Zebrabow: multispectral cell labeling for cell tracing and lineage analysis in zebrafish. Dev. Camb. Engl. *140*, 2835–2846. 10.1242/dev.094631.

216. Haase, R., Royer, L.A., Steinbach, P., Schmidt, D., Dibrov, A., Schmidt, U., Weigert, M., Maghelli, N., Tomancak, P., Jug, F., et al. (2020). CLIJ: GPU-accelerated image processing for everyone. Nat. Methods *17*, 5–6. 10.1038/s41592-019-0650-1.

Erklärung entsprechend §5.5 der Promotionsordnung

Hiermit versichere ich, dass ich die vorliegende Arbeit ohne unzulässige Hilfe Dritter und ohne Benutzung anderer als der angegebenen Hilfsmittel angefertigt habe; die aus fremden Quellen direkt oder indirekt übernommenen Gedanken sind als solche kenntlich gemacht. Die Arbeit wurde bisher weder im Inland noch im Ausland in gleicher oder ähnlicher Form einer anderen Prüfungsbehörde vorgelegt.

Die Dissertation wurde im Zeitraum vom Dezember 2018 bis Dezember 2022 verfasst und von Prof. Dr. Michael Brand, CRTD-TUD, Molekulare Entwicklungsgenetik betreut.

Meine Person betreffend erkläre ich hiermit, dass keine früheren erfolglosen Promotionsverfahren stattgefunden haben.

Ich erkenne die Promotionsordnung des Bereiches für Mathematik und Naturwissenschaften, Technische Universität Dresden, vom 23.02.1011 an, zuletzt geändert durch Beschlüsse des Fakultätsrates vom 15.06.2011 und 18.06.2014.

_____

Datum, *Unterschrift*